PB-217 289

FOAM FRACTIONATION WITH REFLUX

Robert Lemlich

Cincinnati University
Cincinnati, Ohio

28 May 1968

DISTRIBUTED BY:

NTIS
National Technical Information Service
U. S. DEPARTMENT OF COMMERCE
5285 Port Royal Road, Springfield Va. 22151

1

Progress Report

for

December 1, 1966 through May 15, 1968

on the research project

FOAM FRACTIONATION WITH REFLUX

WP - 00161

Reproduced from best available copy.

Summary

Drainage and coalescence within a vertical foam fractionation column were measured experimentally. This was accomplished by constructing and operating a vertical column equipped with a series of electrical conductivity cells mounted internally at various levels. With these cells, the variation in the local foam density along the column was determined from the variation in the local conductance. The change in bubble size was measured photographically. Other variables were determined by conventional means. The surfactants employed included Triton X-100, albumin, and saponin. Reflux ratios ranged from zero to infinity.

The results showed that coalescence decreased as the gas rate and concentration increased. Also, while a higher surface viscosity made for appreciably greater foam stability, it had a smaller effect on foam drainage and hence on foam overflow from the column. This apparent anomaly was tentatively ascribed to non-Newtonian behavior at the surface. The non-Newtonian effect was evaluated quantitatively by applying the writer's theory for foam drainage and overflow to the experimental data.

Finally, consideration was given to the increased separation attainable by vertically elongating the liquid pool so as to establish a concentration gradient within it. A detailed analysis of this phenomenon was prepared in terms of potential flow and penetration theory at the upstream portion of the bubble, plus a renewing wake downstream and an overall solute balance.

The overall experimental and theoretical results have added materially to the understanding of foam fractionation and to the development of a rational design procedure for achieving desired separations.

Results of this research were presented at three national society meetings. Five new publications have appeared or are in press.

The reader's attention is called to the Preface on the next page.

Robert Lemlich

May 28, 1968
University of Cincinnati
Cincinnati, Ohio 45221

Robert Lemlich
Principal Investigator
Professor of Chemical Engineering

Preface

Interest in foam fractionation and allied techniques of separation has burgeoned in recent years. A considerable number of new systems have been separated. Some of these are of direct interest to sewage disposal and the problem of water renovation in general.

Most of the new studies which have been reported are reviewed on pages 26-31 of Part 3 of the present report. Generally speaking, the investigations reported are experimental and specific. However, almost none of them are fundamental, at least in an engineering sense. Therefore they do not yield the kind of information on which rational engineering decisions can truly be made, or on which economic designs can be optimized.

For these reasons, the present writer and his co-workers have studied foam fractionation for a number of years in an effort to uncover the fundamentals which govern the process. In the writer's opinion, he and his co-workers have met with a considerable degree of continuing success in this endeavor. Parts 2 and 3 of the present report are review papers. Most of the fundamentals and engineering principles for foam fractionation described in these two papers are a direct result of this work.

It is the writer's hope that the Federal Water Pollution Control Administration will continue to support this research for the next two years so that the work which has begun can be completed and the rational design of foam fractionation apparatus can become a reality.

Staffing

Principal Investigator: Robert Lemlich, Professor of Chemical Engineering.

Research Assistants: Katherine D. Cannon, masters student in Chemical Engineering.

Indrakumar L. Jashnani, masters student in Chemical Engineering.

Fang-Shung Shih*, doctoral student in Chemical Engineering.

Domestic Travel

The Principal Investigator spoke on the subject of the present progress report at three national society meetings and at four universities. Details of this travel are summarized later under the heading "Other Contributions".

Foreign Travel

none

---

*This student is currently completing the writeup of his Ph.D. research under this project. The research of the two M.S. students is in progress.

Publications*

Since the last progress report (December 1, 1966), three papers have been submitted and accepted for publication, and a fourth and fifth have appeared in print. These papers are listed below as Parts 2-6 of the present progress report.

Part 1 is not a paper. It is instead a summary of recent progress in research under the grant. When complete, a detailed account will be written up as a paper for submission to a recognized journal.

Since the several parts of the present report involve individual papers, each part has its own separate page numbers, nomenclature, references, etc.

	Part
Recent progress: A summary of results obtained for the coalescence, drainage, and overflow of foam together with a study of the considerations involved in deliberately elongating the liquid pool.	1
*Lemlich, R., "Principles of Foam Fractionation", a chapter written for Progress in Separation and Purification, Vol. 1, at the invitation of E. S. Perry, editor, Interscience (1968).	2
*Lemlich, R., "Adsorptive Bubble Separation Methods: Foam Fractionation and Allied Techniques", an invited review paper to be published in Ind. Eng. Chem.	3
*Lemlich, R., "Foam Overflow Rate: Comparison of Theory with Experiment", a communication to be published in Chem. Eng. Science.	4
*Shih, F. S., and Lemlich, R., "A Study of Interstitial Liquid Flow in Foam, Part III: Test of Theory", A.I.Ch.E. Jour. 13, 751 (1967).	5
*Karger, B. L., Grieves, R. B., Lemlich, R., Rubin, A. J., Sebba, F., "Nomenclature Recommendations for Adsorptive Bubble Separation Methods", Separation Science 2, 401 (1967).	6

Other Contributions

The Principal Investigator spoke on the present subject at three national meetings, as follows:

1. American Institute of Chemical Engineers, 59th Annual Meeting, Detroit, Michigan, December 1966, Free Forum.

2. American Chemical Society, 153rd National Meeting, Miami Beach, Florida, April 1967, Division of Water, Air, and Waste Chemistry.

3. American Chemical Society, 154th National Meeting, Chicago, Illinois, September 1967, Division of Industrial and Engineering Chemistry.

The Principal Investigator also spoke on the subject at seminars at four institutions of higher learning, namely:

1. University of Pennsylvania, Philadelphia, Pa., December 1967.
2. Drexel Institute of Technology, Philadelphia, Pa., December 1967.
3. City University of New York, New York, N. Y., March 1968.
4. Columbia University, New York, N. Y., March 1968.

RECENT PROGRESS

Experiment

A foaming column was constructed to measure the bulk foam density at various levels in situ, the rate of coalescence in the rising foam, and the rate of foam overflow.

Figure 1 shows the column. It was constructed from two sections of Pyrex pipe, each 2 inches in internal diameter and 1.5 ft. in length. An inverted U-bend was flanged on top to conduct the foam overflow to a rotary foam breaker. A 12 liter flask for the liquid pool was attached below the column.

The column itself was equipped internally with 8 pairs of electrodes (conductivity cells), equally spaced along its length. The circuit of each electrode pair was independently connected through a double rotary switch to an A.C. bridge. This permitted in situ measurements of electrical resistance, from which local bulk foam densities were determined. Each electrode was made from 1.2 cm diameter platinized platinum foil. It was mounted almost flush with the inner column wall so as to minimize any mechanical disturbance to the rising foam.

The electrodes were calibrated against foam of known density, the latter being determined by simply filling the column (above the liquid level) with foam, measuring the electrical resistance, and then allowing the foam to completely collapse and measuring the resulting rise in liquid level. By varying the initial liquid level, individual electrode pairs could be examined. The specific conductivities of the individual pair were also checked from time to

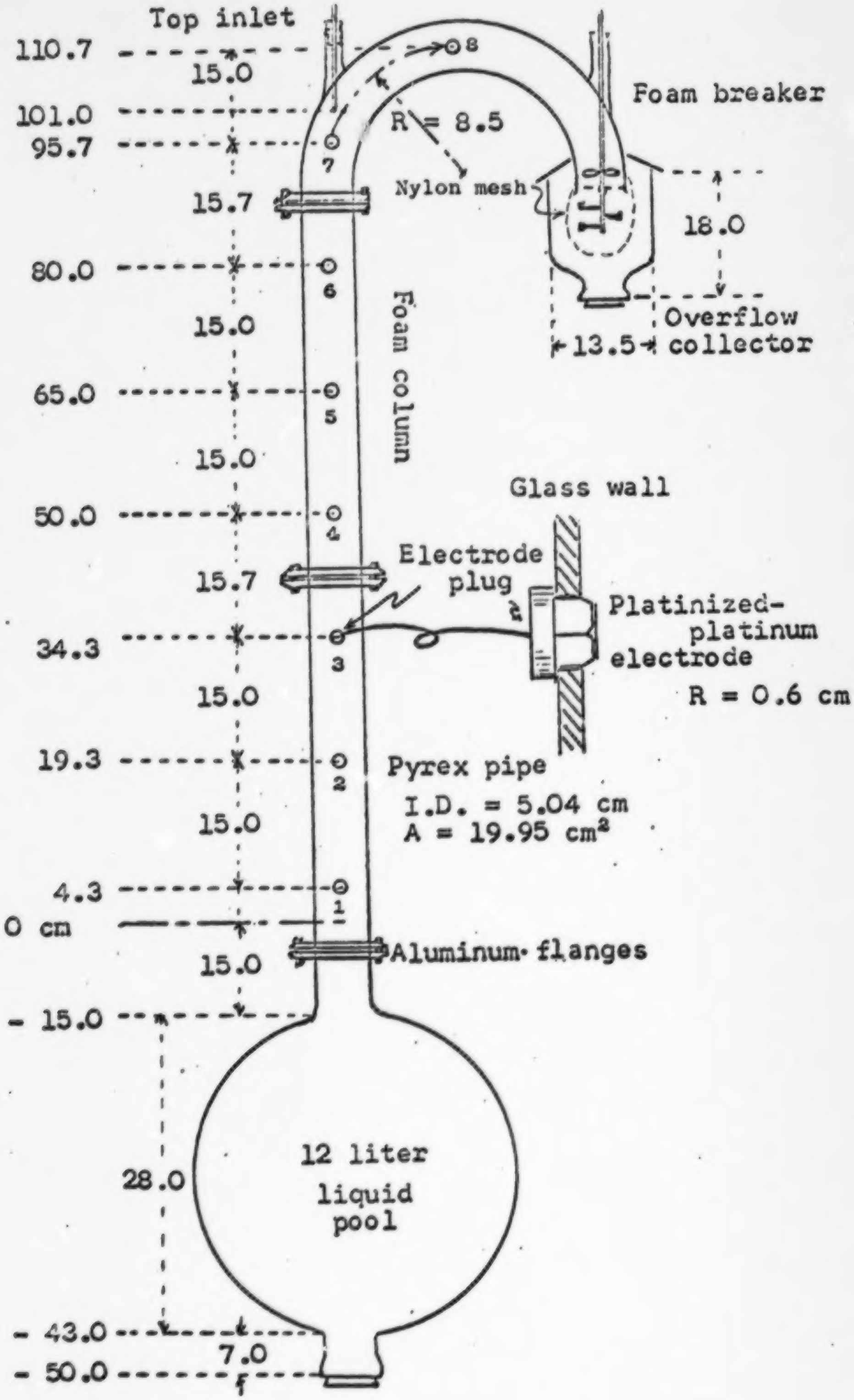
Top inlet
110.7
15.0
101.0
95.7
R = 8.5
8
7
Foam breaker
Nylon mesh
18.0
15.7
80.0
6
15.0
Foam column
Overflow collector
13.5
65.0
5
15.0
Glass wall
50.0
4
Electrode plug
15.7
Platinized-platinum electrode
R = 0.6 cm
34.3
3
15.0
19.3
2
Pyrex pipe
I.D. = 5.04 cm
A = 19.95 cm²
15.0
4.3
1
0 cm
Aluminum flanges
15.0
- 15.0
28.0
12 liter liquid pool
- 43.0
7.0
- 50.0

Figure 1. Foam fractionation column with electrodes.

time against the lowest, and were found to differ by less than 3%.

The foam breaker was of the impeller type, with a variable speed motor. A sack made of nylon mesh (stocking) was hung loosely over the four impellers to further break the foam. Foamate (collapsed foam) dripping from the sack in the collector was passed through a burette for timing its flow rate. It was then returned to the pool at the bottom so as to maintain steady state.

When reflux was employed, part of the foamate was returned to the top of the column via rubber tubing through a Sigmamotor finger pump with an adjustable flow rate. Figure 2 shows the overall experimental setup.

The foam was generated by means of nitrogen gas. This gas was first prehumidified with water in two Rashig-ring packed absorption columns in order to eliminate any spurious evaporative effects in the foaming unit. The gas entered near the bottom of the liquid pool in the flask through one of three bubblers, namely a multi-orificed metal spinneret, an extra course (200 µ opening) sintered glass sparger, and a single glass capillary of 0.6 mm bore. The gas flow rate was measured with a calibrated two-bobbed rotameter.

Bubble sizes in the foam were measured photographically with an Exacta camera fitted with a 2 inch extension tube. Kodak Plus-X film (ASA 125) was employed with a camera setting of f/22 and 1/100 second. Lighting was by means of a 500 watt G.E. photoflood reflector lamp, mounted above the camera, 15 cm from the column at an incident angle of 45°. Care was taken to minimize the duration of exposure of the foam to the resulting thermal radiation.

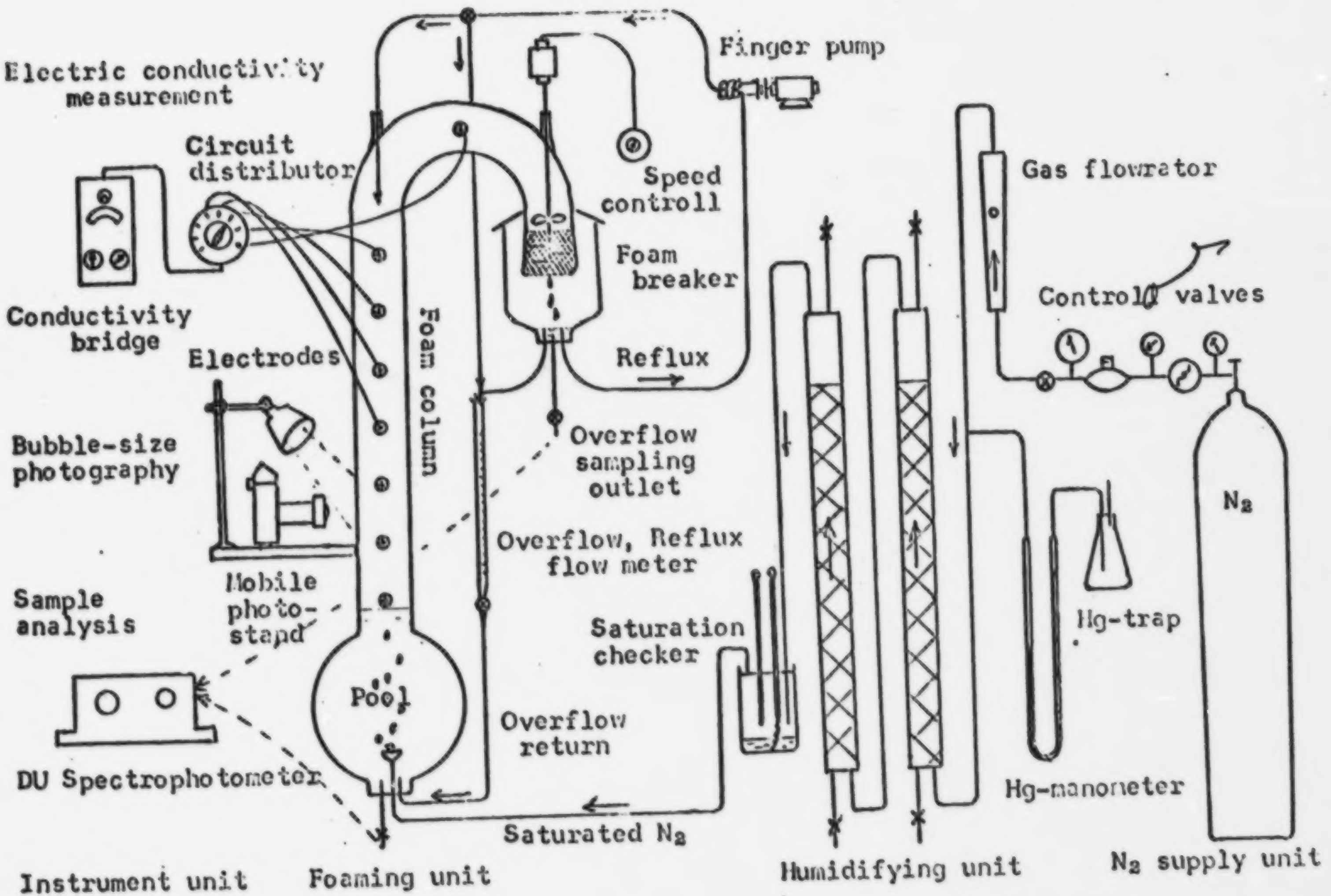
Electric conductivity measurement
Circuit distributor
Conductivity bridge
Electrodes
Bubble-size photography
Mobile photo-stand
Sample analysis
DU Spectrophotometer
Instrument unit
Foam column
Pool
Foaming unit
Speed controll
Foam breaker
Finger pump
Reflux
Overflow sampling outlet
Overflow, Reflux flow meter
Overflow return
Saturated N_2
Saturation checker
Humidifying unit
Gas flowrator
Controll valves
Hg-trap
Hg-manometer
N_2
N_2 supply unit

Figure 2. Experimental setup.

(not to scale)

Besides the major study involving overflowing foam (with and without reflux), some experiments were also conducted with stationary foam. For these, the column was first filled with overflowing foam moving counter-currently to feed trickling down through it from the opening for the reflux inlet. Then the gas was shut off but the feed continued. Local foam densities and bubble sizes in the foam were then measured as with the overflowing foam. The feed rate was also measured. These experiments are termed here "stationary runs". The results of such runs offer another means for examining the details of interstitial flow and drainage.

At the conclusion of some of the stationary runs, the feed was shut off but the foam density measurements were continued. This yielded detailed information regarding the drainage of standing foams in the unsteady state.

Three different systems were employed, namely aqueous solutions of Triton X-100, saponin, and bovine serum albumin. The first (Triton X-100) is a nonionic commercial surfactant. Its aqueous solutions are of low surface viscosity. The second (saponin) is of vegetable origin. Its aqueous solutions are of high surface viscosity. The third (albumin) is of animal origin, and its aqueous solutions are also of high surface viscosity. Thus systems with a wide range of surface viscosities were studied. This was done because surface viscosity is known to have a great effect on foam stability (1,2).

To each aqueous system, KCl was added to bring the concentration of this electrolyte to 0.04 M. This was done to furnish the foam with the necessary electrical conductivity to facilitate measurement of foam density. Control runs showed that the presence of this low concentration of KCl did not affect the foamability or foam overflow rate to any measurable extent. Also, after shaking small amounts of the solution in vials, the appearance of individual thinning films was the same, with or without the KCl. The Triton X-100 solution showed mobile films of low surface viscosity in each case, while the saponin and albumin solutions showed striated "rigid" films of high surface viscosity.

Surfactant concentrations were measured with a Beckman DU spectrophotometer. All experiments were carried out at 25 ± 1°C in a temperature-controlled room.

Results

A total of 109 runs were carried for the three systems. Average bubble diameters ranged from 0.068 to 0.30 cm, gas flow rates from 2.7 to 20.3 cc/sec, and reflux ratios from zero to infinity. Details are being tabulated elsewhere (3).

These results are presently being analyzed. It is too soon to draw final conclusions. However, certain things are already apparent. The most important of these concern the role of surface viscosity.

A high surface viscosity tends to rigidify or immobilize the films. This reduces their rates of thinning and thus increases the stability of the foam by making the films more resistive to rupture.

However, a high surface viscosity does not appear to otherwise greatly affect the rate of foam overflow from a foam fractionation column. In other words, for the same independent variables the rate of foam overflow from the high surface viscosity systems is only moderately greater than that for the low surface viscosity system.

The writer strongly suspects this is due to non-Newtonian behavior of the surface. The back drainage in the foam is chiefly through the interconnecting network of capillaries (Plateau borders). The surfaces of these capillaries are rapidly renewed while those of the films are not. The capillary surfaces are also subjected to greater shear stress. Both of these factors make for non-Newtonian behavior and a lower effective viscosity at the capillary surface. This in turn makes for more back drainage and hence a lower rate of foam overflow than one might otherwise expect.

This tentative conclusion regarding the non-Newtonian behavior of the surface was further verified by the results of the experiments with a feed trickling down through a stationary foam.

In order to obtain a concise quantitative statement of the entire effect, the writer's theory (4,5) for foam drainage and overflow was applied to the experimental data. This theory predicts drainage and overflow without the need for any empirical constants, provided the necessary physical properties are known.

Accordingly, a least squares fit to the data was carried out on an IBM 1620 digital computer, with surface viscosity as the "unknown". The results are summarized in the table below, along with values for films shown for comparison.

Aqueous system	Pool concentration, M	Surface viscosity, dyne sec/cm		
		Foam overflow	Steady drainage	Film mobility
Albumin	1.8×10^{-6} to 1.1×10^{-5}	2.65×10^{-4}	3.07×10^{-4}	10^{-2}
Saponin	3.1×10^{-4} to 8.7×10^{-4}	4.18×10^{-4}	4.64×10^{-4}	10^{-2}
Triton X-100	5.2×10^{-4}	0.84×10^{-4}	1.13×10^{-4}	10^{-4}

It is evident from the third and fourth columns of the table that the effective viscosities in foam of albumin and saponin are higher than Triton X-100. However, they are not nearly so high as shown in the last column which is for individual films. The difference is a quantitative measure of the non-Newtonian behavior of surfaces. The albumin and the saponin are apparently quite non-Newtonian. The Triton X-100, with its simpler molecular structure, is evidently not.

It is also worth pointing out the reasonably good agreement between the third and fourth columns. This evidences the general reliability of the theory and of the experimental results. Good agreement between the theory for foam overflow and the experimental results is also shown by Figure 3. Here, theoretical prediction is plotted against experimental results. The diagonal is the line of theoretical perfection, and the points fall close to it. The standard deviation is 11%.

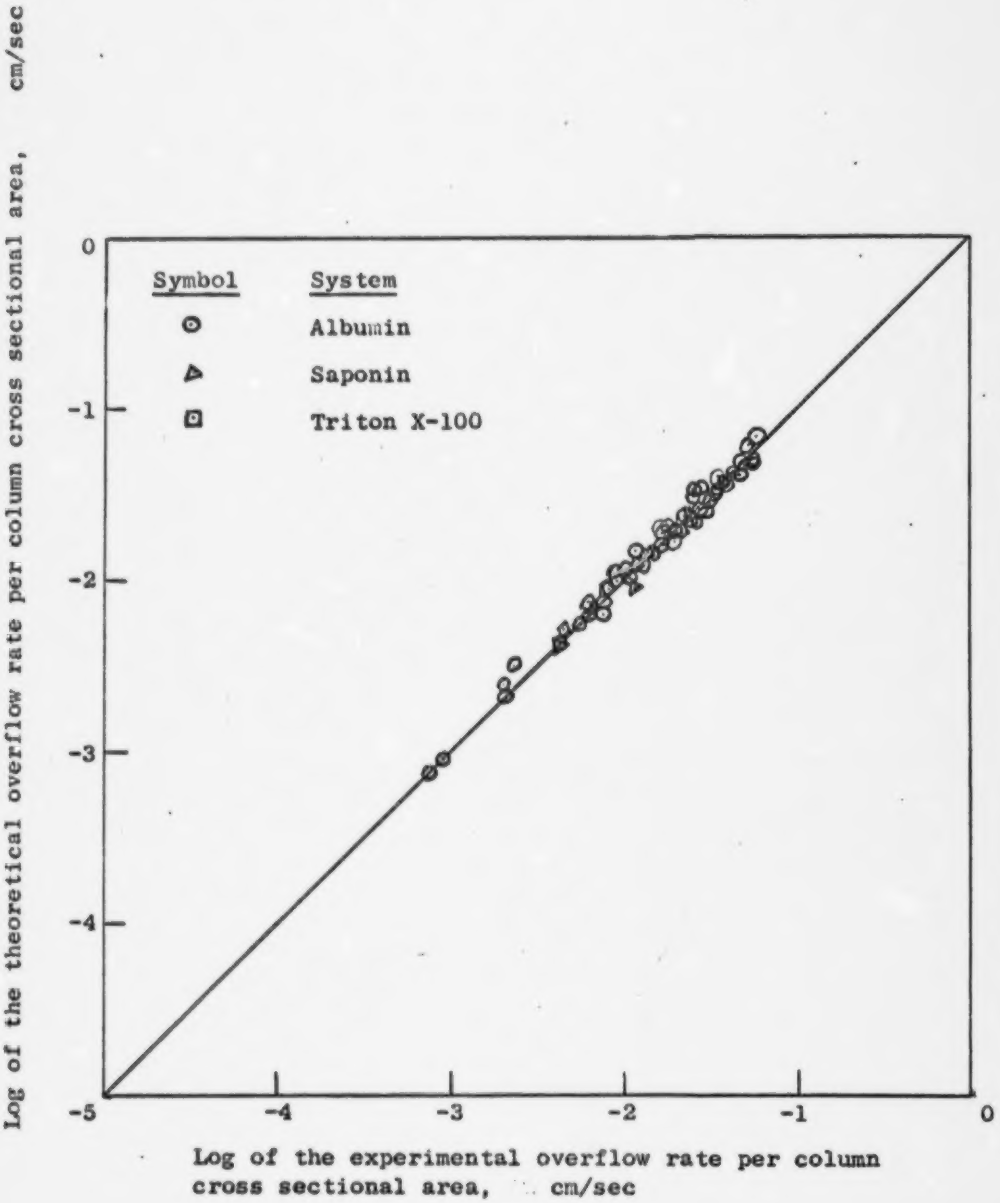

Figure 3. Test of theory (5) for predicting the rate of foam overflow.

Figure 4 shows a test of the theory for drainage through a stationary foam. Here too theoretical prediction is plotted against experimental results, As before, agreement between the points and the diagonal is good, although not as good as for the more important overflow prediction. The standard deviation for Figure 4 is 29%.

Thus, all in all, considering the wide ranges of the variables involved, theoretical prediction accords well with experimental results when the apparent non-Newtonian behavior of the surface is included.

With regard to the density of the foam in the column, the electrical conductivity measurements showed that the density is essentially uniform along the vertical portion of the column provided the foam is stable. This was found to be so for overflowing foam as well as stationary foam fed at steady state. This uniformity accords with theory (4).

The experimental results showed that maximum foam stability was achieved at the higher concentrations of surfactant and at the higher gas rates. The higher the values of these two independent variables, the thicker the films and the more resistive they are to rupture.

At lower values of these variables, coalescence became appreciable up the column. The extent of this coalescence was measured in terms of change in the bubble size distribution up the column and by decrease in the measured foam density up the column.

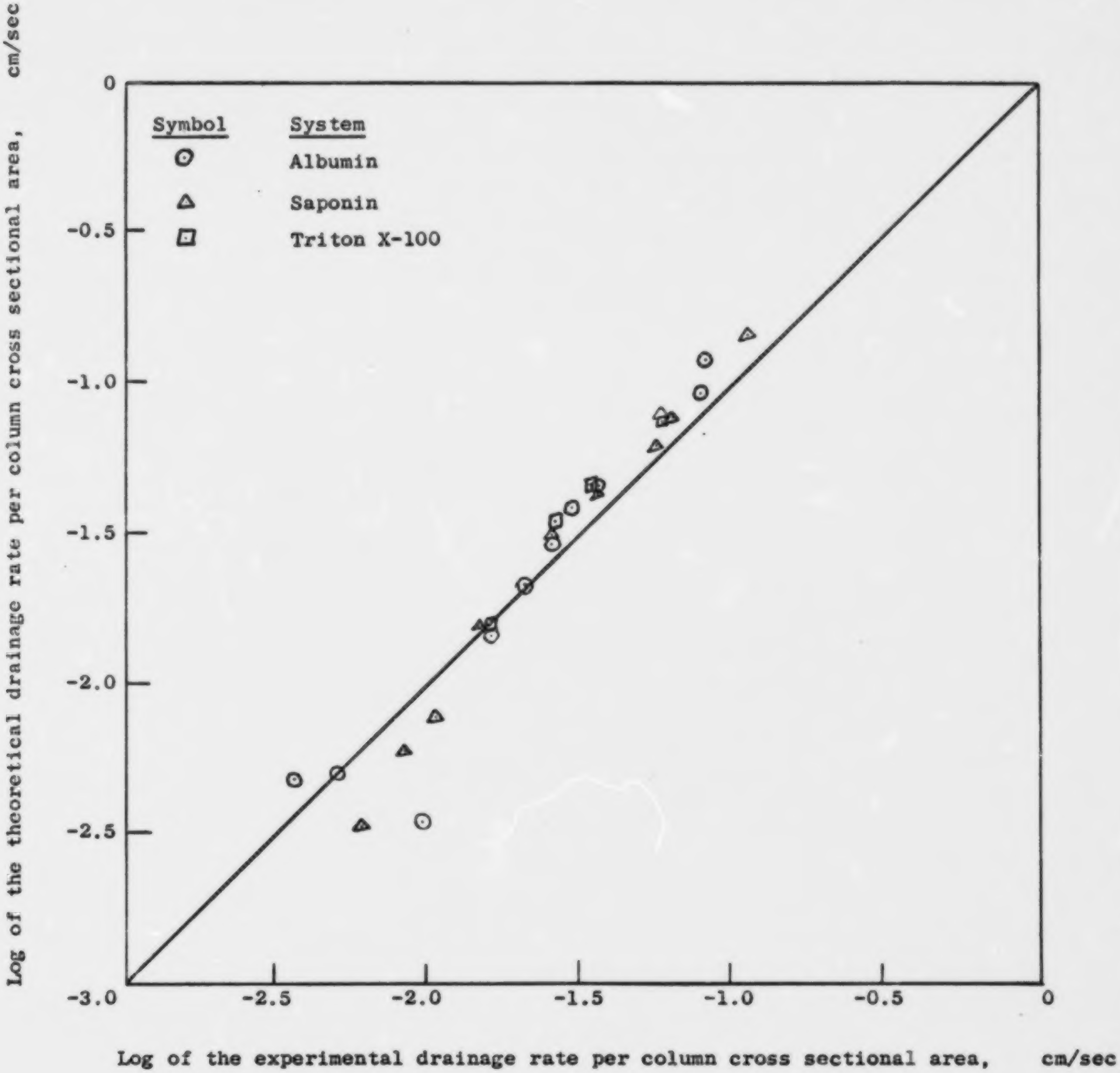

Figure 4. Test of theory (4) for predicting the rate of drainage at steady state through a stationary foam.

Figure 5 shows some typical results. The quantitative cause and effect relationship for these and similar results is under study at this moment.

The Liquid Pool

Normally, the rising gas bubbles in the liquid pool keep it well mixed. As a result, the separation achieved by the pool corresponds to one theoretical stage. However the writer has shown (6,7) that by vertically elongating the liquid pool, more than one theoretical stage can be obtained in the pool. This process has been named "bubble fractionation" (6).

With a foamless (but surface adsorbing) system, bubble fractionation can operate alone. However, it operates more usefully in tandem with the foam fractionation of a foamable system. In other words, it is useful as a booster to foam fractionation.

In an effort to better understand the mechanism operative within the pool, a theoretical analysis of bubble fractionation is currently being developed (8). This analysis extends the writer's existing batchwise theory (9) to continuous flow operation. It also examines the phenomena at the submerged bubble surface and vicinity in terms of potential flow and penetration theory around the upstream portion of the bubble, a renewing wake downstream, and overall material balances. The results of this analysis are not yet complete, but so far appear to be quite illuminating. When complete, the theoretical results will be tested against the experimental results which were obtained in another study (10).

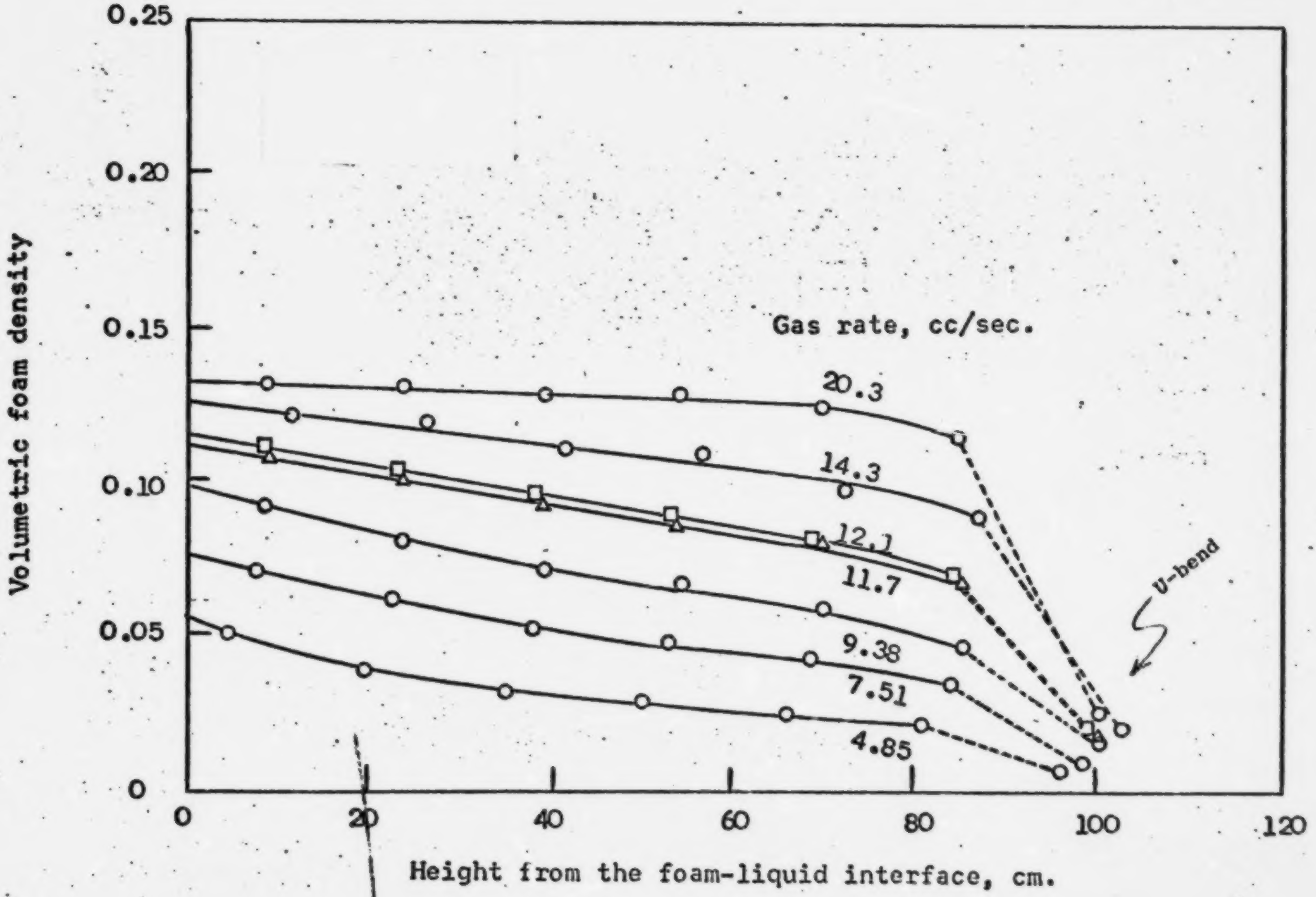

Figure 5. Typical results for the variation of foam density along the column. The last point on each curve is for the conductivity cell in the overhead U-bend. System: Albumin in water with a concentration of 1.8×10^{-6} M in the pool.

The theoretical results are summarized in the appendix which follows:

Appendix

This appendix summarizes the results to date of the new bubble fractionation theory mentioned above. A table of nomenclature and a list of the references cited follow the appendix.

Consider steady state bubble fractionation in continuous flow operation, as shown in Figure 6. A solute balance around the lower end of the column, represented by the dashed loop in Figure 6 yields:

$$L_B c_o + a f \Gamma + B c_B = L_B' c + D_e A_c \frac{dc}{dh} \qquad [1]$$

Both the instantaneous mass balance on the liquid capsule carried with the bubble and the equation for adsorption on the interface are similar to the earlier expressions (9) for batchwise operation.

$$\frac{L_B}{f} \frac{dc}{dh} + a \frac{d\Gamma}{dh} = \frac{k_L a_e}{v_B} (c - c_o) \qquad [2]$$

$$\frac{d\Gamma}{dh} = \frac{k}{v_B} \left(c_o - \frac{\Gamma}{K} \right) \qquad [3]$$

or $$\Gamma = K c_o \qquad [3']$$

Equation 3 and 3' describe reversible adsorption and equilibrium with the adjacent liquid, respectively. The boundary conditions at h = 0 are $c = c_B$ and $\Gamma = 0$. Solutions for four cases were obtained:

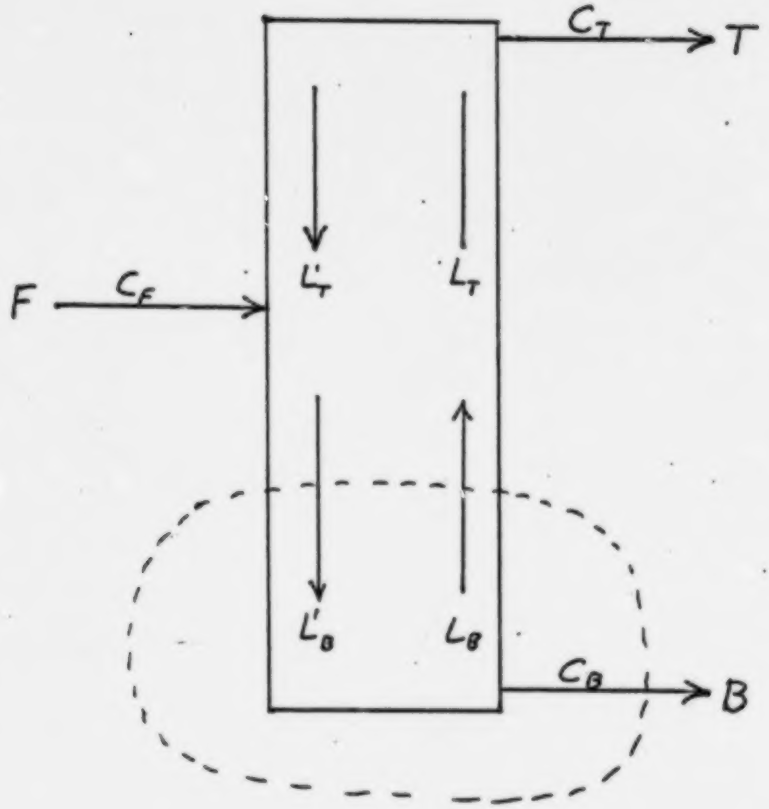
C_T
T
F
C_F
L'_T
L_T
L'_B
L_B
C_B
B

Figure 6. Continuous steady bubble fractionation, showing the material balance envelope over the lower end.

Case I - Axial diffusion negligible compared to gross circulation, and reversible adsorption at the interface.

$$\frac{c}{c_B} = \left(1 - \frac{B}{B - a\rho K}\right)\left(\frac{1}{2\sqrt{\beta^2 + 4\alpha}}\right)\left(\left(\beta + \sqrt{\beta^2 + 4\alpha}\right) \exp\left(\beta - \sqrt{\beta^2 + 4\alpha}\right)\gamma h\right.$$
$$\left. - \left(\beta - \sqrt{\beta^2 + 4\alpha}\right) \exp\left(\beta + \sqrt{\beta^2 + 4\alpha}\right)\gamma h\right) + \frac{B}{B - a\rho K} \qquad [4]$$

where

$$\beta = \frac{k_L a_0}{k a}\left(\frac{L_0'}{L_B} - 1\right) + \left(\frac{L_B'}{L_0} + \frac{L_B'}{a\rho K}\right)$$

$$\alpha = \frac{k_L a_0}{k a}\left(\frac{L_0'}{a\rho K}\left(1 - \frac{L_0'}{L_0}\right) + \frac{L_0'}{L_B}\right)$$

$$\gamma = \frac{-\rho k a}{2 L_0' v_B}$$

Case II - Gross circulation negligible compared to axial diffusion, and reversible adsorption at the interface.

$$\frac{c}{c_B} = \frac{1 + B/a\rho K}{2\sqrt{N^2 + 4M}}\left(N + \sqrt{N^2 + 4M} \exp\left(\frac{-N + \sqrt{N^2 + 4M}}{2}\right) h\right.$$
$$\left. - \left(N - \sqrt{N^2 + 4M} \exp\left(\frac{-N - \sqrt{N^2 + 4M}}{2}\right) h\right)\right) - \frac{B}{a\rho K} \qquad [5]$$

where

$$N = \frac{k}{v_B K}$$

$$M = \frac{k a \rho}{D_e A_c v_B}$$

Case III - Axial diffusion negligible, and equilibrium at the interface.

Stripping section:

$$\frac{C}{C_B} = \frac{K}{a/K - B} \exp\left(\frac{a/K - B}{\mathcal{B}}\right) h - \frac{B}{a/K - B} \qquad [6]$$

Enriching section:

$$\frac{C}{C_T} = \frac{C_F}{C_T} - \frac{T}{a/K + T} \exp\left(\frac{a/K + T}{\mathcal{B}}\right) h - h_F + \frac{T}{a/K + T} \qquad [7]$$

$$\mathcal{B}_{\text{stripping}} = \frac{h_L a_0 / L_B'}{v_B L_B} \left(1 + \frac{Kaf}{L_B}\right)$$

$$\mathcal{B}_{\text{enriching}} = \frac{h_L a_0 / L_T'}{v_T L_T} \left(1 + \frac{Kaf}{L_T}\right)$$

$$h_F = \frac{\mathcal{B}_{\text{stripping}}}{Kaf - B} \log_e \left(\frac{C_F/C_B(Kaf - B)}{Kaf} + B\right)$$

Case IV - Gross circulation negligible, and equilibrium at the interface.

Stripping section:

$$\frac{C}{C_B} = \left(1 + \frac{B}{a/K - B}\right) \exp\left(\frac{a/K - B}{D_e A_c}\right) h - \frac{B}{a/K - B} \qquad [8]$$

Enriching section:

$$\frac{c}{c_T} = \left(\frac{c_F}{c_T} - \frac{T}{1+a/K}\right) \exp\left(\frac{T + Kaf}{D_e A_c}\right)(h - h_F) + \frac{T}{T + a/K} \qquad [9]$$

$$h_F = \frac{D_e A_c}{a/K - B} \log_e \left(\frac{\frac{c_F}{c_B} + \frac{B}{a/K - B}}{1 + \frac{B}{a/K - B}} \right)$$

Equations 7 and 9 were obtained from a material balance around the top of the column above the feed,

$$L_T c_0 + a/\Gamma = L'_T c + D_e A_c \frac{dc}{dh} + T c_T \qquad [10]$$

with the boundary condition $h = h_f$, $C = C_F$. For brevity only the equilibrium case is shown.

The bubble velocity relative to the observer is the sum of the bubble velocity due to its bouyancy, the liquid velocity from the continuous flow, and the basic velocity given to each phase by the displacement effect of the entering gas. This is shown in Equations 11 and 12.

$$v_T = v_0 + T/A_c + G/A_c \qquad [11]$$

$$v_B = v_0 - B/A_c + G/A_c \qquad [12]$$

The present theory was also extended to describe with greater detail the interface and vicinity of the bubble. Liquid passes over the upstream area of the bubble in laminar flow into the renewing turbulent wake in the downstream portion behind the bubble.

An instantaneous solute balance on the liquid flowing around the interface relative to the bubble was made, as shown in the inset figure.

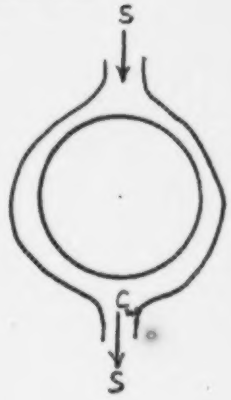

$$\frac{d}{dt}\int \Gamma\, dA\Big)_{\substack{\text{upstream}\\ \text{area}}} + \frac{d}{dt}\int \Gamma\, dA\Big)_{\substack{\text{wake}\\ \text{area}}} + V_w \frac{dc_w}{dt} = S(c - c_w) \qquad [13]$$

Batch operation was considered and a material balance was made around the bottom of the column.

$$Lc + D_e A_c \frac{dc}{dh} = f\left[\left(1 - \frac{v_i}{v}\right)\int_A \Gamma\, dA\Big)_{\substack{\text{upstream}\\ \text{area}}} + \int \Gamma\, dA_w\Big)_{\substack{\text{wake}\\ \text{area}}} \right.$$

$$\left. + c_w\left(V_w\left(1 - \frac{S}{v A_w}\right)\right)\right) \qquad [14]$$

The ratio v_i/v is the fraction of interfacial slip, where v_i is the component of interfacial velocity in the direction of bubble flow relative to the bubble and $S/A_w v$ is the fraction of wake renewal.

To evaluate the surface coverage on the upstream area of the bubble, the equation of motion in spherical coordinates was solved with the assumptions of potential flow.

$$v_r \frac{\partial c}{\partial r} + \frac{v_\theta}{r}\frac{\partial c}{\partial \theta} = D\frac{\partial^2 c}{\partial r^2} \qquad [15]$$

$$\begin{aligned} &\text{I.C.} && \theta = 0 && c = \bar{c} \\ &\text{B.C. 1.)} && r = R && D\frac{\partial c}{\partial r} = \frac{\partial \Gamma}{\partial t} = \frac{v}{R\sin\theta}\frac{\partial \Gamma}{\partial \theta} \qquad [16] \\ &\quad 2.) && r \to \infty && c \to \bar{c} \end{aligned}$$

Interfacial equilibrium is assumed; i.e., $\Gamma = \beta c(R,\theta)$. Diffusion, not adsorption is considered to be the controlling mechanism (12). The result is as follows:

$$\int \Gamma\, dA = \beta\bar{c}\int_0^{\theta_s}\left(1 - \exp\left(\frac{3\ DR}{2v\beta^2}\right)\left(\int_0^{\theta}\sin^3\theta\, d\theta\right)\right.$$
$$\left.\operatorname{erfc}\sqrt{\frac{3\ DR}{2v\beta^2}\int_0^{\theta}\sin^3\theta\, d\theta}\right)2\pi R^2\sin\theta\, d\theta \qquad [17]$$

$$\text{or}\ \int \Gamma\, dA = \beta\bar{c}\ I(\theta) \qquad [18]$$

The equation of motion was also solved using the assumption of the penetration theory:

$$\int \Gamma\, dA = \beta\bar{c}\int_0^{\theta_s}\left(1 - \exp\left(\frac{D\pi R\theta}{\beta^2}\right)\operatorname{erfc}\sqrt{\frac{D\pi R\theta}{\beta^2}}\right)2\pi R^2\sin\theta\, d\theta \qquad [19]$$

Equations 13, 14, and 17 or 18 can be solved simultaneously, first neglecting axial diffusion and secondly gross circulation. The surface coverage in the turbulent wake was considered to be

$$\int_{A_w}\Gamma\, dA_w = \beta c_w .$$

Reproduced from
best available copy.

Case I, neglecting axial diffusion:

$$\frac{c}{c_{\mathcal{B}}} = \exp \frac{s\left(1 - \frac{L-M}{N}\right)}{R + \frac{U(L-M)}{N}} \qquad [20]$$

where

$$M = f\left(1 - v/v_i\right)\mathcal{B}\, I(\theta)$$
$$N = f\left(\mathcal{B} A_w - \left(1 - \frac{s}{A_w v}\right) V_w\right)$$

$$U = V_w + \mathcal{B} A_w$$
$$R = \mathcal{B}\, I(\theta)\, v$$

Case II, neglecting gross circulation:

$$\frac{c}{c_{\mathcal{B}}} = \exp \frac{M+N}{D_e A_c} \qquad [21]$$

and N reduces to $f(\mathcal{B} A_w)$.

Notation

a	total surface area of a bubble	sq.cm.
a_o	surface area of the dragged liquid encapsulating a bubble	sq.cm.
A	upstream area of bubble	sq.cm.
A_c	cross section area of column	sq.cm.
A_w	surface area of a bubble in the turbulent wake	sq.cm.
$\mathcal{B}$	volumetric flow rate of bottom outlet stream	cm^3/sec.
c	solute concentration	g./cm^3.
c_o	solute concentration in capsule dragged by the bubble	g./cm^3.

C_w	solute concentration in wake g./cm^3.
$\bar{c}$	bulk solute concentration g./cm^3.
D_e	axial eddy g./cm.sec.
D	molecular diffusivity g./cm.sec.
f	bubble frequency sec.$^{-1}$
G	volumetric flow rate of gas cm^3/sec.
h	height at any point in column cm.
k	kinetic coefficient g./sec.sq.cm.
k_L	mass transfer coefficient g./sec.sq.cm.
K	equilibrium constant g./sq.cm.
L	volumetric flow rate within the column cm^3/sec.
L'	volumetric flow rate above the feed in a continuous operation column cm^3/sec.
r	radial distance at any point from the center of the bubble cm.
R	radius of a bubble cm.
S	volumetric flow rate around a bubble relative to the bubble cm^3/sec.
T	volumetric flow rate of top outlet stream cm^3/sec.
t	time sec.
v	bubble velocity relative to observer cm./sec.
v_b	bubble velocity due to its bouyancy cm./sec.
V_w	volume of wake cm^3.
v_i	interfacial velocity component in direction of bubble flow relative to the bubble cm./sec.
v_θ	velocity in θ direction around a bubble cm./sec.
v_r	radial velocity around a bubble cm./sec.

Greek

β	adsorption factor cm.
Γ	concentration of solute surface coverage g./cm.^{2}
θ_s	angle measured from top of bubble to point of separation.

Subscripts

B	refers to column below the feed
T	refers to feed
F	refers to column above the feed

Literature Cited

1. Davies, J. T., and Rideal, E. K., "Interfacial Phenomena", Academic Press, New York (1961).

2. Osipow, L. I., "Surface Chemistry, Theory and Industrial Applications" A.C.S. Monograph Series 153, Reinhold, New York (1962).

3. Shih, F. S., "An Investigation to the Effects of Surface Viscosity and Bubble Coalescence in Foam Fractionation", Ph.D. thesis in the process of completion, University of Cincinnati.

4. Leonard, R. A., and Lemlich, R., A.I.Ch.E. Jour. 11, 18 (1965).

5. Fanlo, S., and Lemlich, R., Am. Inst. Chem. Engrs.-Inst. Chem. Engrs. Symp. Ser. (Inst. Chem. Engrs., London) 9, 75 (1965).

6. Dorman, D. C., and Lemlich, R., Nature 207, 145 (1965).

7. Harper, D. O. and Lemlich, R., A.I.Ch.E. Jour. 12, 1220 (1966).

8. Cannon, K. D. "Theoretical Study of Adsorptive Bubble Fractionation", M.S. thesis in preparation, University of Cincinnati.

9. Lemlich, R., A.I.Ch.E. Jour. 12, 802 (1966). Also correction, 13, 1017 (1967).

10. Shah, G. M., "Bubble Fractionation", Ph.D. thesis, University of Cincinnati (1968).

11. Nicklin, D. J., Chem. Eng. Sci. 17, 693 (1962).

12. Farley, R. W., and Schechter, R. S., Chem. Eng. Sci. 21, 1079 (1966).

Note: This paper has been accepted for publication as a chapter in "Progress in Separation and Purification", E. S. Perry, editor, Interscience (1968).

PRINCIPLES OF FOAM FRACTIONATION

by

Robert Lemlich

Department of Chemical Engineering

University of Cincinnati

Cincinnati, Ohio 45221

CONTENTS

I. Introduction

II. Adsorption

- A. Equilibrium
- B. Effect of Micelles on Adsorption
- C. Adsorption Measured through Foam Fractionation
- D. Illustrative Problem #1
- E. Illustrative Problem #2

III. Modes of Column Operation

IV. Typical Column Performance

V. Theory of Column Operation and Performance

- A. Simple Mode
- B. Stripping Mode
- C. Illustrative Problem #3
- D. Illustrative Problem #4
- E. Enriching Mode
- F. Combined Mode
- G. Illustrative Problem #5
- H. Finite Columns
  - 1. Operating lines and equilibrium curves
  - 2. Transfer units
  - 3. Effect of micelles on column performance
  - 4. Column efficiency
- I. Illustrative Problem #6

VI. Bubble Fractionation

(continued)

VII. Foam Drainage and Overflow
    A. Theory
    B. Surface Viscosity and Other Properties
    C. Implications of the Theory
    D. Illustrative Problem #7
    E. Illustrative Problem #8
    F. Experimental Confirmation
VIII. Coalescence
    A. Gas Diffusion
    B. Film Rupture
    C. External Coalescence
IX. Gas Emulsions
X. Closure
XI. Acknowledgement
XII. Notation.
XIII. Literature Cited

I. INTRODUCTION

Foam fractionation is a method of partially separating the components of a solution by virtue of differences in their surface activities. The basic idea behind the operation can be explained in the following way:

Consider an open-topped vessel containing a liquid solution. Whatever might be the composition in the bulk of the liquid, the composition of the surface will usually be different. Thus if the surface molecules could be skimmed off, a partial separation of components could be effected.

Obviously such a procedure would be very awkward. A means for generating greater surface is required. This can be accomplished by deliberately sparging with air or some other gas. The gas is introduced near the bottom of the liquid and bubbles rise to the top. If the system foams, the foam will overflow, carrying off selectively adsorbed solute on the surface of the bubbles.

A schematic diagram representing a simple batch operation is shown in Figure 1a. Simple continuous operation is shown in Fig. 1b. A special case which is discussed later is shown in Fig. 1c. Foam fractionation can also occur "incidentally' as when foam is produced by shaking or by the release of dissolved gas. The difference in composition between beer foam and liquid is an example of the latter.

Quite a number of different solutions have now been successfully foam fractionated. These of course include situations in which the solute to be separated is itself surface active The large-scale removal of detergents from sewage and the laboratory separation of proteins are examples. However foam fractionation has also been used for the separation of non-surface active solutes. This has been accomplished by the addition of a suitable surfactant which either combines with the solute in question or simply adsorbs it at the bubble surface. In either case the solute is then carried off in the foam. A good example here is the removal of trace radioactive cations. An ion or other solute which is not itself surface active, but which is surface adsorbed through the addition of a surfactant, is termed a "colligend" (1). For an extensive compilation of various solutions which have been foam fractionated by one means or another, the reader is referred to the reviews by Schoen (2), Rubin and Gaden (3), Cassidy (4), and Shedlovsky (5). The present chapter deals primarily with the principles of foam fractionation. Some of these have only recently come to light.

Foam fractionation is actually just one member of a group of related separation techniques which are based on selective adsorption at the surface of rising bubbles. Recently the generic name "adsorptive bubble separation methods" was proposed for the group, with "adsubble methods" as a convenient contraction (6).

The sizes of the particles separated in the various adsubble methods range from molecular (and sometimes colloidal) in foam fractionation to macroscopic in the familiar froth flotation (ore flotation). Between these two extremes, and to some extent overlapping them and each other, can be found the methods of ion flotation (1,7), microflotation (8,9), and precipitate flotation (10). Nonfoaming adsubble methods include solvent sublation (1) and bubble fractionation (11).

Needless to say, foam fractionation and the other adsubble methods should never be confused with gas desorption. The latter involves adsorption of volatile material into the interior of the bubbles. The adsubble methods involve adsorption of nonvolatile material at the surface of the bubbles. Furthermore, the adsubble methods can enrich as well as strip. Gas desorption can only strip.

b

II. ADSORPTION

A. Equilibrium

The equilibrium adsorption of dissolved material at a gas-liquid interface is given by Gibbs (12) as Equation 1 where γ is the surface tension, a_i is the activity of the i-th component, $\underset{\sim}{R}$ is the gas constant, T is the absolute temperature, and Γ_i is the surface concentration (sometimes termed "surface excess") of adsorbed component i. Typical units for Γ_i are gm.mol per sq.cm.

$$d\gamma = -\underset{\sim}{R}T\sum\Gamma_i \, d\ln a_i \tag{1}$$

Unfortunately, this equation is often difficult to apply in practice. Generally speaking, it requires knowledge of activity coefficients so as to obtain activities, and precise measurement of surface tension changes which are sometimes very small. As a result, it is usually practical to apply it only in certain special cases. Foremost among these is the case of a single nonionic surface active solute in otherwise pure solvent at sufficiently low concentration that the activity coefficient is constant. A nonionic detergent in water below the critical micelle concentration (c.m.c.) is an example. For this case, Equation 1 simplifies to Equation 2,

$$\Gamma = -\frac{1}{\underset{\sim}{R}T}\frac{d\gamma}{d\ln C} \tag{2}$$

where the concentration of surfactant is Γ at the surface and C in the bulk. Equation 2 has been well confirmed by experiment.

With a simple uni-univalent ionic surfactant, Equation 1 simplifies into Equation 3 below the critical micelle concentration.

$$\Gamma = \frac{-1}{2\underset{\sim}{R}T}\frac{d\gamma}{d\ln C} \tag{3}$$

However, if a considerable excess of one of the ions should be present in solution (due for example to the presence of a salt) the factor of 2 will not appear because C_i for that ion will be constant. Thus Equation 2 will apply instead. Even in the absence of excess ions, experimental results obtained by foaming have not always confirmed the factor of 2 in Equation 3. The reasons for this are not yet clear.

Figure 2 shows the typical shape of a plot of γ versus ln C for a surfactant in water. In accord with Equation 2 or 3, the linear portion of the curve at concentrations below the c.m.c. corresponds to constant Γ. This represents saturation of the surface. Above the c.m.c. Equations 2 and 3 do not apply. The micelles constitute another species. Nevertheless, the bulk of available evidence indicates that essentially the same constant Γ applies above the c.m.c. as well, and the addition of further surfactant goes primarily to the formation of micelles. The entire region of constant Γ is generally believed to represent saturation or complete coverage of the surface with a monolayer.

Figure 3 shows a typical curve for Γ versus concentration. According to simple adsorption theory, the lower portion of the curve is linear and can be expressed by Equation 4.

$$\Gamma = K\ C \tag{4}$$

The upper portion levels off at saturation. For un-ionized material, the entire curve can be approximated by a Langmuir isotherm (13)

$$\Gamma = \frac{K\ C}{1+K'C} \tag{5}$$

where K and K' are constant. Thus K/K' is Γ at saturation. On the basis of the size of the molecules and their close packing at the surface, for many surfactants Γ is approximately 3×10^{-10} gm.mol/cm.^{2} at saturation (14).

The general shape of the curve in Figure 3 often applies not only to the adsorption of a surfactant at the surface but also to the adsorption of a colligend on that surfactant layer. Of course the particular curves will differ one from the other. Also, the adsorption of the particular colligend will be affected by the surfactant concentration (14), especially if micelles are formed since these will compete for adsorption against the surfactant at the surface (1,15). Below the c.m.c. the adsorption of colligend counterions is theoretically unaffected by surfactant concentration provided of course that sufficient surfactant is present to saturate the surface with a surface active monolayer. If the surfactant present is insufficient for this, then K for the colligend counterion is no longer constant but theoretically becomes directly proportional to Γ for the surfactant. However foaming is difficult at such low surfactant concentrations.

The surface adsorption of a colligend through chelation or the formation of some other surface active compound with the surfactant can also be affected by surfactant concentration. It has been suggested that this occurs partly through competition for surface adsorption between the compound on the one hand and the unreacted surfactant on the other (16).

B. Effect of Micelles on Adsorption

It is possible to estimate the effect of micelles on the adsorption of a colligend on a surface active monolayer under equilibrium conditions, assuming a linear isotherm and assuming the surfactant molecules constituting the monolayer are E times as effective in adsorbing the colligend as are the surfactant molecules which constitute the micelles. This is accomplished in the following way:

Let the concentration of unadsorbed colligend counterions be C_1 in the absence of micelles but at sufficient surfactant concentration to assure a surfactant monolayer. Let C_2 be the concentration of unadsorbed colligend counterions in the presence of micelles. Then by Equation 4,

$$\Gamma_1 = K\,C_1 \qquad (6)$$

and

$$\Gamma_2 = K\,C_2 \qquad (7)$$

where Γ_1 and Γ_2 are the concentration of adsorbed colligend counterion at the surface in the absence and in the presence of micelles respectively. In the latter case the ratio of colligend adsorbed at the surface to surfactant adsorbed at the surface is $K\,C_2/\Gamma_s$ where Γ_s is the concentration of surfactant at the surface. Assuming all surfactant added above the c.m.c. goes to the formation of micelles, the quantity of colligend counterion adsorbed by the micelles per unit volume of solution is then $\frac{(C_s-C_{sc})K\,C_2}{\Gamma_s E}$ where C_s is the surfactant concentration in the solution, and C_{sc} is the c.m.c. Striking a mass balance for the colligend counterion in a unit volume of pool liquid yields Equation 8.

$$\frac{(C_s-C_{sc})K\,C_2}{\Gamma_s E} + C_2 = C_1 \qquad (8)$$

The mass balance represented by Equation 8 neglects the adsorption at the surface of the bubbles in the liquid pool since the holdup at the surface is generally small compared to the material in the pool. (If otherwise, Equation 8 can be modified to incorporate the holdup with little difficulty.) Combining Equations 6, 7, and 8, yields

$$\Gamma_2 = \frac{\Gamma_1}{1 + \frac{(C_s-C_{sc})K}{\Gamma_s E}} \qquad (9)$$

Equation 9 gives the effect of the micelles on Γ for the colligend counterion. The effect on the apparent equilibrium constant can be obtained by defining $K = K_1 = \Gamma_1/C_1$ and $K_2 = \Gamma_2/C_1$, and combining these definitions with Equation 9.

The result is $\frac{1}{K_2} = \frac{1}{K_1} + \frac{C_s - C_{sc}}{\Gamma_s E}$.

C. Adsorption Measured through Foam Fractionation

For a surfactant, or for a colligend adsorbed on the surfactant layer, Γ can be found by foam fractionating in the simple mode. In the foam, the component in question is partly in the interstitial liquid and partly adsorbed at the bubble surfaces. For spherical bubbles of various diameter d_i, each present in proportion to the number n_i, the rate of surface overflow in the foam is 6G/d where G is the volumetric gas flow rate and d is determined according to Equation 10.

$$d = \frac{\sum n_i d_i^{3}}{\sum n_i d_i^{2}} \qquad (10)$$

Thus the rate of overflow of the component in the adsorbed state is $6G\Gamma/d$.

If there is no bubble coalescence in the foam, the concentration in the interstitial liquid will be essentially that in the liquid pool, C_W. Thus, from the foregoing,

$$C_Q Q = C_W Q + 6G\Gamma/d \qquad (11)$$

where Q is the volumetric rate of foam overflow on a gas-free (collapsed) basis, and C_Q is the concentration in the collapsed foam. Rearranging yields Equation 12 (17).

$$\Gamma = (C_Q - C_W)\,\frac{Qd}{6G} \qquad (12)$$

Thus, from measurements of Q, d, G, C_Q, and C_W, Γ can be found.

Figure 4 shows some apparatus for making such measurements which was dedeveloped during the course of the author's work (17). It is a foam fractionation column operating in the simple mode according to Figure 1c, with return of collapsed foam to the bottom in order to maintain steady state conditions in a convenient manner. The feed inlet is located near the bubbler to counteract local depletion of adsorbable material in the pool. However, if the surfactant concentration in the return stream should be above the c.m.c. and the micelles should be too slow to dissociate upon subsequent dilution in the liquid pool, then any adverse adsorptive effect by such micelles can be avoided by not returning the collapsed foam and feeding the pool with fresh feed instead. Alternatively, but somewhat less satisfactorily, a short batchwise run can be conducted with a liquid pool large enough to maintain a sufficiently constant concentration throughout the run.

Prehumidified nitrogen is used in order to avoid any spurious evaporative effects. A very low height of foam is employed to reduce foam residence time so as to minimize coalescence within the foam. A substantial gas rate also helps, partly by reducing foam residence time and partly by producing a wetter foam (meaning a foam of higher liquid content) which is less likely to coalesce. Such internal coalescence not only alters bubble sizes but releases adsorbed material into the interstitial liquid, some of which drains back down to the pool. This reduces the applicability of Equations 11 and 12. It may also set up an undesirable local concentration gradient below the pool surface. The sum of these errors inclines toward a falsely high Γ. If necessary, in order to minimize any vertical concentration gradient in the liquid pool, the column can be widened to encourage pool mixing. Then with sufficient pool height to assure a close approach to equilibrium between bubble surface and pool liquid, and with negligible coalescence within the rising foam, the apparatus operates essentially as a one-theoretical-stage separator.

At low concentrations of surfactant, the foam is especially unstable and so is allowed to overflow freely from the column into the inverted Erlenmeyer flask where it is easily broken by gently stirring with a bent rod. Any bends or constrictions would have promoted excessive internal coalescence by straining the foam thus rupturing bubbles. For high concentrations of surfactant, this is less serious and gentle bends may be tolerated. However sharp constrictions are not employed until the foam has passed over its highest point so that internal coalescence induced by the constrictions will not cause liquid to drain back through the rising foam. The stable foam overflow produced by a high concentration of surfactant is conveniently broken by being whirled through a spinning perforated can inside a large inverted plastic bottle.

Bubble diameters are measured either optically or photographically. This is convenient to do through the glass walls of the column. However there are certain sources of error which should be recognized. The foam bubbles distort somewhat at the walls. There is also the question of whether the local distribution of bubble sizes at the wall is the same as that in the interior of the foam. Finally, even if it is, observations at the wall (or at any plane, even one cut through frozen foam) are not representative of the bubble distribution as a whole because the plane tends to miss the smaller bubbles and hit the larger ones. These points are considered in detail by de Vries (18).

Fortunately, much of the difficulty can be obviated by selecting a sparger (bubbler) which gives bubbles of fairly uniform size. To this end, a fritted glass bubbler should not be used. Rather, a group of carefully matched capillary tubes or a good spinneret should be employed. Except for its low capacity, a single short capillary tube is best of all.

Bubble diameters can be optically or photographically measured in the liquid pool. Optical distortion due to curvature of the glass can be avoided by immersing the lower part of the column in an external pool of liquid with flat glass walls.

Γ can also be measured by operating continuously in the simple mode as shown in Figure 1b. Experimentally, this is somewhat more cumbersome than the recyclic operation of Figure 1c. However, recycle of micelles is avoided and Equation 16, which is derived later, can be applied to find Γ. Furthermore, if internal coalescence is a problem, the very similar Equation 24 can be applied with the bracketed term approximated by the constant 6.3. This is discussed later.

The reader is referred to the author's publication for further details (17). For a discussion of chemical equilibrium between surface and bulk, the reader is referred to Sebba (1).

D. Illustrative Problem #1

Statement:

A continuous foam fractionation column is operating in the simple mode with 4 cm^3/sec. of prehumidified nitrogen. Collapsed foam, which is collected overhead at the rate of 0.2 cm^3/sec. contains 5×10^{-7} gm.mol/cm^3 of surfactant and 5×10^{-12} gm.mol/cm^3 of a colligend counterion. The average bubble size according to Equation 10 is 0.1 cm. Liquid withdrawn from the pool contains 2×10^{-7} gm.mol/cm^3 of surfactant and 2×10^{-13} gm.mol/cm^3 of the colligend. If internal coalescence is negligible, estimate the surface concentration for the surfactant and for the colligend.

Solution:

Applying Equation 12 to the surfactant,

$$\Gamma = \frac{(5\times10^{-7}-2\times10^{-7}) \times 0.2 \times 0.1}{6 \times 4}$$

$$\Gamma = 2.5 \times 10^{-10} \text{ gm.mol surfactant per cm}^2$$

Now applying Equation 12 to the colligend,

$$\Gamma = \frac{(5\mathrm{x}10^{-12}-2\mathrm{x}10^{-13}) \times 0.2 \times 0.1}{6 \times 4}$$

$$\Gamma = 4 \times 10^{-15} \text{ gm.ion per cm}^2$$

E. Illustrative Problem #2

Statement:

For the system of the previous problem, if the critical micelle concentration of the surfactant is 7 x 10^{-7} gm.mol/cm^3., estimate the surface concentration of the adsorbed colligend when the concentration of the surfactant in the solution is 9 x 10^{-7} gm.mol/cm^3. Assume the surfactant molecules that constitute the micelles are equally effective in adsorbing colligend as are the surfactant molecules that constitute the surface monolayer.

Solution:

For this system, E = 1. From Equation 6 and the results of the previous problem,

$$K = \frac{\Gamma_1}{C_1} = \frac{4 \times 10^{-15}}{2 \times 10^{-13}} = 0.02 \text{ cm.}$$

Substituting in Equation 9,

$$\Gamma_2 = \frac{4 \times 10^{-15}}{1 + \frac{(9\mathrm{x}10^{-7}-7\mathrm{x}10^{-7}) \times 0.02}{2.5 \times 10^{-10}}}$$

$$\Gamma_2 = 2.35 \times 10^{-16} \text{ gm.ion per cm}^2$$

III. MODES OF COLUMN OPERATION

A foam fractionation column can be operated in several modes. These include the simple mode which has already been discussed, the stripping mode, the enriching mode, and the combined mode. For comparison, the four modes are shown for continuous operation in Figure 5.

In the stripping mode, feed enters the foam some distance above the liquid pool and trickles down countercurrently through the rising foam. This tends to replace interstitial liquid of pool composition with interstitial liquid of feed composition. The overall result is an improvement in the degree of stripping. Quantitatively, this is expressed as an increase in the decontamination factor C_F/C_W or a decrease in the stripping ratio C_W/C_F, where C_W is the concentration in the pool or bottoms and C_F is the concentration in the feed.

It is interesting to note that stripping operation can be so successful in removing surfactant that insufficient remains to properly remove the colligend if any. In such event some additional surfactant can be added to the pool.

The enriching mode involves the use of reflux. A portion of the collapsed overhead is fed back to the top of the column. From there it trickles back down through the rising foam. Since the reflux is much richer than the rising interstitial liquid, the mass transfer resulting from this countercurrent action can greatly cascade the enrichment and yield a much higher concentration in the overhead product than would be obtainable without reflux (19).

If D is the rate at which net overhead product is withdrawn, RD is the rate of reflux flow, where R is the reflux ratio. R can vary from zero (no reflux -- simple mode) to infinity (total reflux). By simple material balance, $Q = (R+1)D$.

C_D is defined as the concentration in the net overhead product. Thus $C_D = C_Q$. The enriching ratio C_D/C_F is a useful measure of the degree of enrichment.

Figure 5 shows the use of external reflux. However this is not the only source of reflux. Bubble coalescence in the rising foam releases adsorbed material plus some liquid, both of which drain back down through the foam. This constitutes internal reflux. Indeed, some internal coalescence, and hence some internal reflux, is nearly always present in foam fractionation.

Internal reflux can be deliberately increased by widening the column, either along its entire length or just for some distance at the top. This slows the linear rate of foam rise and so permits more thorough drainage of interstitial liquid. This drainage does not itself represent true (useful) reflux. However, it does increase the concentration in the overhead product by reducing the liquid content. It also thins the films separating bubbles. Widening increases their residence time in the column. Both of these effects make for more frequent film rupture in the column. The resulting coalescence releases enriched liquid which constitutes true reflux.

For columns of large diameter, an expanded section at the top may not prove satisfactory if some foam forms pockets in the expanded section thus forcing the rest of the foam to pass through without slowing down sufficiently. In such a situation, Haas and Johnson (20) recommend a horizontal drainage section instead.

Of course lengthening the column is another means for encouraging internal coalescence and reflux by increasing the residence time. The greater length also furnishes increased opportunity for countercurrent contact between the internal streams thus increasing the overall enrichment.

In batch operation, a long column with internal coalescence can be employed to effect the separation of a complex mixture into fractions according to differences in surface activity. This is accomplished by first running the column for a while with a gas rate just sufficient to drive the foam up nearly to the top of the column. Under these conditions the rate of foam generation just balances the rate of internal coalescence, and the column operates under total internal reflux.

The gas rate is then raised very slowly and successive fractions of foam are collected separately. The essentially complete removal of a component is sometimes signaled by a sudden drop in foam height within the column. In any case, the gas rate is continually raised until no more foam comes off. The last bit of foam, which is too unstable to reach the top, can be collected from one or more ports lower down the column. The final overall result is a separation into fractions, the sharpness of which depends in part on the composition of the original charge, the height of the column, and the control of the gas rate.

The enriching mode and the stripping mode can be combined to furnish the advantages of both. The resulting combined mode is shown in Figure 5 for continuous operation.

IV. TYPICAL COLUMN PERFORMANCE

Figure 6 shows some apparatus employed by the author (21) to study typical overall column performance. The column was of glass, 174 cm. tall, with an internal diameter of 4.8 cm. The liquid pool comprised approximately 110 cm. of this height. Foam filled the remaining 64 cm. and overflowed into a rotary foam breaker. Reflux was returned through a multichannel pump. Net overhead product and bottoms were withdrawn through other channels of the pump.

Feed consisted of a 2.2×10^{-4} molar aqueous solution of the commercial surfactant Triton X-100 which has the nominal formula $C_8H_{17}-C_6H_4-(OCH_2CH_2)_{9.7}OH$. It was fed through one channel of the pump at the rate of 32 cm^3/minute to one of three feed locations.

A factorial group of nine runs were conducted with the feed entering the liquid pool 5 cm. below the foam-pool interface. Results are shown in Figures 7 and 8. (The original reference shows the origin and unity as lower limits for Figures 7 and 8 respectively. However this is not necessarily the case.)

Figure 7 reveals that increasing the gas rate decreases C_W/C_F; that is, it improves the degree of stripping. Higher gas rates generate more surface per unit time and so carry up adsorbed surfactant more rapidly. However increasing the reflux ratio is of little effect on stripping. On the other hand, increasing the reflux ratio greatly increases enrichment, as is to be expected. At total reflux the surfactant concentration in the overhead was approximately 70 times that in the feed. This is shown in Figure 8. This figure also reveals that increasing the gas rate decreases the enrichment. A high gas rate means a wetter foam, and hence more carryover of interstitial liquid as well as less internal reflux. R in Figures 7 and 8 refers only to the external reflux.

Lowering the feed inlet to a point approximately midway up the liquid pool was of only slight effect. However raising it to a level 16 cm. above the foam-pool interface improved the stripping considerably. This follows from the countercurrent action mentioned earlier. The subject of countercurrent action is further discussed later.

V. THEORY OF COLUMN OPERATION AND PERFORMANCE

It is possible to make certain quantitative predictions regarding the performance of foam fractionation columns.

A. Simple Mode

As shown earlier, Equation 11 applies to operation in the simple mode. Rearranging that equation gives

$$C_Q = C_W + \frac{6\ G\ \Gamma_W}{Q\ d} \qquad (13)$$

where the subscript in Γ_W is added to emphasize that Γ_W is in equilibrium with C_W. By overall mass balance for continuous operation,

$$F = Q + W \tag{14}$$

and

$$C_F F = C_Q Q + C_W W \tag{15}$$

Combining Equations 13, 14, and 15 yields Equation 16 for continuous operation in the simple mode (22).

$$C_W = C_F - \frac{6\ G\ \Gamma_W}{F\ d} \tag{16}$$

B. Stripping Mode

For a long stripping column; that is, one in which the feed enters the foam at a sufficient height above the pool, the downflowing interstitial liquid may closely approach equilibrium with the rising interstitial liquid. The concentration pinch will occur at the feed level. The rising interstitial liquid at the top of the column will have a concentration of C_F (if internal coalescence above the feed inlet is negligible). Replacing C_W in Equation 11 with C_F, replacing Γ with Γ_F, and replacing the constant 6 with 6.59 (for reasons stated later) gives

$$C_Q = C_F + \frac{6.59\ G\ \Gamma_F}{Q\ d} \tag{17}$$

where Γ_F is the surface concentration in equilibrium with C_F. A height of several feet is often sufficient to assure a close pinch. Combining Equations 14, 15, and 17 yields Equation 18 for a long stripping column (22).

$$C_W = C_F - \frac{6.59\ G\ \Gamma_F}{W\ d} \tag{18}$$

Since W must be less than F, and Γ_F cannot be less than Γ_W, it is clear that C_W from Equation 18 must be lower than C_W from Equation 16. With Γ a known function of C, the comparison permits one to estimate how much further the bottoms can be purified by stripping operation as compared to simple operation.

The small change in the constant was made for the following reasons:

Reproduced from best available copy.

The original constant 6 is based on spherical bubbles. In a well-drained foam the bubbles press against each other and are therefore more polyhedral. This is especially so with bubbles of uniform size. Within the foam, the dodecahedral shape predominates (23,24,25). (This may not seem so under casual observation through a glass retaining wall. However it must be borne in mind that at the glass the bubbles are connected to a continuous wall and not just to each other.) For a regular dodecahedron the ratio of surface to volume is 6.59/d. Accordingly, the constant in Equations 17 and 18 is more properly 6.59.

However, no such change is made for the simple mode. The constant remains 6 in Equations 11, 12, 13, and 16. This is because here the additional surface adsorption, which occurs after the spherical bubbles leave the pool and distort to form polyhedral bubbles in the foam, occurs at the expense of material already in the interstitial liquid. In the simple mode this liquid is not replaced by any fresh incoming stream. Accordingly, the incremental adsorption resulting from the distortion contributes no net increase to the upflow of material. Therefore the constant 6 remains unchanged for the simple mode.

The preceding equations, as well as those to follow, must not be used beyond the range of reason. For example, indiscriminate substitution of numbers could yield negative values for C_W. This of course would be absurd.

C. Illustrative Problem #3

Statement:

A foam fractionation column operating continuously in the simple mode gives a decontamination factor of 4.0 for the removal of a particular detergent from water under a certain set of conditions wherein the foam overflow rate (on a gas-free basis) is 0.05 times the feed. Under similar conditions, what should the decontamination factor theoretically be for highly efficient stripping?

Solution:

Rearranging Equation 16,

$$1 - \frac{C_W}{C_F} = \frac{6\ G\ \Gamma_W}{FC_Fd}$$

Rearranging Equation 18,

$$1 - \frac{C_W}{C_F} = \frac{6.59\ G\ \Gamma_F}{WC_Fd}$$

Assuming Γ is constant (meaning the adsorbed detergent forms a saturated monolayer), and then dividing the second equation by the first while noting that $W = 0.95F$ here, yields upon substitution of the given decontamination factor

$$\frac{1 - \left(\frac{C_W}{C_F}\right)_{strip}}{1 - \frac{1}{4}} = \frac{6.59}{6 \times 0.95}$$

Solving, $\left(\frac{C_F}{C_W}\right)_{strip} = 7.5$ which is the theoretical decontamination factor for stripping operation. Of course it must be borne in mind that in changing from the simple mode to the stripping mode, "similar conditions" may be difficult to achieve in practice. In particular, the lower C_W for stripping may make for a higher surface tension and hence a larger d.

D. Illustrative Problem #4

Statement:

The system of the previous problem also contains a colligend counterion which is present at a trace level of concentration. For this colligend the decontamination factor is 1.8 for continuous operation in the simple mode. Under similar conditions, what should it theoretically be for highly efficient stripping?

Solution:

Since the concentration is very low, the adsorption isotherm should be linear. Therefore, from Equation 4, $\Gamma_W = KC_W$ and $\Gamma_F = KC_F$.

Rearranging Equation 16 and substituting for Γ_W,

$$\frac{C_F}{C_W} - 1 = \frac{6\ G\ K}{F\ d}$$

Rearranging Equation 18 and substituting for Γ_F,

$$1 - \frac{C_W}{C_F} = \frac{6.59\ G\ K}{W\ d}$$

Noting that W = 0.95F here, substituting the given decontamination factor for the simple mode, and dividing the second equation by the first, yields

$$\frac{1 - \left(\frac{C_W}{C_F}\right)_{strip}}{1.8 - 1} = \frac{6.59}{6 \times 0.95}$$

Solving, $\left(\frac{C_F}{C_W}\right)_{strip}$ = 13.3 which is the theoretical decontamination factor for stripping operation.

E. Enriching Mode

Figure 9 shows the flow of material for that portion of an enriching column which is situated above the liquid pool. This portion is of course the foam. Q' is the rate of the upward flowing interstitial liquid leaving the pool. S is the surface to volume ratio for a foam bubble, namely 6/d for a sphere or 6.59/d for a regular dodecahedron. C_L is the concentration in the downflowing interstitial liquid just before it enters the liquid pool, and C_D is the concentration in the collapsed foam product overhead.

A material balance over the envelope shown in Figure 9 yields Equation 19 (17).

$$\frac{C_D}{C_W} = \frac{(R+1)G\,S\,\Gamma_W}{Q\,C_W} + \frac{C_L}{C_W} + \frac{(R+1)Q'(1-C_L/C_W)}{Q} \tag{19}$$

As was the case for the stripping column, if the enriching column is sufficiently long the downflowing interstitial liquid may closely approach equilibrium with the rising interstitial liquid. The pinch will occur just above the liquid pool. Then $C_L = C_W$ and Equation 19 reduces to Equation 20 (17).

$$C_D = C_W + \frac{G\,S\,\Gamma_W}{D} \tag{20}$$

Careful consideration shows that here the incremental adsorption due to the distortion of bubbles from spheres to dodecahedra can only be partly compensated from the downflowing liquid (reflux). Said analysis shows that effectively $S = \left(6.59 - \frac{0.59}{R+1}\right)\frac{1}{d}$. Substituting in Equation 20 yields Equation 21 for long enriching columns (22).

$$C_D = C_W + \left(6.59 - \frac{0.59}{R+1}\right)\frac{G\,\Gamma_W}{D\,d} \tag{21}$$

The range of the bracketed coefficient is only 6 to 6.59 over the entire possible R range of 0 to ∞.

It is worth noting that Equation 13 is a special case of Equation 21. Also, since $D = \frac{Q}{R+1}$, it is evident that the use of reflux can greatly increase the degree of enrichment.

If the pool is fed continuously at rate F and bled continuously at rate W, an overall balance states that

$$F = D + W \tag{22}$$

and

$$C_F F = C_D D + C_W W \tag{23}$$

Combining Equations 21, 22, and 23 gives Equation 24.

$$C_W = C_F - \left[6.50 - \frac{0.59}{R+1}\right] \frac{G\,\Gamma_W}{F\,d} \qquad (24)$$

Comparison with Equation 16 which was derived from the simple mode confirms that, unlike the situation for enrichment, the use of reflux does little to improve the degree of stripping. However, for a given C_W and C_F the use of reflux does reduce D/F. This can be of value.

The various equations developed for the several modes apply to the surfactant as well as to any colligend present. As mentioned earlier, Γ for surfactant can usually be taken as fixed.

Under some conditions, C_D may exceed the critical micelle concentration. Thus micelles may be present in the reflux. These of course would not adversely affect Γ or C_D for the surfactant. Interestingly enough, for a sufficiently long column, theoretically the micelles should not affect C_W or C_D for any colligend either! In fact, for such a column there should be no overall effect at all. To be sure, the micelles may shift the equilibrium adversely, but by the analysis leading to Equation 21 the overall performance of a sufficiently long enricher should not be affected by the shift. In such an enricher, any micelles in the downflowing interstitial liquid are all transferred to the rising interstitial liquid by the time the downflowing liquid reaches the pool. The transferred micelles are then carried up and out the top where a portion of them are continuously bled off in the net overhead product.

The upflowing interstitial stream is larger than the downflowing interstitial stream. This means that any pinch must occur at the start of the upflowing interstitial stream. This can be shown in several ways, including an analogy with an equivalent proof based on the Second Law of Thermodynamics for a long counterflow water-to-water heat exchanger (26). The upflowing stream originates from the pool and so at its start has a concentration of C_W

in the interstitial liquid and Γ_W at its surface.

Of course the immunity to the effect of micelles does not extend to short columns. For such columns any adverse shift in equilibrium must be balanced off against the beneficial cascading effect of reflux. However, even in such cases, the net effect of using reflux may still be very favorable to the enrichment. Naturally, for the surfactant itself, no adverse effect would be expected at all. Short columns will be considered in some detail later.

F. Combined Mode

For a long combined column; that is, a column consisting of a sufficiently long stripping section and a sufficiently long enriching section, the concentration pinch between the counterflowing streams will occur at the level of the feed. So, by means of an analysis similar to that which preceded, Equation 25 is obtained for a long column operating continuously in the combined mode (22).

$$C_D = C_F + \frac{6.59\ G\ \Gamma_F}{Dd} \tag{25}$$

Equation 17 is a special case of Equation 25. Combining Equation 25 with an overall balance gives

$$C_W = C_F - \frac{6.59\ G\ \Gamma_F}{Wd} \tag{26}$$

Equation 26 is identical with Equation 18.

G. Illustrative Problem #5

Statement:

A continuous foam fractionation column is to operate in the combined mode to remove and concentrate a surfactant, which has a surface concentration of 3×10^{-10} gm.mol/cm^2, from a feed containing 5×10^{-7} gm.mol/cm^3 of the surfactant. The ratio of gas rate to total collapsed overflow rate is to be 30. With a properly averaged bubble diameter of 0.2 cm, what is the richest overhead that can be expected for a reflux ratio of 10?

Solution:

The richest overhead would be obtained with a very long column.

Substituting Q = (R+1)D into Equation 25 gives

$$C_D = C_F + \frac{6.59(R+1)G\Gamma_F}{Qd}$$

G/Q is given as 30. Substituting numerical values,

$$C_D = 5 \times 10^{-7} + \frac{6.59(10+1)30\times3\times10^{-10}}{0.2}$$

$C_D = 3.76 \times 10^{-6}$ gm.mol/cm^3. maximum.

H. Finite Columns

At this point, the question naturally arises as to how long a column must be in order to qualify as "sufficiently" long. Unfortunately, no general answer can be given short of infinity. Too many factors are involved. At modest reflux ratios, a height of several feet may give a reasonably close approach. At higher reflux ratios, a much greater height may be needed. The author's experience with aqueous solutions of the commercial anionic surfactant Aresket-300 showed roughly a 90% approach to theoretical C_D/C_W at reflux ratios in the neighborhood of 2 with an enriching column 100 cm. tall (17). Roughly comparable results were obtained with Triton X-100 (27).

1. Operating lines and equilibrium curves

The foregoing equations for long columns can be viewed as limiting equations. Actual performance for short columns can be examined from the familiar points of view which have been established for contacting operations in general. These include the concepts of the theoretical (perfect) stage and the transfer unit (28).

For stripping assemblies, an equilibrium curve of Γ versus C has been used in conjunction with an operating line of slope $\frac{\Delta\Gamma}{\Delta C} = \frac{F}{GS}$ (20,21). This implies $GS\Delta\Gamma = F\Delta C$. Such an equality neglects changes in the solute content of the upflowing interstitial liquid. For some situations this approximation is quite satisfactory. However, for other stripping conditions and for refluxing columns (enriching or combined), the approximation may lead to significant error. When the surface is saturated with the substance in question (as for example a surfactant) the method breaks down completely. For these reasons the present author prefers a different approach which takes into account the material in the upflowing liquid. This approach is outlined next.

Consider the counterflowing streams at some level within a continuous foam fractionation column which may be a stripper, an enricher, or a combination of both. Let the upflowing stream rate be U, and let the concentration in the upflowing interstitial liquid be C. The upflowing rate of the pertinent component is then $UC + GS\Gamma$. Define an effective stream concentration $\bar{C}$ such that $U\bar{C} = UC + GS\Gamma$. Then,

$$\bar{C} = C + \frac{GS\Gamma}{U} \tag{27}$$

The upflowing interstitial liquid at any level in the column is assumed to be in equilibrium with the upflowing surface at that level. (While this assumption may not be exact, it is clearly more realistic than ignoring the liquid upflow entirely!) Γ can now be related to C from a known equilibrium relationship such as Figure 3. Then, with S as say 6.59/d, $\bar{C}$ is computed for various values of C at the G/U ratio involved. $\bar{C}$ is then plotted against C to give a new equilibrium diagram.

For the important special case of the linear isotherm, Equation 4 applies. The new equilibrium curve is therefore a straight line through the origin, namely

$$\bar{C} = \left(1 + \frac{GSK}{U}\right)C \tag{28}$$

At the other extreme, if Γ is constant, the new equilibrium curve is a straight line but with an intercept of $GS\Gamma/U$ and a slope of unity.

On the same coordinates of $\bar{C}$ versus C, the operating line is now plotted. By simple material balance it will have a slope of $\frac{\Delta\bar{C}}{\Delta C} = \frac{L}{U}$ where L is the interstitial liquid downflow rate. Actual placement of the line depends of course on entrance and exit conditions.

The flow rates of the counterflowing streams can be estimated directly from the inlet and outlet stream rates. Thus for a stripper, L = F and U = Q = F - W. For an enricher, L = RD and U = Q = (R+1)D. However L and U so determined are really only the apparent downflow and the apparent upflow. The true downflow and the true upflow should include the internal recycle of liquid. This recycle is in addition to any from internal coalescence. For example, the true upflow in an enricher is really Q' which, in the absence of internal coalescence, is constant up to the reflux inlet level. At that level part of Q' "turns around" to join RD and both descend through the column.

The internal recycle results from the fact that the interstitial channels are not of fixed dimensions but can expand or contract in a complicated way to accommodate interstitial flow. The amount of recycle can be estimated for any given situation by means of the author's theory for interstitial drainage and overflow which is discussed later. However the computation is somewhat complicated. So for simplicity, L and U will be taken at their apparent values. This implies that mass transfer takes place between the apparent streams rather than the true streams. Within a consistent set of calculations, the results are satisfactory for many purposes.

After the operating line is placed, theoretical stages can be stepped off between it and the equilibrium curve. Figure 10 illustrates the calculation with a stripper where Equation 4 applies, and Figure 11 illustrates a combined column where Γ is constant.

2. Transfer Units

As an alternative to theoretical stages, the number of transfer units can be determined for the foam. Based on the upflowing stream, this number N_U is given by

$$N_U = \int_{\overline{C}_W^*}^{\overline{C}_Q} \frac{d\overline{C}}{\overline{C}^* - \overline{C}} \tag{29}$$

where $\overline{C}$ is related to C by the operating line, and $\overline{C}^*$ is related to C by the equilibrium curve. The lower limit of the integral is the concentration in the upflowing stream just above the pool. Equating it to $\overline{C}_W^*$ is predicated on the pool behaving as a theoretical stage.

Based on the downflowing stream, the number of transfer units N_L is given for the foam by

$$N_L = \int_{C_L}^{C_{top}} \frac{dC}{C - C^*} \tag{30}$$

where C is related to $\overline{C}$ by the operating line, and C^* is related to $\overline{C}$ by the equilibrium curve. C_L is the concentration in the downflowing stream just before it enters the pool. Taking the pool as a theoretical stage, C_L can be found from C_W by material balance around the pool. Of course if one wishes to lump together the separation achieved by the pool and the transfer units in the foam, a lower integration limit of C_W can be used in both Equations 29 and 30, provided the feed inlet is not to the liquid pool.

When the equilibrium curve can be expressed by a simple equation, the number of transfer units can be found by substitution followed by direct integration, and the number of theoretical stages can be found by the calculus of finite differences (30). For example, with a continuous stripping column a material balance yields Equations 31, 32, and 33, and Equation 28 gives Equations 34 and 35.

$$F = Q + W \tag{31}$$

$$C = \frac{Q}{F}\bar{C} + \frac{W}{F}C_W \tag{32}$$

$$C_Q = \frac{F}{Q}C_F - \frac{W}{Q}C_W \tag{33}$$

$$\bar{C}^* = \left(1 + \frac{GSK}{Q}\right)C \tag{34}$$

$$\bar{C}_W^* = \left(1 + \frac{GSK}{Q}\right)C_W \tag{35}$$

Combining Equations 29 and 31-35 yields Equation 36 for a continuous stripper operating with a system for which equilibrium adsorption is governed by the linear isotherm $\Gamma = KC$.

$$N_U = \frac{F}{GSK-W}\ln\frac{F(GSK-W)\dfrac{C_F}{C_W} + FW}{GSK(GSK+F-W)} \tag{36}$$

3. Effect of micelles on column performance

If micelles are a factor, they can be taken into account. In a refluxing column their effect on the adsorption equilibrium of a colligend should be greatest at the top of the column because that is where their concentration is the greatest. Further down the column their effect diminishes as their concentration decreases. For a sufficiently long column their effect vanishes, as discussed earlier.

Equation 9 cannot be used directly to estimate the effect of micelles introduced by reflux into the foam. Equation 9 is derived from Equation 8, and the latter is based on a material balance within the pool where the ratio of surface to volume is small. In the foam this ratio is large and so Equation 8 would first have to be modified to include surface adsorption by adding a term of the order $GSKC_1/U$ to the right-hand side and a term of the order $GSKC_2/U$ to the left-hand side. These changes would in turn modify Equation 9. Also, the variation in C_s along the column must be included. This can be accomplished by stagewise or transfer unit calculation for the surfactant to give values for C_s at each stage or transfer unit, and then substituting these values into the modified Equation 9 to give Γ_2 for the colligend at each stage or transfer unit. Thus $\bar{C}$ at each stage or transfer unit can be found from Equation 27 with $\Gamma = \Gamma_2$. Stagewise or transfer unit calculations can then be carried out for the colligend. Trial and error may be necessary to obtain a match.

4. Column efficiency

As in the case with other contacting operations, the determination of the number of theoretical stages or transfer units is often only part of the picture. The efficiency of the actual stages, or the actual column height equivalent to a theoretical stage (abbreviated H.E.T.S.) is frequently required too. Alternatively, the column height equivalent to a transfer unit (abbreviated H.T.U.) may be needed.

These quantities are difficult to predict and, generally speaking, must be determined by experiment. They depend on the intimacy of contact between the countercurrent streams. Fortunately, true foam is by its nature a good packing. This is especially true for relatively dry foam; that is, foam of relatively low liquid content. The interstitial suction opposes channeling and tends to distribute the downcoming liquid evenly over the cross section of the column, thus assuring good contact. H.T.U. values as low as 1 cm. have been reported (20).

A single axially located feed inlet generally gives a reasonably uniform distribution of feed in a foam column which does not exceed 2 inches in diameter. In wider columns a feed distributor is advisable, especially for wetter foam. In a 24 inch diameter column, a distributor which supplied 37 streams on 3-3/4 inch triangular spacing reportedly proved satisfactory (20). The streams impinged on baffles and then dripped into the foam with minimal kinetic energy.

As foam becomes wetter, the interstitial suction decreases and channeling becomes more likely. When the volumetric fraction of the foam occupied by the liquid reaches the void fraction for close packed spheres (which is 0.26 for uniform spheres), the bubbles become free to move. Further increase in the liquid fraction, especially if much beyond 0.30, makes for excessive channeling and poor contact (20,31).

Stages have also been investigated. Alternately placed mixing and settling stages have been used. These were made by constructing a column of alternately narrow and wide diameter (14). However, insofar as the present author is aware, it has not been established that such a configuration is superior to a uniform column of the wider diameter.

Sieve plates, with foam rising up the erstwhile downcomers and liquid dripping down through the holes, gave indifferent results (32). So did screen plates. Bubble cap plates passing foam through the slots yielded efficiencies of up to 30% (14). Individual bubbled pools in countercurrent array have been suggested (29).

It appears from the available evidence that submerging the bubbler one foot below the pool surface provides more than enough depth to assure a close approach to equilibrium. Thus the pool at the bottom of a foam fractionation column can generally be considered to be one theoretical stage.

I. Illustrative Problem #6

Statement:

An experimental foam fractionation column is operated as a continuous stripper with no bottom stream. In other words, after passing down and up the column, the entire feed exits as the overflow foam. The feed is aqueous and contains surfactant plus 10^{-14} gm.mol/cm.^{3} of an undesirable ion. When the volumetric gas rate is 20 times the volumetric feed rate, the bubble surface is 100 cm.^{2} per cm.^{3} of gas and the liquid pool contains 10^{-15} gm.mol/cm.^{3} of the ion. The linear equilibrium adsorption constant for the ion is 10^{-4} cm. A very small aqueous stream of concentrated surfactant is added to the pool in order to maintain sufficient surfactant, but without exceeding the critical micelle concentration. Estimate the concentration in the pool if the height of the foam is doubled.

Solution:

This problem can be attacked directly with Equation 36. However it is more instructive to show the use of the prior equations.

In the present problem, $L = F = U = Q$ and $\frac{G}{F} = 20$. From Equation 28 or 34,

$$\bar{C}^* = \left(1 + \frac{GSK}{Q}\right) C$$

By substitution, $\bar{C}^* = (1 + 20 \times 100 \times 10^{-4})\, C = 1.2C$

and $\bar{C}_W^* = 1.2C_W = 1.2 \times 10^{-15}$

Since $W = 0$, by simple material balance

$$\overline{C} = C$$

and $$C_Q = C_F = 10^{-14}$$

By substitution, $\overline{C}^* = 1.2\overline{C}$

Substitution in Equation 29,

$$N_U = \int_{1.2\times10^{-15}}^{10^{-14}} \frac{d\overline{C}}{0.2\overline{C}} = 10.6$$

Let the new situation with the height doubled be denoted by a prime. Thus $N_U' = 2 \times 10.6 = 21.2$ since doubling the foam height of a stripper (with negligible internal coalescence) should double the number of transfer units in the foam. Substituting in Equation 29 for the new situation

$$21.2 = \int_{1.2C_W'}^{10^{-14}} \frac{d\overline{C}}{0.2\overline{C}} = 5 \ln \frac{10^{-14}}{1.2C_W'}$$

Solving, $C_W' = 1.2 \times 10^{-16}$ gm.mol/cm.^{3} in the pool.

VI. BUBBLE FRACTIONATION

Oddly enough, there are some situations where the pool can constitute more than one theoretical stage! If the pool itself is tall and narrow, downflowing liquid arriving at the pool surface may not mix thoroughly with the rest of the liquid in the pool. As a result, a vertical concentration gradient will set up in the pool. This gradient will further enrich the surface of the rising bubbles before they have even left the pool. Under these conditions, the pool will act as more than a single theoretical stage. In other words, the pool will exhibit a stage efficiency of over 100%.

This happy phenomenon is not to be expected with operation that is truly in the simple mode; that is, without internal coalescence. Without a rich downflow, little beneficial gradient will form in the pool. With the long stripper, enricher, and combined column, the downflow to the pool surface is there -- but, as discussed earlier, it does not arrive rich. Thus only with the short counterflow columns, especially the enricher, can a large gradient form.*

An interesting extreme case of this phenomenon occurs with total internal reflux which may even be virtually instantaneous. This last situation is tantamount to having no foam formation at all. When the bubbles reach the pool surface the gas in them merely passes off, leaving the adsorbed material behind. The concentration gradient so developed can then be put to use since it represents a partial separation of the components in the liquid. The author has named this technique Bubble Fractionation. Its potential application is to surface active systems which, because of low concentration, or for some other reason, foam very slightly or not at all. Batch operation is shown in Figure 12a.

If a bit of foam does form but is ignored in that rich liquid is withdrawn from the pool, the technique is still bubble fractionation. However if the foam is withdrawn, then the technique is of course foam fractionation but with bubble fractionation assisting if there is a vertical concentration gradient in the pool. Indeed, deliberately using bubble fractionation may sufficiently enrich the upper layers of the liquid pool to permit foam fractionation of an otherwise unfoamable system. Thus bubble fractionation can act as a booster to foam fractionation operating above it.

The separation attainable in bubble fractionation is enhanced by increasing the height of the pool and the generation of bubbles. Certain soluble dyes have been effective in giving a separation visible to the eye. However, undesirable impurities, especially those more surface active than the dye, must be carefully eliminated lest they pre-empt the bubble surface and prevent the dye from concentrating sufficiently. In batch operation with several parts per million of crystal violet chloride dissolved in a column of water several cm. in diameter and several feet tall, the concentration at the top reached as high as 10 times that at the bottom under favorable conditions.

---

*However, a small stripping gradient is always possible.

Continuous bubble fractionation is shown in Figure 12b. Rich liquid is withdrawn from the top and lean liquid from the bottom. Feed enters between the two, preferably at or near the level of matching concentration.

Further discussion of bubble fractionation is beyond the scope of the present paper. For additional information, including a theoretical approach, the reader is referred to the author's work on the subject (11,33,34).

VII. FOAM DRAINAGE AND OVERFLOW

A. Theory

So far, little has been said about quantitatively estimating the magnitude of the foam overflow or the magnitude of the true interstitial liquid flow. These are clearly important in developing a comprehensive picture of foam fractionation. Accordingly, a brief outline will now be presented of the theory for foam drainage and overflow developed during the course of the author's work (22). Results of this theory agree fairly well with available experimental data (27,32,35). For further details of theory or experiment, the interested reader is referred to the original papers.

The bubbles in a foam press one against the other, more or less flattening the faces or films in between. These faces intersect three at a time to form channels or capillaries which are often called Plateau borders (abbreviated here as PB). With bubbles of uniform size, this means a dihedral angle of 120° between intersecting films, which in turn implies that the bubbles are nearly regular dodecahedra (23,24,25). This can be shown from geometrical considerations.

The regular dodecahedron was therefore selected as the model for the shape of a typical bubble within the foam. The typical bubble is thus considered as having 12 congruent regular pentagonal faces. Of course it is recognized that in reality bubbles will deviate from this ideal, so alternatively the model can be viewed as a kind of average of shapes. At this point it is again worth mentioning that the view through a glass retaining wall can be misleading to the casual observer because local packing distorts the bubble shapes from what they are in the interior of the foam.

Foam drainage occurs primarily through the interconnecting network of capillaries rather than from film to film (25,36). The problem is therefore to predict the flow through the capillaries.

Figure 13a showed two capillaries in cross section. The curvature of their boundaries exerts a suction on the films. Figure 13b is a magnified view of a single capillary. The capillary boundary is pictured as being of radius r_o. The cross section exhibits six-fold symmetry. Thus flow through only one such symmetrical section need be examined.

Flow through the capillaries is incompressible and laminar. Accordingly, for steady rectilinear flow through a vertical capillary, the equation of motion in cylindrical form (37) for a Newtonian liquid with constant density ρ and viscosity μ is

$$-\frac{\rho}{\mu}\left(g - \frac{1}{\rho}\frac{\partial p}{\partial z}\right) = \frac{1}{r}\frac{\partial}{\partial r}\left(r\frac{\partial v_z}{\partial r}\right) + \frac{1}{r^2}\frac{\partial^2 v_z}{\partial \theta^2} \qquad (37)$$

where g is the acceleration of gravity, r the radial coordinate, θ the angular coordinate, Z the axial coordinate (in this case vertically downward), v_z the linear axial velocity, and $\partial p/\partial Z$ the axial pressure gradient.

The boundary conditions at the two straight borders of the symmetrical section are simply those of mirror symmetry. However at the curved wall the situation is more complicated. With some foams, such as those of protein origin, the curved wall may be essentially rigid due to the formation of the well-known protein skin. Under such conditions, v_z at the wall is zero. However, this rigidity is not generally the case. With other foams, such as detergent foams, the wall can move. Of course there is still some resistance. The measure of this drag resistance is the surface viscosity μ_s which typically has the units of dyne sec./cm. This can be compared with dyne sec./cm.^{2} for the conventional viscosity μ which is its three-dimensional analog. Assuming μ_s to be Newtonian and constant, a momentum balance at the capillary wall yields Equation 38 as the boundary condition at the wall.

$$\frac{\partial^2 v_z}{\partial \theta^2} = -\frac{\mu r_o^2}{\mu_s}\frac{\partial v_z}{\partial r} \qquad (38)$$

The dimensionless quantity $M = \frac{\mu r_o}{\mu_s}$ is a measure of the relative fluidity of the wall. Motion is viewed relative to the center of the junction of the capillary and the flat film for reasons discussed in the original papers (22,32) and subsequently (38). This location is shown as point A in Figure 13b. Points B and C represent similar locations.

Equation 37 was solved with the three boundary conditions by means of finite differences at 53 nodal points. This was accomplished with a digital computer to solve the resulting matric equation via Crout's reduction (39). Velocity contours were obtained. These are shown in dimensionless form in Figure 14 for a rigid capillary wall of $M = 0$, in Figure 15 for a moderately fluid wall of $M = 2.48$, and in Figure 16 for a very fluid wall of $M = 61.9$.

However, the capillaries are generally not vertical. For a capillary inclined at some angle α to the horizontal, the axial component of gravity is $g \sin\alpha$. The axial pressure gradient is also that for the vertical multiplied by $\sin\alpha$. Therefore the axial velocity is now $v_z \sin\alpha$ where v_z is for a similar capillary which is vertical. The downward vertical component of the axial velocity is accordingly $v_z \sin^2\alpha$. This is all relative to a "moving observer", designated MO, moving upward with the foam bubbles. Accordingly, the vertical component is now written $v_{z,MO} \sin^2\alpha$. Relative to a "stationary observer", SO, standing on the surface of the Earth, the foam bubbles move upward at a linear velocity of $v_{f,SO}$. Subtracting yields $v_{f,SO}-v_{z,MO}\sin^2\alpha$ as the net upward velocity at a point in a capillary, relative to a stationary observer. Multiplying this net velocity by the differential horizontal cross section dA_{PBh} and integrating over the entire horizontal cross section of all the capillaries at some arbitrary level in the foam column will give the net upward flow of interstitial liquid, Q_{SO}.

Said integration requires knowledge of the number of capillaries at the column cross section as well as the distribution of their inclination α. This was determined in the following way:

From geometrical considerations it can be shown that the probability of a single random capillary being oriented at α is $\cos\alpha\, d\alpha$. For a capillary that is inclined at α, but otherwise randomly located in the column, the probability of intersection by a particular horizontal plane is obviously $P \sin\alpha$ where P is the capillary packing factor defined as capillary length divided by foam column height. Therefore the compound probability of a capillary being at α and also being at a particular horizontal plane (cross section of a column) is the product or $P \sin\alpha \cos\alpha\, d\alpha$. The last expression becomes the number of such capillaries when there are many capillaries in the column, as is actually the case of course. This assumes the capillaries are random.

Equation 39 indicates this aforementioned integration for Q_{SO}.

$$Q_{SO} = P \int_0^{\pi/2} \int_{A_{PBh}} (v_{f,SO} - v_{z,MO} \sin^2\alpha) \sin\alpha \cos\alpha \, d\alpha \, dA_{PBh} \qquad (39)$$

It is convenient to replace $A_{PBh} \sin\alpha$ with A_{PB} which is the capillary cross section perpendicular to the capillary axis. P is related to bubble diameter and column cross section by geometry. The bulk foam is presumed to move in plug flow. This is generally the case in a column of uniform cross section because of the structural rigidity of the bulk foam.

Equation 39 was recast into dimensionless form and the double integration carried out numerically with a digital computer. The results are expressed as dimensionless curves in the original paper. These curves permit estimation of the drainage rate, upflow rate, and bulk foam density. All that are required are physical properties and conditions of operation. No empirical constants are required. The theory is more rigorous and complete than earlier theories of other workers. These earlier theories suffer from three vitiating assumptions, namely that the interstitial flow takes place through channels which are vertical with rigid walls and of either substantially circular (40,41) or parallel plane (12,42,43,44) cross section.

The results for column overflow can be simplified to give Equation 40 for dry foam; that is, for foam of low liquid content.

$$Q = \frac{G^2 \mu}{A g \rho d_o^2} \phi\left(\frac{\mu^3 G}{\mu_s^2 g \rho A}\right) \qquad (40)$$

As before, Q is the volumetric rate of foam overflow on a gas-free basis. A is the cross sectional area of the column. For bubbles of nonuniform size, the appropriate average bubble diameter d_o is given by Equation 41.

$$d_o = \left(\frac{\Sigma n_i d_i^3}{\Sigma n_i d_i}\right)^{\frac{1}{2}} \qquad (41)$$

Function ϕ was evaluated theoretically according to two alternatives regarding the detailed relationship between interstitial downflow and bulk foam upflow (22,27). The two evaluations are shown as curves in Figure 17. The difference between the curves is small over much of the range (35). However, the asymptotes do differ appreciably. Additional work is in progress to examine this difference further. In the meantime the author recommends that the solid curve be used for Equation 40.

For moderately wet foam, the theoretical correction necessary for the higher liquid content can be conveniently approximated by simply multiplying Q from Equation 40 by the quantity (1 + 3 Q/G). This gives a corrected Q.

When internal coalescence is present, d_o must be taken at the top of the column.* This is important. A small but significant degree of coalescence can easily go unnoticed to the eye, especially with bubbles that are nonuniform to begin with. For very severe internal coalescence, extremely wet foam, highly nonuniform bubble sizes, or very nonuniform or tortuous column cross section, the theoretical model breaks down.

B. Surface Viscosity and Other Properties

With dilute solutions, μ and ρ can usually be conveniently taken as those of the solvent which is generally water. However, the surface viscosity μ_s is a separate property. It can be measured in several ways. Unfortunately, there is a lack of consensus on the best way for doing so. Different methods give quite different results. This is due partly to differences in technique and the presence of impurities, and partly to the fundamental nature of surface viscosity. It is not simple. Surface flow can involve not only shear but dilation and elasticity (45). Temperature can have a marked effect too, especially if "melting" of a rigid surface layer occurs.

---

* But d is another matter. An average between top and bottom has been suggested (27). However, on theoretical grounds, it is more correct to take d at the pool surface for Equations 21 and 24, and at the feed level for Equations 17, 18, 25 and 26.

Fortunately, ϕ is not a highly sensitive function of μ_s. In fact, for high values of μ_s as are common with protein solutions, ϕ approaches an asymptote which is independent of μ_s. Joly (46) has compiled measurements of μ_s for various aqueous systems. Typical values range from under 10^{-4} dyne sec./cm. for some detergent solutions to over 10^{-1} dyne sec./cm. for some protein solutions.

The present author has found the method of Mysels (36) to be useful as a simple means for roughly measuring μ_s in foam. In this method, μ_s is obtained from the motion of the black spots which form in a well drained film. Such films can be obtained in a foam column by simply shutting off the gas flow and feed flow, thus allowing the standing foam to drain thoroughly. As such drainage proceeds, various colors appear in the bubble faces due to the diffraction of light. If a film does not break prematurely, its color eventually turns silver-white with a thickness t_w on the order of 10^{-5} cm. Black spots form in this film. The thickness t_b of these spots is on the order of 10^{-6} cm. and their blackness stems from the diffractive cancellation of light. Being thinner than the surrounding white film, the black spots are buoyant and therefore rise up through (within) the film. This is shown schematically in Figure 18. Refined methods for measuring t_w and t_b exist (36,47). However, in view of other uncertainties, undue effort in this connection is not warranted here.

The inclination angle β of the film from the horizontal, the radius r_b of a more or less circular black spot, and the linear velocity u within the film for this same black spot are all estimated optically. The results are then substituted in Equation 42 which is essentially the surface analog of

Lamb's relationship (48) for a buoyant, infinitely long, horizontal cylinder rising at terminal velocity through a homogeneous viscous fluid.

$$\mu_s = \frac{-r_b^2 \rho g (t_w - t_b) \sin\beta}{8\ u} \left[0.0772 + \ln \frac{u r_b \rho t_w}{8 \mu_s} \right] - \frac{\mu t_w}{2} \qquad (42)$$

The term $\mu t_w/2$ is generally negligible. Solution for μ_s is by trial.

Since the method is only very approximate, but the measurements are so easy to obtain, the determination should be repeated many times and the results for μ_s averaged so as to achieve greater reliability. In the work of the present author (32), 16 such determinations for aqueous Triton X-100 at 25°C yielded a mean μ_s of 1.01×10^{-4} dyne sec./cm. with a standard deviation of 0.47×10^{-4} dyne sec./cm. for the individual measurements. By statistical t-test this corresponds to a 95% confidence interval of $\pm 0.25 \times 10^{-4}$ dyne sec./cm. on the mean.

There is another way to estimate μ_s. One can run a foam column with the system in question, measure (or otherwise evaluate) Q, G, A, μ, g, ρ, and d_o, and substitute in Equation 40 using the wetness correction factor (1 + 3 Q/G) if required. Then from ϕ in Figure 17, μ_s can be found. Naturally, μ_s determined in this manner will suffer from whatever shortcomings exist in the theory. On the other hand, for subsequent use in estimating Q under changed conditions, μ_s determined in such a manner offers the prospect of cancelling these shortcomings as well as cancelling the experimental error.

C. Implications of the Theory

Besides providing a theoretical estimate of Q by Equation 40 for any mode of column operation, the drainage theory also provides means for estimating the bulk foam density and the interstitial liquid upflow and downflow rates at any level in the column, barring internal coalescence. The quantitative considerations are beyond the scope of the present chapter and the interested reader must be referred to the original paper for further information (22).

The present discussion will be restricted to certain general results of the theory. Perhaps the most significant of these relate to $\mathcal{E}$, the volumetric density of the bulk foam, which is expressed as interstitial liquid volume divided by bulk foam volume.

According to the drainage theory, $\mathcal{E}$ within any section of the column should be uniform along the column provided there is no internal coalescence and provided any reflux or feed entering the foam is well distributed over the column cross section. For example, in a combined column, $\mathcal{E}$ should be uniform from the surface of the liquid pool up to the feed inlet, and then uniform at another value from the feed inlet up to the reflux inlet, and then uniform again at still another value from the reflux inlet up to the top of the column. This means that the H.T.U. or the H.E.T.S. in any section of a column is theoretically uniform along that section because the foam is uniform. It also means that increasing the height of a column which is truly operating in the simple mode should be of no value since, odd as it may appear at first glance, there is theoretically no change in $\mathcal{E}$ with height. Of course, if significant internal coalescence is present (as it often is), the situation would be quite different. Finally, the theory shows that $\mathcal{E}$ at the top of the column is not equal to $\frac{Q}{Q+G}$ as one might have thought offhand. Rather, $\mathcal{E}$ is somewhat greater than $\frac{Q}{Q+G}$. This inequality is related to the true interstitial downflow, upflow, and recycle mentioned earlier.

D. Illustrative Problem #7

Statement:

A foam fractionation column of 7 cm. diameter is to operate at 25°C with the surfactant Triton X-100 in water. If the gas rate is 90 $cm.^3/sec.$ and the average bubble diameter according to Equation 41 is 0.12 cm. at the top of the column, estimate the rate of foam overflow.

Solution:

Taking the viscosity and density of the solution as equal to those for water at 25°C, $\mu = 8.94 \times 10^{-3}$ dyne $sec./cm.^2$ and $\rho = 1.00$ $gm./cm.^3$

$A = \frac{\pi}{4} \times 7^2 = 38.5$ $cm.^2$ Substituting in Equation 40,

$$Q = \frac{90^2 \times 8.94 \times 10^{-3}}{38.5 \times 980 \times 1.00 \times 0.12^2} \phi\left(\frac{(8.94 \times 10^{-3})^3 \times 90}{(1.01 \times 10^{-4})^2 \times 980 \times 1.00 \times 38.5}\right)$$

$Q = 0.133 \times \phi(0.167)$

$\log_{10} 0.167 = -0.78$

From the solid curve of Figure 17, $\log_{10}\phi = 1.54$. Therefore, $\phi = 34.7$.

Substituting, $Q = 0.133 \times 34.7 = 4.62$.

Applying the wetness factor of $(1 + 3\ Q/G)$,

$$Q = \left(1 + \frac{3 \times 4.62}{90}\right) 4.62 = 5.34$$

Rounding off, $Q = 5.3$ $cm.^3/sec.$ of foam overflow on a gas-free basis. Neglecting the small density of gas, this represents 5.3 gm./sec. of foam overflow.

E. Illustrative Problem #8

Statement:

Estimate the approximate range of relative change in the overflow rate of a fairly dry foam from a foam fractionation column if the gas rate is doubled but the bubble sizes remain unchanged.

Solution:

At high ϕ, such as might be the case with the comparatively high μ_s of a protein foam, ϕ approaches a constant asymptote. This is shown in Figure 17. Thus from Equation 40, Q is directly (linearly) proportional to G^2. Therefore, in this case, doubling G should quadruple Q. Since the foam is fairly dry, to a first approximation the wetness correction is neglected.

At lower ϕ, such as might be the case with lower μ_s in a detergent foam, the solid curve in Figure 17 becomes approximately linear with a slope of about -0.27. This means ϕ is directly proportional to $G^{-0.27}$. Thus from Equation 40, Q is directly proportional to $G^{1.73}$. Therefore doubling G multiplies Q by $2^{1.73}$ or about 3.3. Again the wetness correction is neglected.

Thus, for a fairly dry foam, the effect of doubling G should be to multiply Q by a factor ranging from about 3.3 to 4.0.

F. Experimental Confirmation

Experimental confirmation of the theory has been obtained in various ways. Figure 19 shows one of several columns which were used for this purpose (27). The column was of glass with an internal diameter of 4.6 cm. It was surrounded with a circulating water jacket to maintain the temperature at 25°C. Pairs of calibrated electrodes (not shown) were mounted within the foam column at 7 locations along its length in order to measure local electrical conductivity and hence local bulk foam density. The column was run both with and without reflux. Collapsed net overhead product was returned as feed to the liquid pool. The system was the nonionic surfactant Triton X-100 in water with a bit of sodium chloride added to provide sufficient electrical conductivity for easy measurement.

Figure 20 shows some typical experimental results (27). The reciprocal of the local bulk foam density is plotted against its corresponding level in the foam column. Curve A and curved B are each straight and horizontal. This means $1/\mathcal{S}$ is uniform along the column, and therefore so is $\mathcal{S}$. Thus with or without reflux, when internal coalescence is negligible the uniformity in $\mathcal{S}$ which is predicted by theory is borne out by experiment. In this connection it is of interest to note that Haas and Johnson (20) report little variation in H.T.U. with column length for a stripping column under good operating conditions. Such uniformity also accords with the theory.

Of course if internal coalescence is not negligible $\mathcal{S}$ will decrease up the column, which means of course that $1/\mathcal{S}$ will increase. Curve C illustrates this for a case of severe internal coalescence.

Experimental results (27,32,38,49) also verify the prediction of Q by Equation 40. Data were assembled (35) from 46 runs at 25°C with three different columns. The system was aqueous Triton X-100 at pool concentrations ranging from 2×10^{-7} to 20×10^{-7} gm.mol/cm.^{3} R ranged from 0 to 13, A ranged from 13.1 to 16.6 cm.^{2}, d_o ranged from 0.05 to 0.40 cm., G ranged from 1.3 to to 10.4 cm.^{3}/sec. and Q ranged from 0.001 to 0.405 cm.^{3}/sec. Stripping operation was employed in some runs by feeding a solution of 5×10^{-7} gm.mol/cm.^{3} into the foam. For all runs, a comparison was then made between Q measured experimentally, and Q predicted by Equation 40 utilizing the solid curve of Figure 17 and the wetness correction factor $(1 + 3\ Q/G)$. The surface viscosity was taken to be 1.01×10^{-4} dyne sec./cm., as determined separately from the motion of the black spots.

Figure 21 shows the results of the test. Theoretical Q/A is plotted against experimental Q/A. The diagonal is the line of theoretical perfection. Deviation from the line is quite modest, especially in view of the wide range of variables involved. Over more than a 400-fold range of foam overflow rate, the average deviation of theory from experiment is only 26%. This is deemed to be fairly good agreement for such a wide range.

Of course, the agreement could be improved even further by using μ_s determined from some of the operating data for the column, as described earlier. Such determinations in a pool-fed column showed that μ_s increased somewhat as the interstitial concentration was raised either by the use of reflux or by the use of a higher pool concentration. However, such values of μ_s were not employed in the test. For the sake of impartiality, only the one aforementioned value determined from the independent method of black spots was used.

The drainage theory can also be used to relate the bulk foam density of a stationary foam to the rate of a continuous liquid feed draining down through the foam keeping it wet. This applies at steady state and in the absence of appreciable coalescence. The theory predicts that $\mathcal{S}$ will be uniform along the column. Of course, if the feed is stopped, allowing the foam to drain in unsteady state, $\mathcal{S}$ will begin to vary along the column and with time.

The procedure for relating $\mathcal{S}$ to L at steady state, or vice versa, does not involve ϕ. Also, it does not involve any empirical constants. It is summarized by an information flow diagram presented elsewhere (35). Comparison of theory against experiment yields favorable agreement (35).

From experimental data for aqueous Triton X-100 taken with the column shown in Figure 19, true L and true U were obtained (38) from the drainage theory. L and U so determined include the internal recycle mentioned earlier. Mass transfer coefficients were then obtained for the transfer of surfactant between the two true interstitial streams under conditions of reflux. Of course the bubble surfaces were saturated.

Values for the said mass transfer coefficient k_L based quite arbitrarily on the capillary wall area a_o are presented elsewhere (27). Those values are easily converted to transfer units since it can be readily shown that $N_U = k_L a_o/U$ for this case. Dividing the column height of 100 cm. by N_U gives the height of a transfer unit. Values so obtained for H.T.U. ranged from 4 to 21 cm. for that series of experiments.

VIII. COALESCENCE

As indicated earlier, bubble coalescence within the rising foam can be important. This internal coalescence stems from two sources. One is the diffusion of gas from small bubbles to large bubbles. While this is not usually significant with respect to foam fractionation, with a sufficiently high column residence time it can be. The second source is the rupture of films which separates bubbles. This can easily be very significant.

A. Gas Diffusion

When an interface between two fluids is curved, a pressure difference exists across it. This pressure difference Δp is related to γ and the radii of curvature r_1 and r_2 by the equation of Laplace and Young, namely

$$\Delta p = \gamma \left(\frac{1}{r_1} + \frac{1}{r_2} \right) \tag{43}$$

Thus, for example, the suction of the capillaries which was referred to earlier can be estimated by setting $r_1 = r_o$ and $r_2 = \infty$. This gives suction $\Delta p = \gamma/r_o$.

For the present discussion, Equation 43 is applied directly to a bubble. For a spherical bubble of radius $\bar{R}$ in air, $r_1 = r_2 = \bar{R}$. Also, there are two nearly equal surfaces, an inner and an outer. So for this case, Equation 43 yields $\Delta p = 4\gamma/\bar{R}$ where Δp is the pressure excess within the bubble with respect to the atmosphere around it. For a spherical bubble submerged within a liquid, the pressure excess with respect to the adjacent liquid is $\Delta p = 2\gamma/\bar{R}$ since there is only one bubble surface. Thus the pressure difference between two submerged spherical bubbles of unequal size is $\Delta p = 2\gamma\left(\frac{1}{\bar{R}} - \frac{1}{\bar{R}'}\right)$ where $\bar{R}'$ is the radius of the larger bubble and $\bar{R}$ is the radius of the smaller. This pressure difference causes gas to diffuse from the smaller bubble, through the liquid, into the larger bubble. This difference makes the larger bubble grow still larger and the smaller bubble grow still smaller, thus increasing the driving force and hence the rate even further. Given sufficient time, the smaller bubble will disappear altogether.

Since it is impossible to have perfectly identical bubbles in a dispersion it is evident that some change must always occur in the distribution of bubble sizes. The rate of this change depends not only on the deviation in bubble sizes but also on the resistance to gas diffusion from bubble to bubble. De Vries (18) has derived and experimentally verified certain relationships which describe how the distribution of bubble sizes changes with time under the influence of gas diffusion. According to his work, if the number of bubbles of radius $\bar{R}$ is $F(\bar{R})d\bar{R}$, and if Equation 44 describes the frequency distribution $F(\bar{R})$ in terms of $\bar{R}$ and a distribution parameter b, then Equation 45 gives the effect of interbubble gas diffusion on b as it changes from b_o to b_γ over time interval τ.

$$F(\bar{R}) = \frac{6b\bar{R}}{\left(1+b\bar{R}^2\right)^4} \tag{44}$$

$$b_\gamma = \frac{b_o}{(1+k\tau)^2} \tag{45}$$

The quantity k treated as a constant is expressed by Equation 46, where $\underline{\underline{R}}$ is the gas constant, T the absolute temperature, $\bar{D}$ the diffusivity of gas in liquid, $\bar{S}$ the solubility (per unit pressure) of gas in liquid, p_a the atmospheric pressure, and t the average distance between bubbles.

$$k = \frac{4\underline{\underline{R}}T\bar{D}\bar{S}\gamma b}{p_a t} \tag{46}$$

While strictly speaking the foregoing relationships are for spherical bubbles, they should nevertheless apply in a general sort of way to polyhedral foams as well.

B. Film Rupture

The persistence of foam results from the persistence of the films separating the bubbles. The latter characteristic is a manifestation of the film elasticity which is defined by Gibbs (12) as $2sd\gamma/ds$ where s is the surface of the film.

Physically, this elasticity stems from a depletion of surfactant at the film surface when the surface is stretched. This depletion raises the surface tension which results in the exertion of a restoring force which opposes rupture.

Stretching depletes the adsorbed surfactant for two reasons. Firstly, there is the momentary depletion due to the inability of surfactant molecules to diffuse instantaneously from the interior of the film to the surface. This is known as the Marangoni effect. Secondly, in thin films the limited supply of surfactant in the interior may be insufficient to completely recoat the surface regardless of diffusion rate. This is termed the Gibbs effect. The relative importance of the two effects is still a matter of controversy. A third effect, which can be important with some ionic surfactants in thin films, is the electrostatic repulsion between the charged surfaces. This opposes film thinning and rupture.

It is very difficult to predict rupture. Kitchener (45) summarizes some of the approaches which have been employed. They yield activation energies which are directly proportional to the square of the film thickness. Various suggestions have been put forth as to the causative agents for rupture. These include thermal fluctuation, pressure fluctuation, spontaneous nucleation of vapor, external vibration, cosmic radiation, and local internal stress resulting from readjustment of the packing as the bubble sizes change due to interbubble gas diffusion.

C. External Coalescence

Generally speaking, it is desirable to collapse the foam overflow. If external reflux is employed, this is a necessity. However, even otherwise, it is frequently desirable since uncollapsed foam occupies a great deal of volume.

Some foams collapse readily upon standing. Others require special measures. Slowly rotating perforated centrifuges have been used successfully in a number of the investigations already cited. Discharging from the foam breaker on to a Teflon sheet instead of glass was found to be helpful in reducing any foam which remained uncollapsed (20).

An ingenious method, which has been applied in a large unit for foaming pollutants from sewage, is to run collapsed foam on to uncollapsed foam thereby mechanically breaking the latter (50). Of course, for very persistent foams this method may be difficult to apply successfully.

Other methods for collapsing foam include sonic and ultrasonic vibration, thermal means, and chemical additives. The last is not suitable for operation with external reflux, or where the additive would constitute an undesirable contaminant in the collapsed foam. For laboratory purposes the choice of method is largely one of convenience. With larger units the relative costs may prove decisive.

IX. GAS EMULSIONS

If the gas rate to a foam fractionation column is increased, the rate of bubble formation will be increased. This in turn will increase the rate at which surface, and therefore adsorbed material, flows off overhead. However, the liquid content of the foam will also be increased, so the concentration of the collapsed overhead will be lower. Furthermore, the wetter the foam, the poorer the contact is likely to be between countercurrent streams if such streams are involved. These disadvantages of excessive liquid content were pointed out earlier.

If the gas rate is increased still further, the foam bubbles separate. There are no longer films between the bubbles (which have become quite spherical). The rising gas-liquid dispersion becomes a gas emulsion (51). It is no longer a true foam.

The great propensity toward channeling in gas emulsions makes them poorly suited to stripping or refluxing operation. However, for simple operation, in situations where very high adsorptive throughput is required per unit cross sectional area of the column, the generation of a gas emulsion may be desirable. Of course the resulting additional external drainage load must not be overlooked.

Separation by means of gas emulsions are discussed by Wace and Banfield (14) who present relationships for throughput. They find maximum throughput at a $\mathcal{S}$ of 0.56. Above that $\mathcal{S}$ the rising dispersion becomes indistinguishable from the highly aerated pool. For bubbles of 0.1 cm. diameter, a $\mathcal{S}$ of 0.56 reportedly corresponds to a superficial gas velocity G/A of about 2.2 cm./sec. They also report that throughput is not a sensitive function of bubble diameter, and a broad maximum in throughput exists at a diameter of 0.08 cm.

X. CLOSURE

Foam fractionation is not a new technique. It has been a laboratory curiosity for a number of years. However, only recently has the technique been examined from a fundamental point of view. This fundamental approach has been stimulated in part by a greater recognition of the potentialities of the technique in large scale separations. Foam fractionation shows particular promise as an economical means for removing substances present at low concentrations from large volumes of liquid.

The material which has been presented in this chapter summarizes the principles of foam fractionation as they have been developed to date. Some of these ideas can be extended to the other adsubble methods. For example, where a foam is involved, the fundamentals of drainage apply. Where a partition process is involved, the concept of the transfer unit applies. It is the author's conviction that through the application of principles, more rational designs of processes can be prepared and more fruitful results obtained.

XI. ACKNOWLEDGEMENT

The present work is supported in part by F.W.P.C.A. Research Grants WP-00161 and WP-00814 from the U.S. Department of Interior.

XII. NOTATION

A = horizontal cross sectional area of the column, cm.^{2}

A_{PB} = cross sectional area of a capillary taken perpendicular to its axis, cm.^{2}

A_{PBh} = horizontal cross sectional area of a capillary, cm.^{2}

a_i = activity of component i.

a_o = wall area of the capillaries, cm.^{2}

b = bubble distribution parameter, cm.$^{-2}$

b_o = bubble distribution parameter at the start of interbubble gas diffusion, cm.$^{-2}$

b_τ = bubble distribution parameter after time interval τ, cm.$^{-2}$

C = concentration in the liquid, gm. mol/cm.^{3}

$\bar{C}$ = effective upflow concentration, gm. mol/cm.^{3} on a gas-free basis.

$\bar{C}^*$ = effective upflow concentration in equilibrium with C, gm. mol/cm.^{3} on a gas-free basis.

C^* = downflow concentration in equilibrium with $\bar{C}$, gm. mol/cm.^{3}

D = volumetric rate of collapsed net overflow product, cm.^{3}/sec.

$\bar{D}$ = diffusivity of gas in liquid, cm.^{2}/sec.

$\mathcal{D}$ = volumetric foam density (volumetric fraction of liquid in the foam).

d = bubble diameter or surface average bubble diameter, cm.

d_i = individual bubble diameter, cm.

d_o = edge average bubble diameter, cm.

E = relative adsorptive effectiveness of surfactant in the surface versus surfactant in the micelles.

F = volumetric feed rate, cm.^{3}/sec.

$F(\bar{R})$ = frequency distribution function for $\bar{R}$, cm.$^{-1}$

G = volumetric gas rate, cm.^{3}/sec.

g = acceleration of gravity, cm./sec.^{2}

K = equilibrium constant for adsorption, cm.

K' = auxiliary constant for Langmuir isotherm, cm.^{3}/gm.mol.

k = redistribution parameter for interbubble gas diffusion, sec.$^{-1}$

k_L = mass transfer coefficient, cm./sec.

L = volumetric rate of interstitial liquid downflow, cm.^{3}/sec.

M = dimensionless viscosity modulus $\mu r_o/\mu_s$.

N_L = number of transfer units based on the downflowing stream.

N_U = number of transfer units based on the upflowing stream.

n_i = number of bubbles with diameter d_i.

P = capillary packing factor (total length of capillaries within a unit height of foam).

Q = volumetric rate of foam overflow on a gas-free basis, cm.^{3}/sec.

Q' = volumetric rate of upflow on a gas-free basis just above the liquid pool, cm.^{3}/sec.

Q_{SO} = volumetric rate of net upflow of interstitial liquid relative to a stationary observer, cm.^{3}/sec.

p = pressure, dyne/cm.^{2}

p_a = atmospheric pressure, dyne/cm.^{2}

$\underset{\sim}{R}$ = gas constant, erg/gm.mol°K.

R = reflux ratio.

$\overline{R}$ = bubble radius, cm.

$\overline{R}'$ = radius of the larger bubble, cm.

r = radial coordinate, cm.

r_b = radius of approximately circular black spot, cm.

r_o = radius of curvature of the capillary wall, cm.

r_1 = radius of surface curvature, cm.

r_2 = radius of surface curvature taken in a plane perpendicular to that for r_1, cm.

s = film surface, cm.^{2}

S = ratio of surface to volume, cm.$^{-1}$

$\overline{S}$ = solubility of gas in liquid per unit pressure, gm.mol/erg.

T = absolute temperature, °K.

t = film thickness or distance separating bubbles, cm.

t_b = film thickness of black spot, cm.

t_w = thickness of silver-white film, cm.

U = volumetric rate of interstitial liquid upflow, cm.^{3}/sec.

u = linear velocity of a black spot moving within a silver-white film, cm./sec.

v_z = linear velocity downward at a point within a vertical capillary, cm./sec.

$v_{z,MO}$ = v_z but emphasizing that motion is relative to the rising foam bubbles, cm./sec.

$v_{f,SO}$ = linear upward velocity of the foam bubbles relative to a stationary observer, cm./sec.

W = volumetric rate of bottoms takeoff, cm.^{3}/sec.

Greek:

α = angle which a capillary makes with a horizontal plane.

β = angle which a bubble face makes with a horizontal plane.

Γ = concentration at the surface, gm.mol/cm.^{2}

γ = surface tension, dyne/cm.

Δ = difference.

μ = viscosity, dyne sec./cm.^{2}

μ_s = surface viscosity, dyne sec./cm.

π = 3.1459...

ρ = liquid density, gm./cm.^{3}

τ = time interval, sec.

ϕ = dimensionless function.

Subscripts for C, $\overline{C}$, $\overline{C}^*$, K and Γ only:

D = collapsed net overhead product.

F = feed.

i = particular component.

L = downflow just above the pool.

Q = foam overflow on a gas-free basis.

s = surfactant.

sc = critical micelle.
top = at the top of the downflowing stream.
W = pool or bottoms.

1 = in the absence of micelles.

2 = in the presence of micelles.

XIII. LITERATURE CITED

1. F. Sebba, Ion Flotation, Elsevier, New York, 1962.
2. H. M. Schoen, Ann. New York Acad. Sci., 137, Art. 1, 148 (1966).
3. E. Rubin and E. L. Gaden, Jr., "Foam Separation", Ch.5 in H. M. Schoen, Ed., New Chemical Engineering Separation Techniques, Interscience, New York, 1962.
4. H. G. Cassidy, "Fundamentals of Chromatography" Vol. X in A. Weissberger, Ed., Technique of Organic Chemistry, Interscience, New York, 1957.
5. L. Shedlovsky, Ann. New York Acad. Sci., 49, Art. 2, 279 (1948).
6. R. Lemlich, Chem. Eng., 73, No. 21, 7 (1966).
7. F. Sebba, Nature, 184, 1062 (1959).
8. A. Dognon and H. Dumontet, Compt. Rend. Soc. Biol., 135, 884 (1941).
9. A. J. Rubin, E. A. Cassell, O. Henderson, J. D. Johnson, and J. C. Lamb, Biotechnol. Bioeng., 8, 135 (1966).
10. R. E. Baarson and C. L. Ray, "Precipitate Flotation, a New Metal Extraction and Concentration Technique", Am. Inst. Mining, Metallurgical and Petroleum Engineers Symp., Dallas, Texas, 1963.
11. D. C. Dorman and R. Lemlich, Nature, 207, 145 (1965).
12. J. W. Gibbs, Collected Works, Longmans Green, New York, 1928.
13. J. T. Davies and E. K. Rideal, Interfacial Phenomena, 2nd ed., Academic Press, New York, 1963.

14. P. F. Wace and D. L. Banfield, Chem. Proc. Eng., 47, No. 10, 70 (1966).

15. P. F. Wace and R. Lemlich, discussion, Am. Inst. Chem. Engrs. - Inst. Chem. Engrs. Symp. Ser. (Inst. Chem. Engrs., London) No. 9, 85 (1965).

16. R. W. Schnepf, E. L. Gaden, Jr., E. Y. Mirocznik, and E. Schonfeld, Chem. Eng. Prog., 55, No. 5, 42 (1959).

17. C. A. Brunner and R. Lemlich, Ind. Eng. Chem. Fundamentals 2, 297 (1963).

18. A. J. de Vries, Foam Stability, Rubber-Stichting, Delft, 1957.

19. R. Lemlich and E. Lavi, Science, 134, No. 3473, 191 (1961).

20. P. A. Haas and H. F. Johnson, Am. Inst. Chem. Engrs. J., 11, 319 (1965).

21. D. O. Harper and R. Lemlich, Ind. Eng. Chem. Process Design and Development, 4, 13 (1965).

22. R. A. Leonard and R. Lemlich, Am. Inst. Chem. Engrs. J., 11, 18 (1965).

23. A. W. Adamson, Physical Chemistry of Surfaces, Interscience, New York 1960.

24. J. J. Bikerman, Foams: Theory and Industrial Applications, Reinhold, New York, 1953.

25. E. Manegold, Schaum, Strassenbau, Chemie und Technik Verlagsgesellschaft m. b. H., Heidelberg, 1953.

26. R. Lemlich, J. Chem. Eng. Educ. (Cincinnati), 3, No. 2, 53 (1965).

27. S. Fanlo and R. Lemlich, Am. Inst. Chem. Engrs. - Inst. Chem. Engrs. Symp. Ser. (Inst. Chem. Engrs., London) No. 9, 75 (1965).

28. R. H. Perry, C. H. Chilton, S. D. Kirkpatrick, Chemical Engineers Handbook, 4th ed., McGraw-Hill, New York, 1963.

29. D. L. Banfield, I. H. Newson, and P. J. Alder, Am. Inst. Chem. Engrs. - Inst. Chem. Engrs. Joint Symp. Preprint 1.1, Inst. Chem. Engrs., London, 1965.

30. E. J. Henley and H. K. Staffin, Stagewise Process Design, Wiley, New York, 1963.

31. I. H. Newson, J. Appl. Chem., 16, 43 (1966).

32. R. A. Leonard and R. Lemlich, Am. Inst. Chem. Engrs. J., 11, 25 (1965).

33. R. Lemlich, Am. Inst. Chem. Engrs. J., 12, 802 (1966).

34. D. O. Harper and R. Lemlich, Am. Inst. Chem. Engrs. J., 12, 1220 (1966).

35. F. S. Shih and R. Lemlich, Am. Inst. Chem. Engrs.J. in press.

36. K. J. Mysels, K. Shinoda, and S. Frankel, Soap Films, Studies of their Thinning, Pergamon, New York, 1959.

37. R. B. Bird, W. E. Stewart, and E. N. Lightfoot, Transport Phenomena, Wiley, 1960.

38. S. Fanlo, Ph.D. Dissertation, University of Cincinnati, 1964.

39. F. B. Hildebrand, Introduction to Numerical Analysis, McGraw-Hill, New York, 1956.

40. P. A. Haas and H. F. Johnson, "A Model and Experimental Results for Drainage of Solution between Foam Bubbles", Am. Chem. Soc. national meeting, Chicago, 1964.

41. G. D. Miles, L. Shedlovsky, and J. Ross, J. Phys. Chem., 49, 93 (1945).

42. A. P. Brady and S. Ross, J. Am. Chem. Soc., 66, 1348 (1944).

43. W. M. Jacobi, K. E. Woodcock, and C. S. Grove, Jr., Ind. Eng. Chem. 48, 2046 (1956).

44. S. Ross, J. Phys. Chem., 47, 266 (1943).

45. J. A. Kitchener, "Foam and Free Liquid Films", Ch. 2 in J. F. Danielli, K. G. A. Pankurst, and A. C. Riddiford, Eds., Recent Progress in Surface Science, Vol. I, Academic Press, New York, 1964.

46. M. Joly, "Surface Viscosity", Ch. 1 in J. F. Danielli, K. G. A. Pankhurst, and A. C. Riddiford, Eds., Recent Progress in Surface Science, Vol. I, Academic Press, New York, 1964.

47. K. J. Mysels, J. Phys. Chem., 68, 3441 (1964).

48. H. Lamb, Hydrodynamics, 6th ed., Dover, New York, 1945.

49. R. A. Leonard, Ph.D. Dissertation, University of Cincinnati, 1964.

50. C. A. Brunner and D. G. Stephan, Ind. Eng. Chem., 57, No. 5, 40 (1965).

51. J. J. Bikerman, Ind. Eng. Chem., 57, No. 1, 56, (1965).

LIST OF FIGURES

Figure 1. Foam fractionation in the simple mode: a) Batchwise operation, b) Continuous flow operation, c) Continuous operation with recycle of collapsed overflow as feed.

Figure 2. Typical curve for surface tension versus logarithm of concentration in the liquid.

Figure 3. Typical curve showing the effect of concentration in the liquid on concentration at the surface.

Figure 4. Standard separator.

Figure 5. Continuous foam fractionation columns showing four modes of operation.

Figure 6. Apparatus for studying overall column performance in various modes of operation.

Figure 7. Typical stripping performance from an enriching column separating a surfactant from water. Decreasing ordinate represents improvement in the degree of stripping.

Figure 8. Typical enriching performance for an enriching column separating a surfactant from water. Increasing ordinate represents improvement in the degree of enrichment.

Figure 9. Material balance around an enriching column.

Figure 10. Graphical stagewise calculation (via apparent streams) for a stripper. The equilibrium curve is based on a linear isotherm $\Gamma = KC$.

Figure 11. Graphical stagewise calculation (via apparent streams) for a stripper-enricher combination with feed entering at the match point. The equilibrium curve is based on a constant surface concentration Γ.

Figure 12. Bubble fractionation: a) Batchwise operation, b) Continuous flow operation.

Figure 13. Capillaries (Plateau borders) in cross section. a) Two capillaries with the film between them. b) A magnified view of one capillary, illustrating the six-fold symmetry. Capillary wall DWE has the radius r_o from point P.

Figure 14. Dimensionless velocity contours within a capillary with a rigid wall; i.e., with $M = 0$. The film thickness shown here is negligible.

Figure 15. Dimensionless velocity contours within a capillary with a moderately fluid wall of $M = 2.48$. The film thickness shown here is negligible.

Figure 16. Dimensionless velocity contours within a capillary with a very fluid wall of $M = 61.9$. The film thickness shown here is negligible.

Figure 17. Theoretical evaluation of ϕ. The solid curve (27) has an asymptote of $\log_{10}\phi = 2.41$. The broken curve (22) has an asymptote of $\log_{10}\phi = 2.27$. Use of the solid curve is recommended (35).

Figure 18. Typical pattern of black in white film, showing the rising black spots.

Figure 19. Foam fractionation column equipped for reflux and return. Seven pairs of electrodes (not shown) are located within the column to measure the bulk foam density at various levels.

Figure 20. Typical measurements of bulk foam density at various levels within the vertical foam column.

Figure 21. Test of theory for predicting the foam overflow rate.

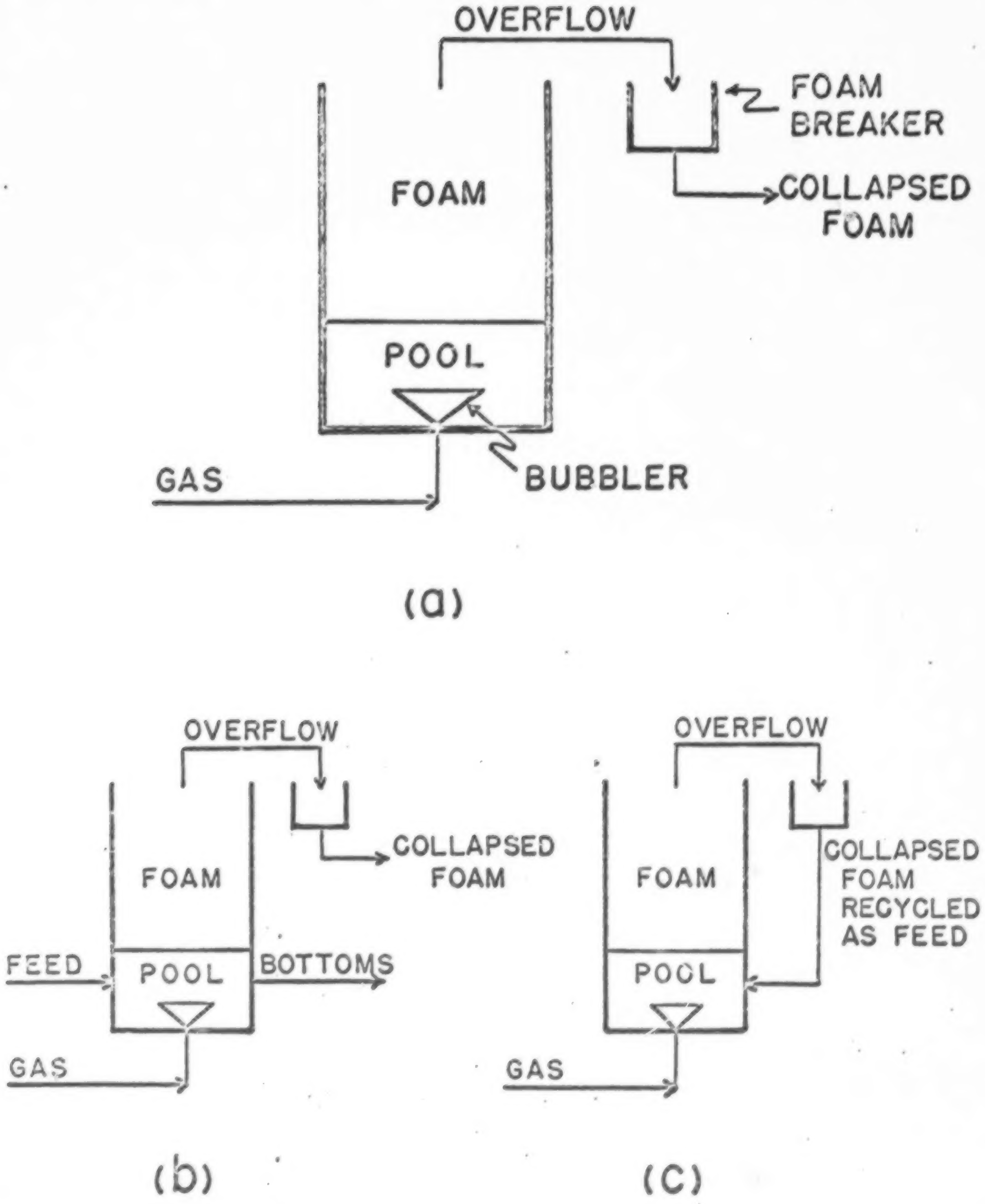
OVERFLOW
FOAM BREAKER
FOAM
COLLAPSED FOAM
POOL
GAS
BUBBLER
(a)
OVERFLOW
COLLAPSED FOAM
FOAM
FEED
POOL
BOTTOMS
GAS
(b)
OVERFLOW
COLLAPSED FOAM RECYCLED AS FEED
FOAM
POOL
GAS
(c)

Figure 1. Foam fractionation in the simple mode: a) Batchwise operation, b) Continuous flow operation, c) Continuous operation with recycle of collapsed overflow as feed.

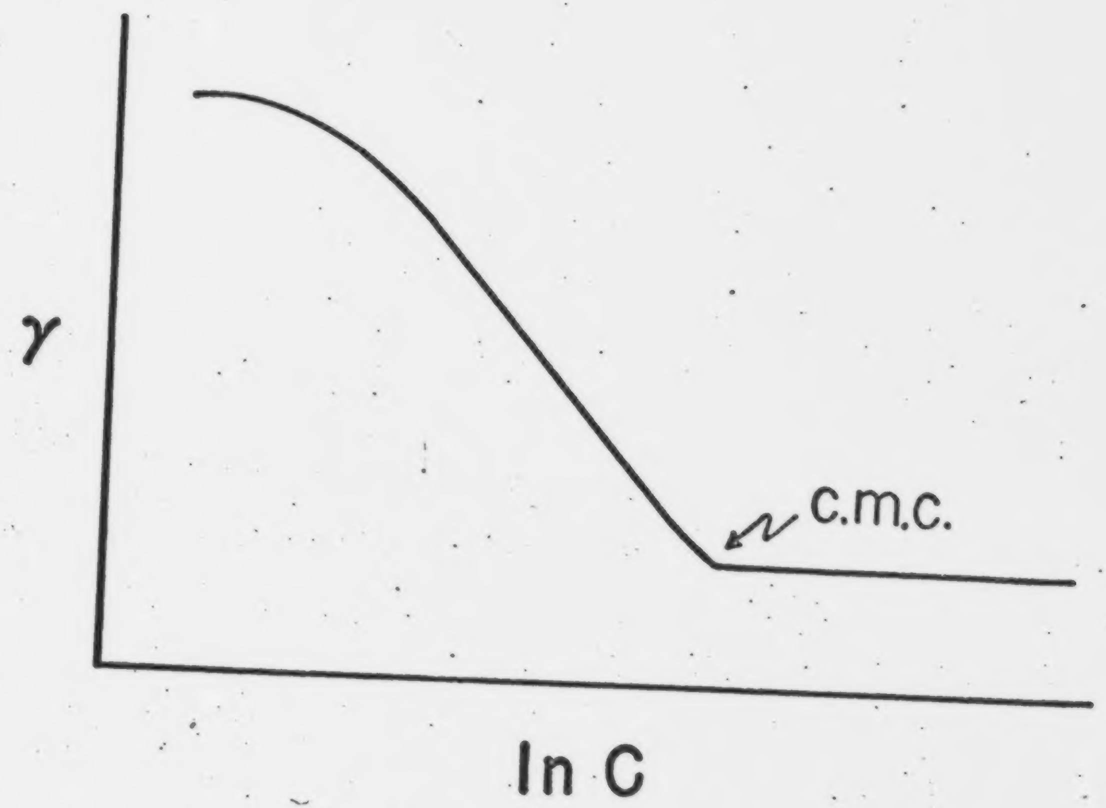

Figure 2. Typical curve for surface tension versus logarithm of concentration in the liquid.

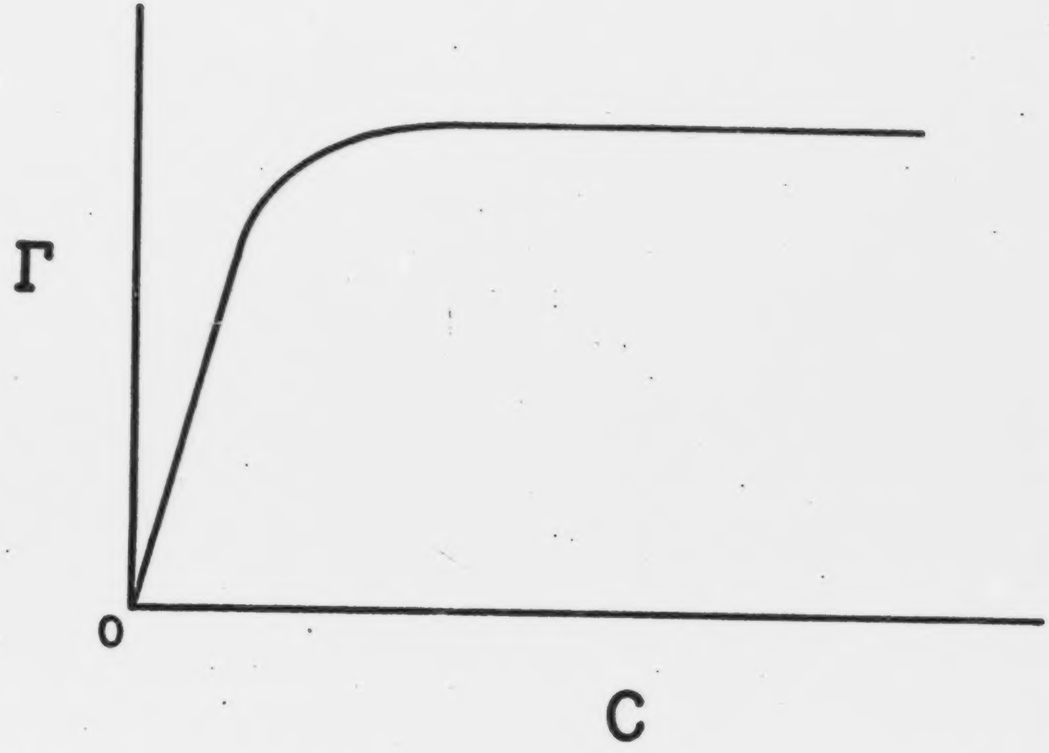

Figure 3. Typical curve showing the effect of concentration in the liquid on concentration at the surface.

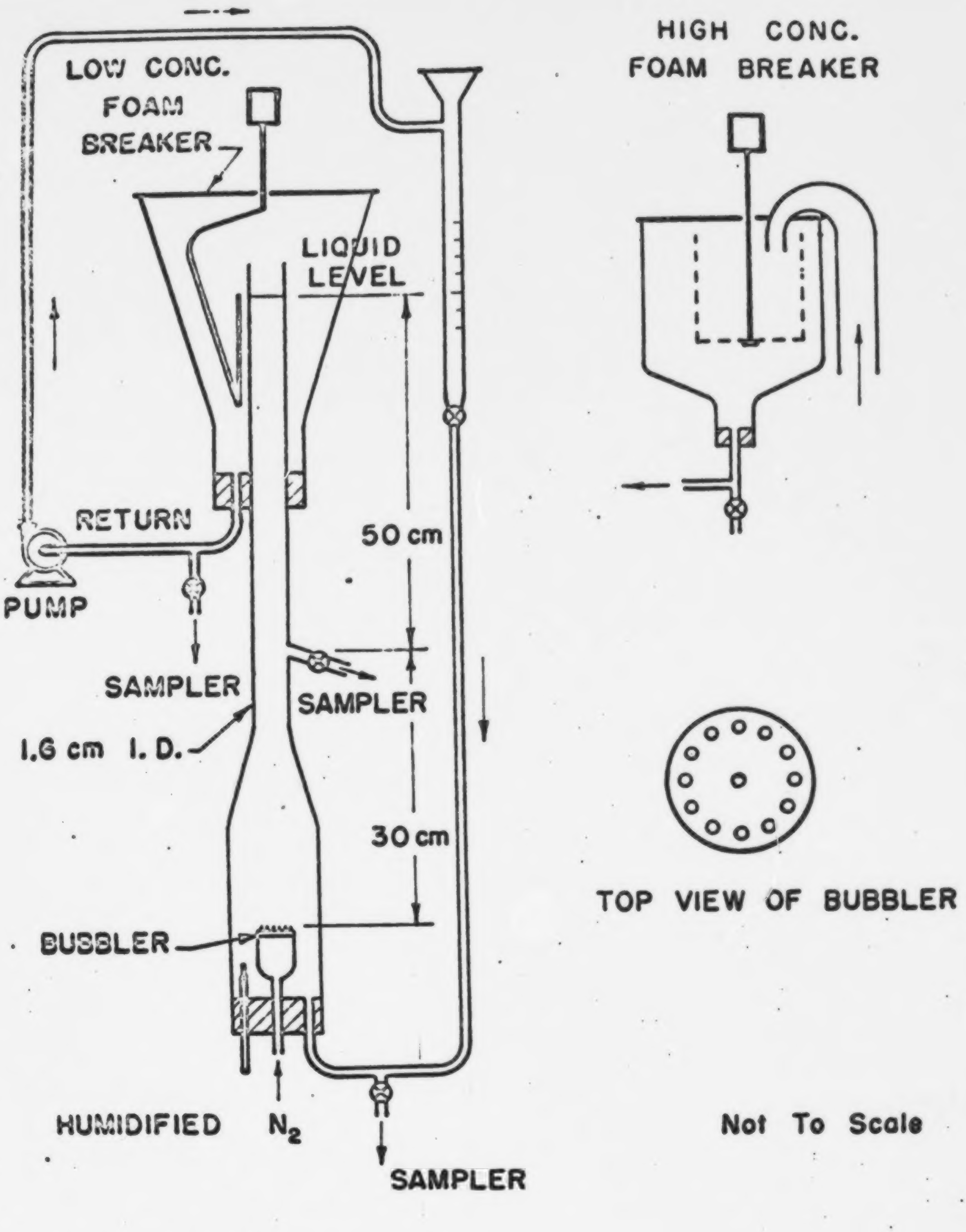
LOW CONC.
FOAM
BREAKER
HIGH CONC.
FOAM BREAKER
LIQUID
LEVEL
RETURN
PUMP
50 cm
SAMPLER
SAMPLER
1.6 cm I. D.
30 cm
TOP VIEW OF BUBBLER
BUBBLER
HUMIDIFIED N_2
Not To Scale
SAMPLER

Figure 4. Standard Separator.

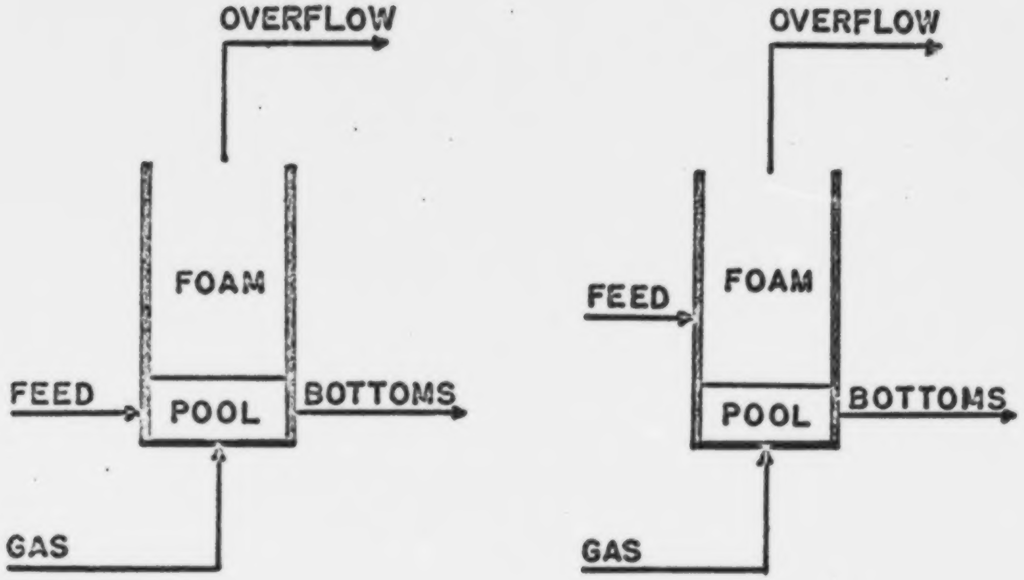
OVERFLOW
FOAM
FEED
POOL
BOTTOMS
GAS
OVERFLOW
FEED
FOAM
POOL
BOTTOMS
GAS

SIMPLE STRIPPER

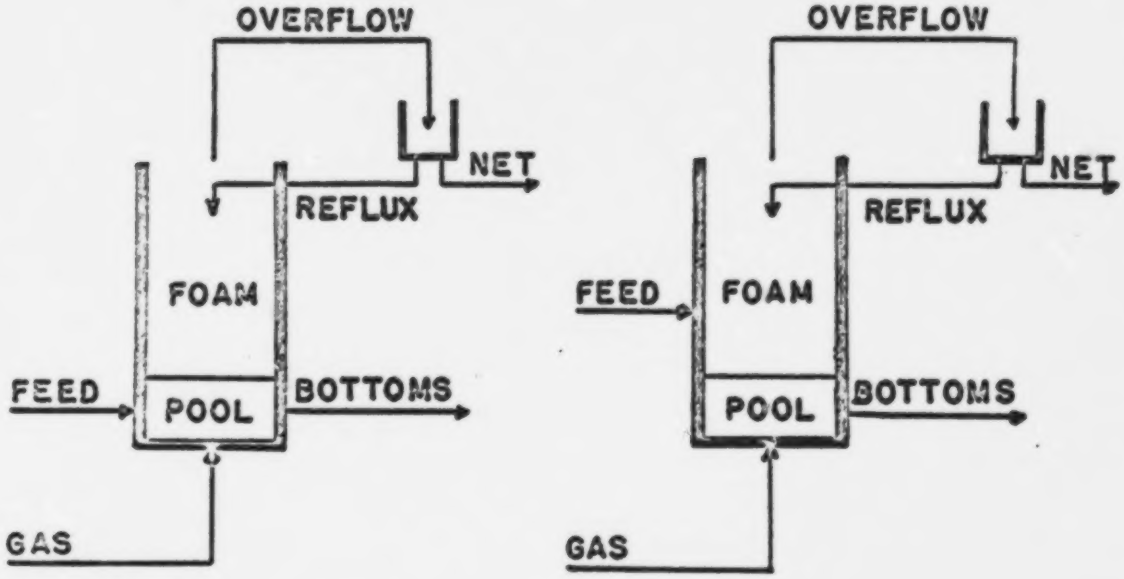
OVERFLOW
NET
REFLUX
FOAM
FEED
POOL
BOTTOMS
GAS
OVERFLOW
NET
REFLUX
FEED
FOAM
POOL
BOTTOMS
GAS

ENRICHER COMBINED

Figure 5. Continuous foam fractionation columns showing four modes of operation.

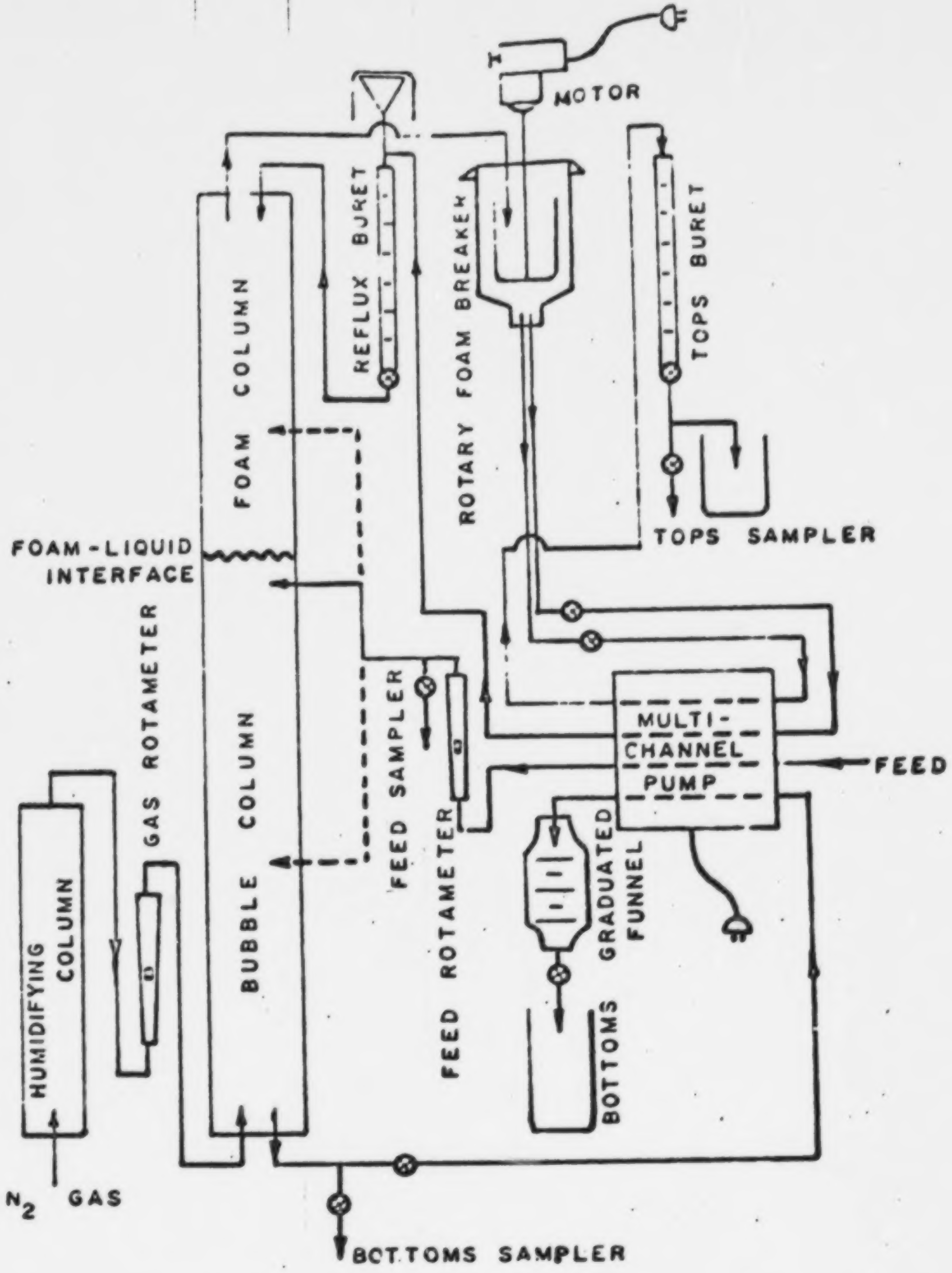
MOTOR
REFLUX BURET
ROTARY FOAM BREAKER
TOPS BURET
FOAM COLUMN
TOPS SAMPLER
FOAM-LIQUID INTERFACE
GAS ROTAMETER
FEED SAMPLER
MULTI-CHANNEL PUMP
FEED
BUBBLE COLUMN
FEED ROTAMETER
GRADUATED FUNNEL
HUMIDIFYING COLUMN
BOTTOMS
N2 GAS
BOTTOMS SAMPLER

Figure 6. Apparatus for studying overall column performance in various modes of operation.

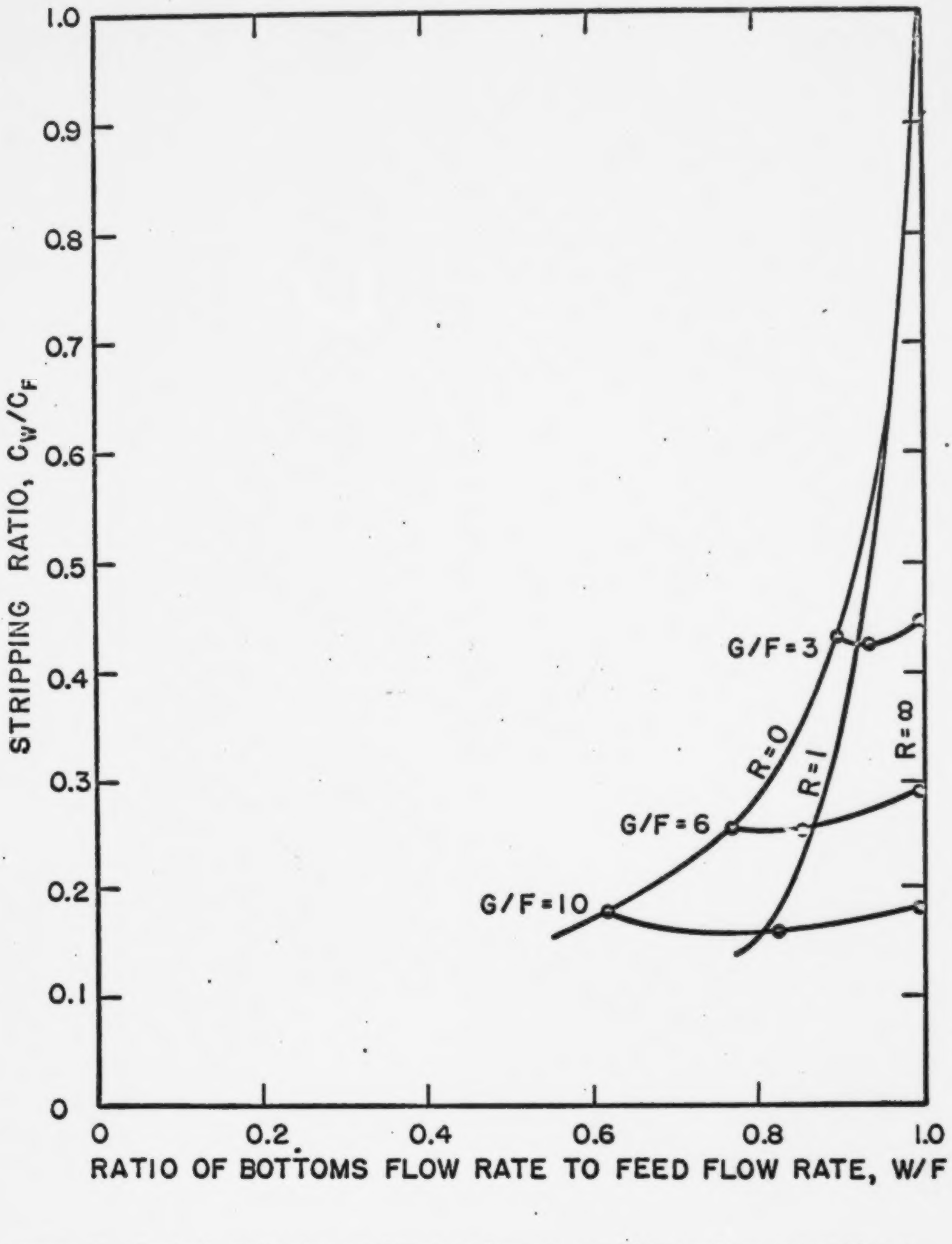

Figure 7. Typical stripping performance from an enriching column separating a surfactant from water. Decreasing ordinate represents improvement in the degree of stripping.

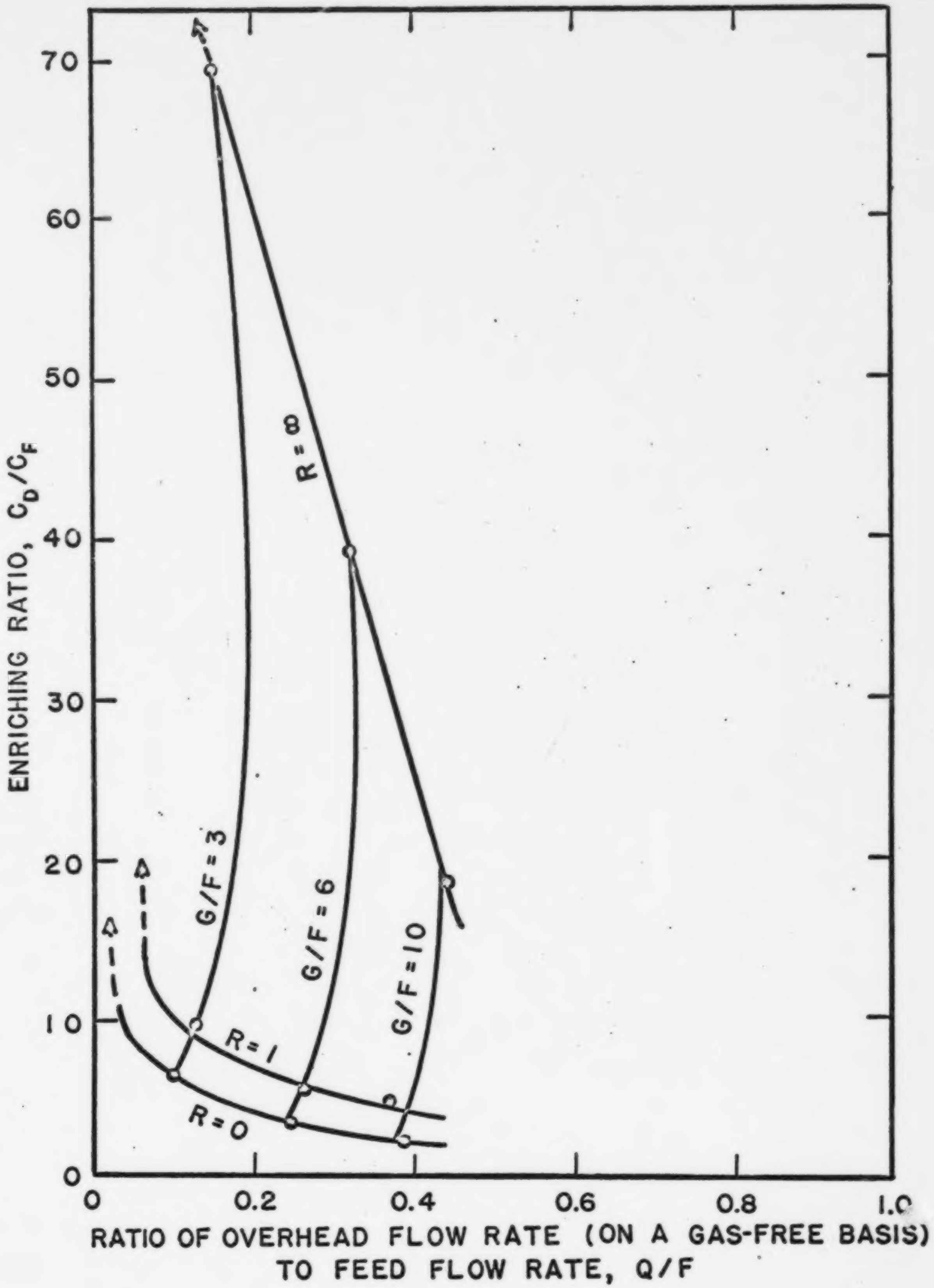

Figure 8. Typical enriching performance for an enriching column separating a surfactant from water. Increasing ordinate represents improvement in the degree of enrichment.

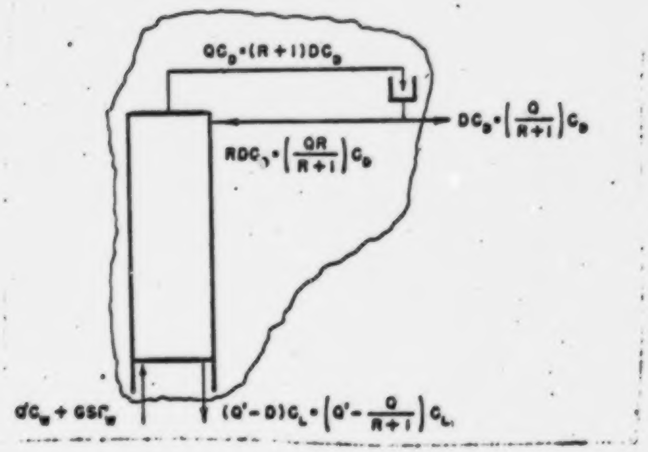
$QC_D = (R+1)DC_D$
$DC_D = \left(\frac{Q}{R+1}\right)C_D$
$RDC_D = \left(\frac{QR}{R+1}\right)C_D$
$Q'C_W + GS\Gamma_W$
$(Q'-D)C_L = \left(Q'-\frac{Q}{R+1}\right)C_L$

Figure 9. Material balance around an enriching column.

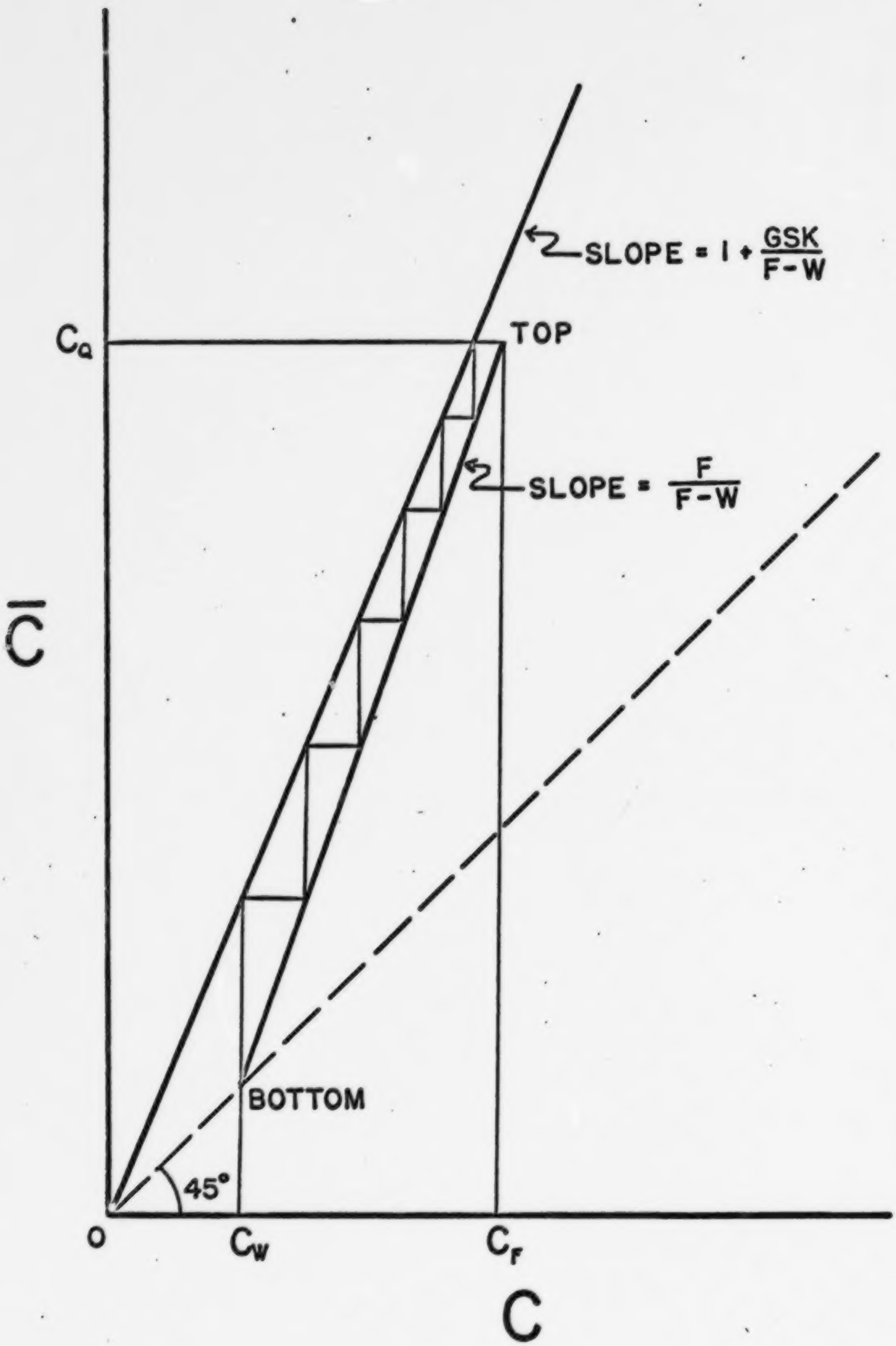
SLOPE = $1 + \frac{GSK}{F-W}$
C_a
TOP
SLOPE = $\frac{F}{F-W}$
$\bar{C}$
BOTTOM
45°
0
C_W
C_F
C

Figure 10. Graphical stagewise calculation (via apparent streams) for a stripper. The equilibrium curve is based on a linear isotherm $\Gamma = KC$.

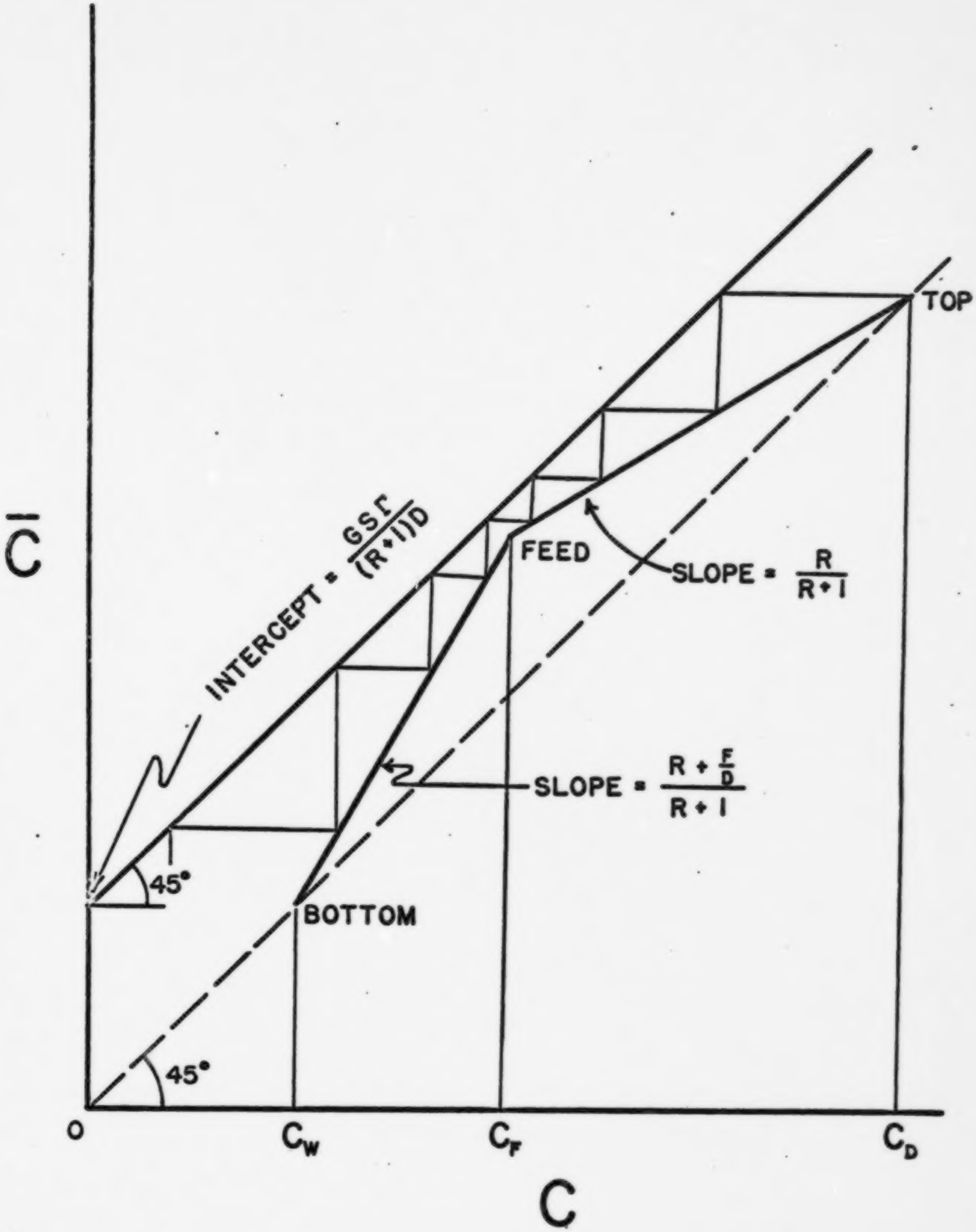

TOP
INTERCEPT = $\frac{GS\Gamma}{(R+1)D}$
FEED
SLOPE = $\frac{R}{R+1}$
SLOPE = $\frac{R+\frac{F}{D}}{R+1}$
45°
BOTTOM
45°
O
C_W
C_F
C_D
$\bar{C}$
C

Figure 11. Graphical stagewise calculation (via apparent streams) for a stripper-enricher combination with feed entering at the match point. The equilibrium curve is based [illegible] Γ.

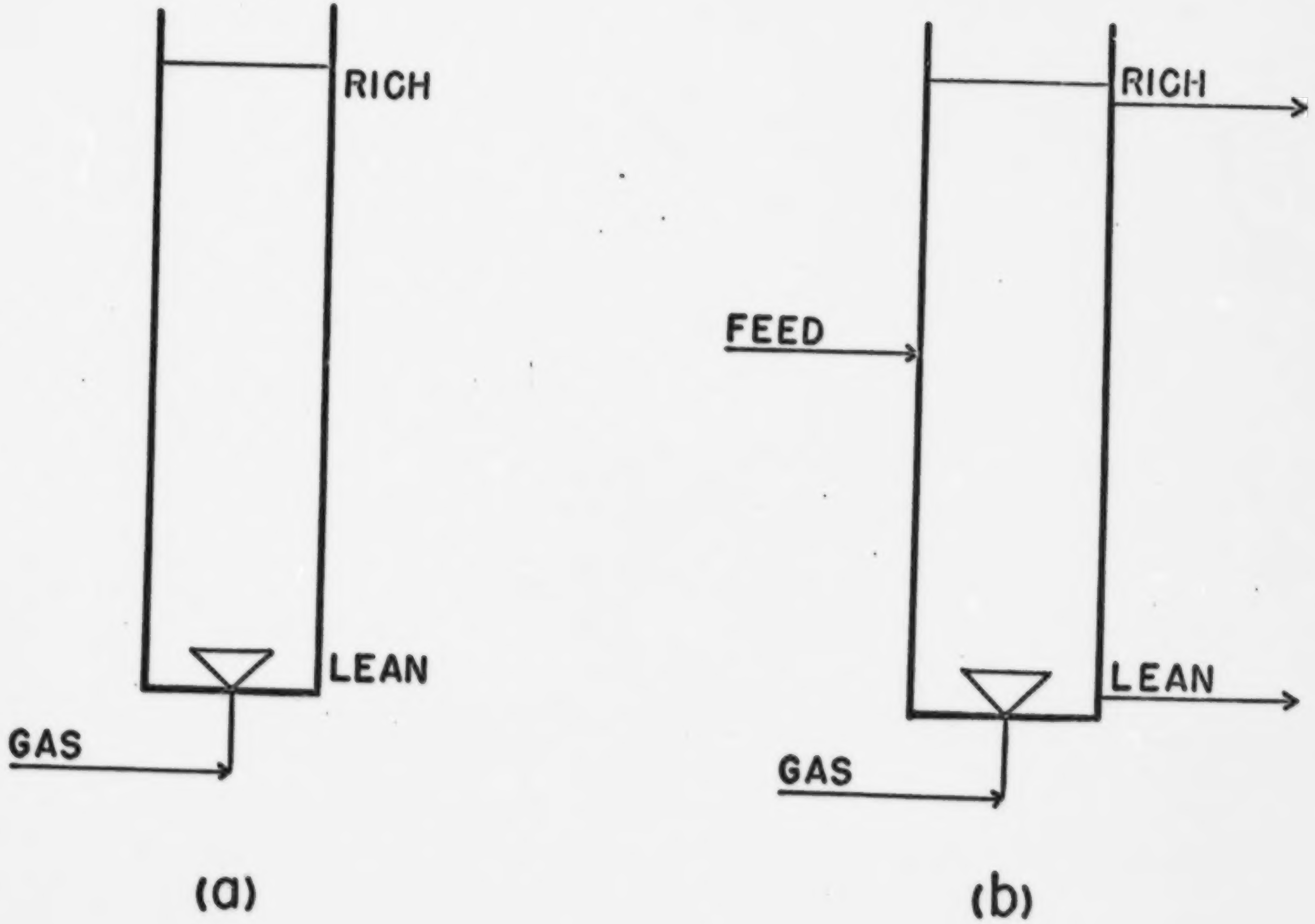
RICH
LEAN
GAS
(a)
FEED
RICH
LEAN
GAS
(b)

Figure 12. Bubble fractionation: a) Batchwise operation, b) Continuous flow operation.

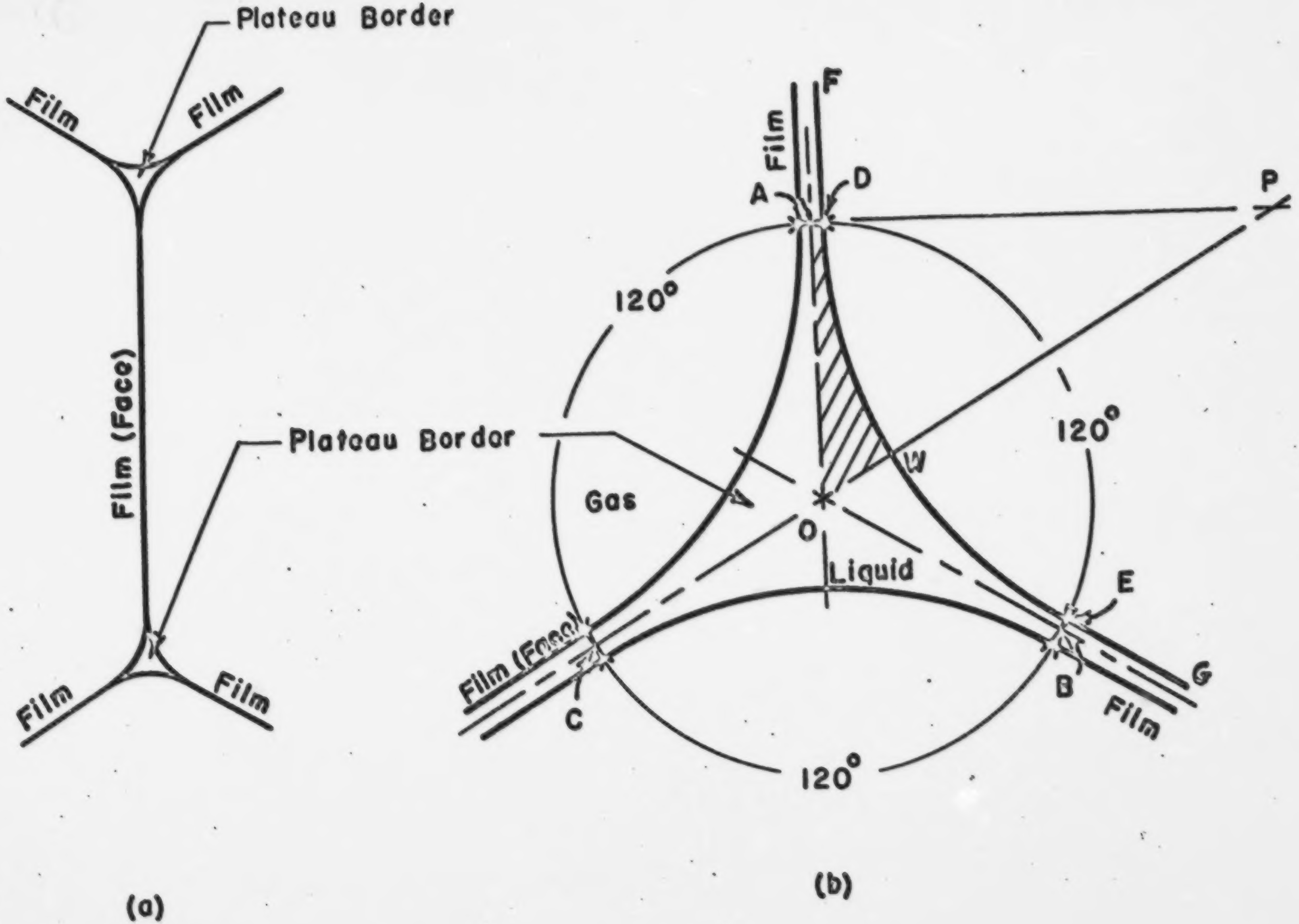
Plateau Border
Film
Film
Film (Face)
Plateau Border
Film
Film
(a)
F
Film
A
D
P
120°
120°
120°
W
Gas
O
Liquid
E
Film (Face)
C
B
G
Film
(b)

Figure 13. Capillaries (Plateau borders) in cross section. a) Two capillaries with the film between them. b) A magnified view of one capillary, illustrating the six-fold symmetry. Capillary wall DWE has the radius r. from point P.

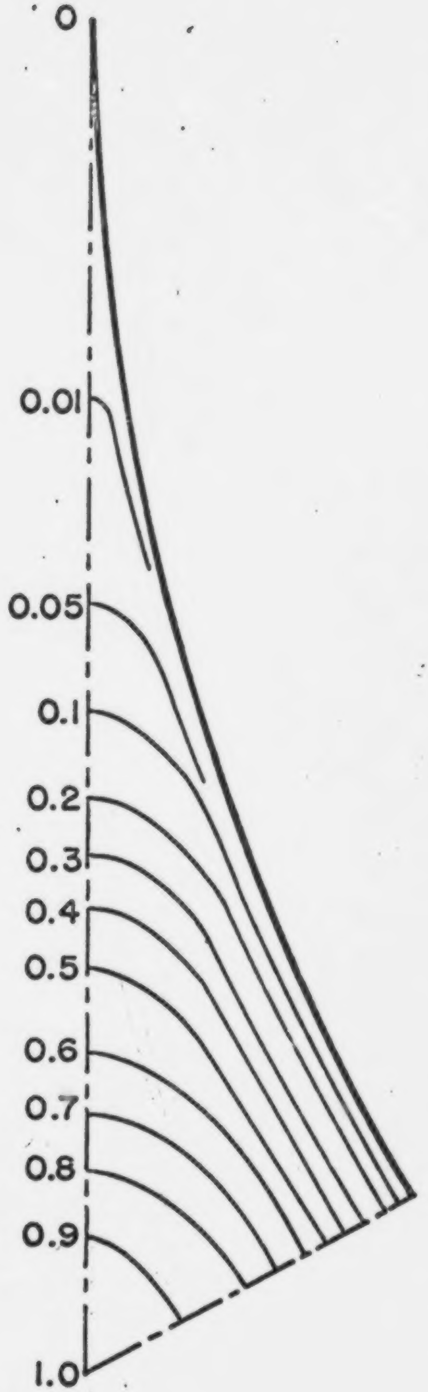

Figure 14. Dimensionless velocity contours within a capillary with a rigid wall; i.e., with $M = 0$. The film thickness shown here is negligible.

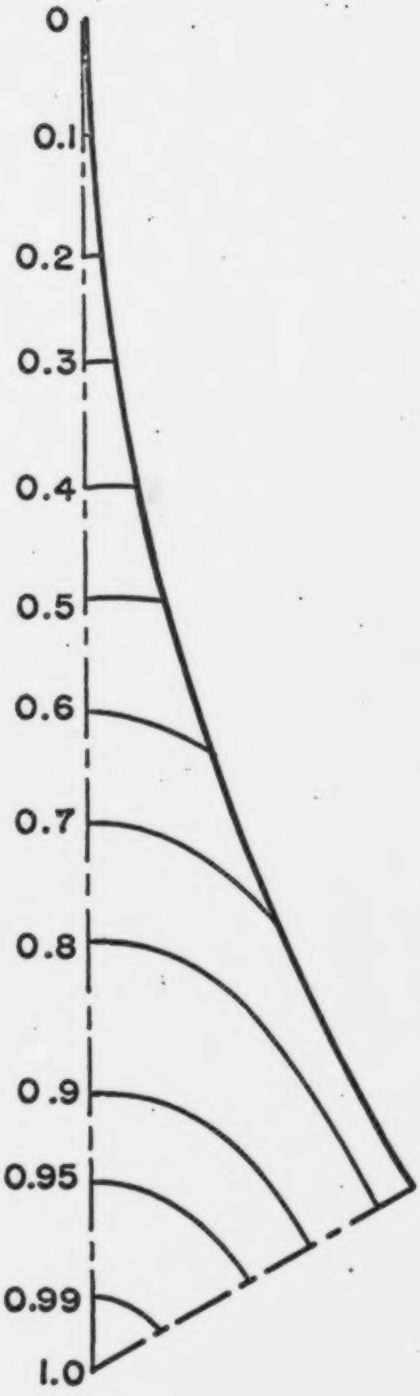

Figure 15. Dimensionless velocity contours within a capillary with a moderately fluid wall of M = 2.48. The film thickness shown here is negligible.

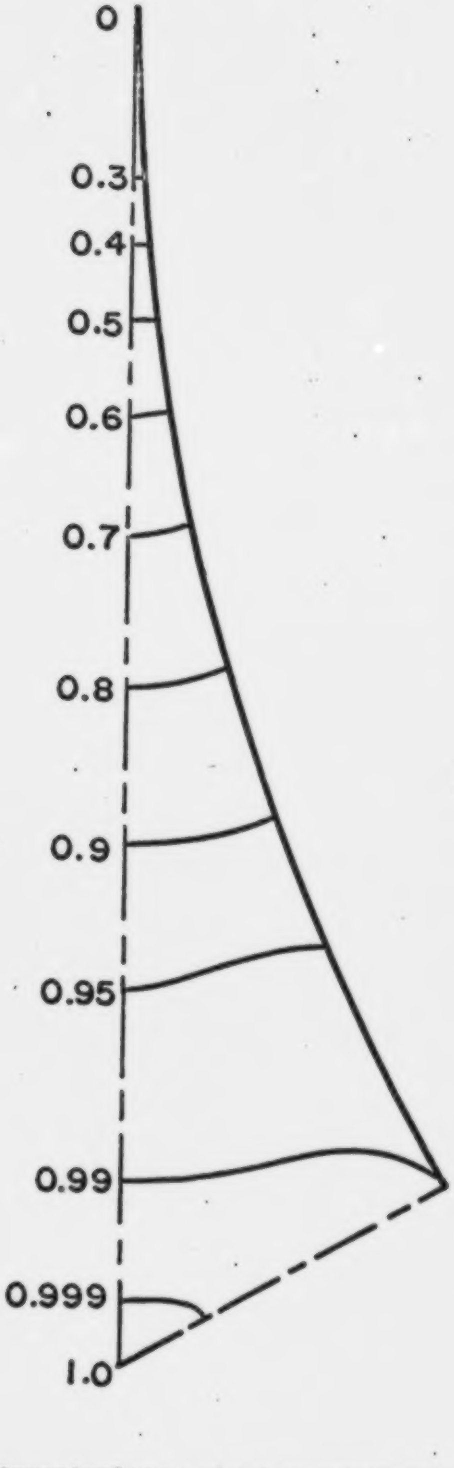

Figure 16. Dimensionless velocity contours within a capillary with a very fluid wall of $M = 61.9$. The film thickness shown here is [illegible]

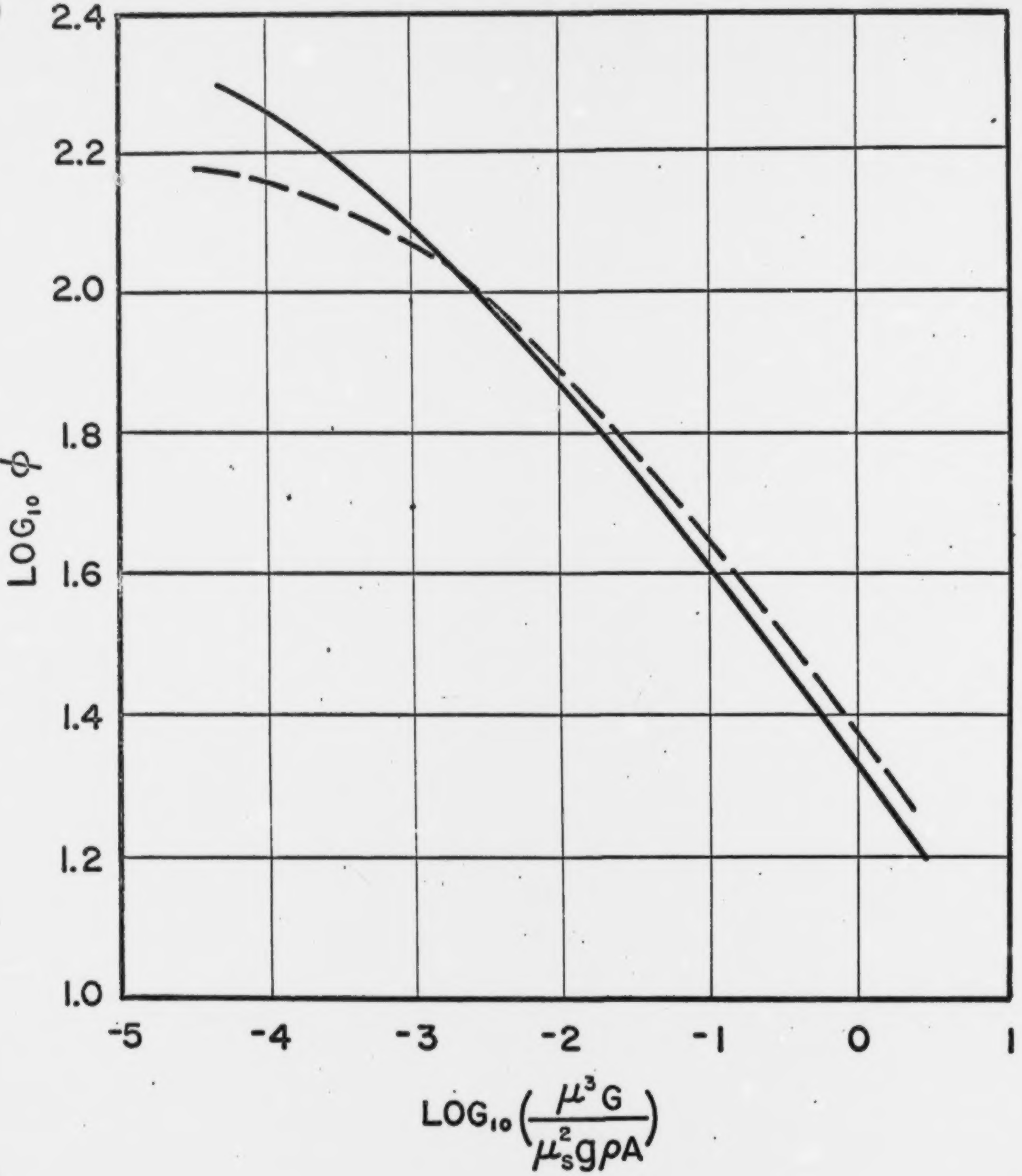

Figure 17. Theoretical evaluation of ϕ. The solid curve (27) has an asymptote of $\log_{10}\phi = 2.41$. The broken curve (22) has an asymptote of $\log_{10}\phi = 2.27$. Use of the solid curve is recommended (35).

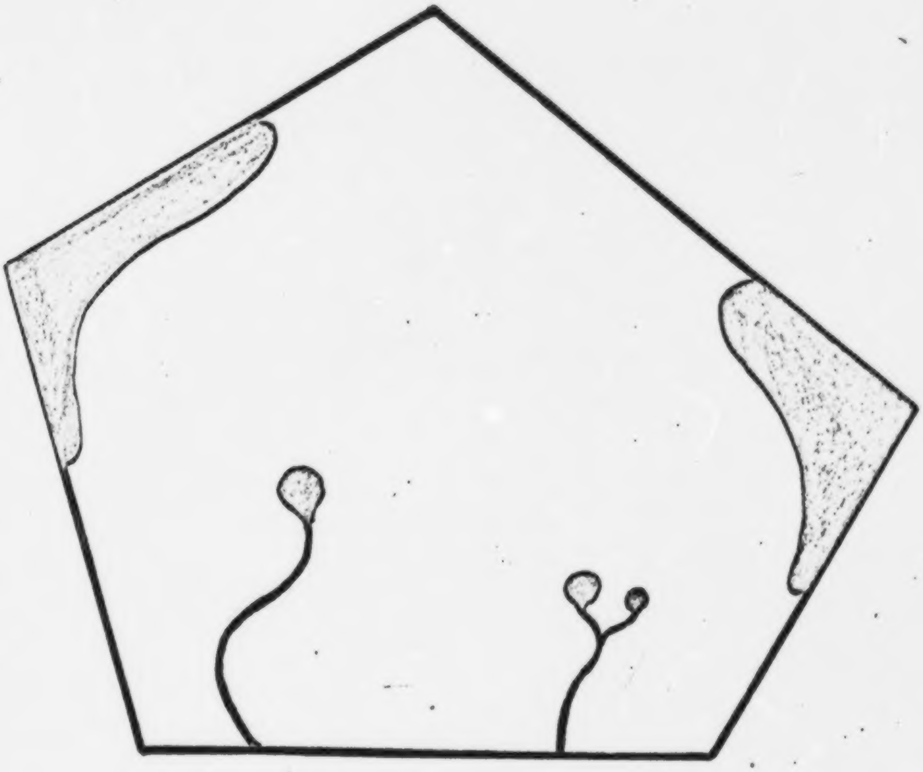

Figure 18. Typical pattern of black in white film, showing the rising black spots.

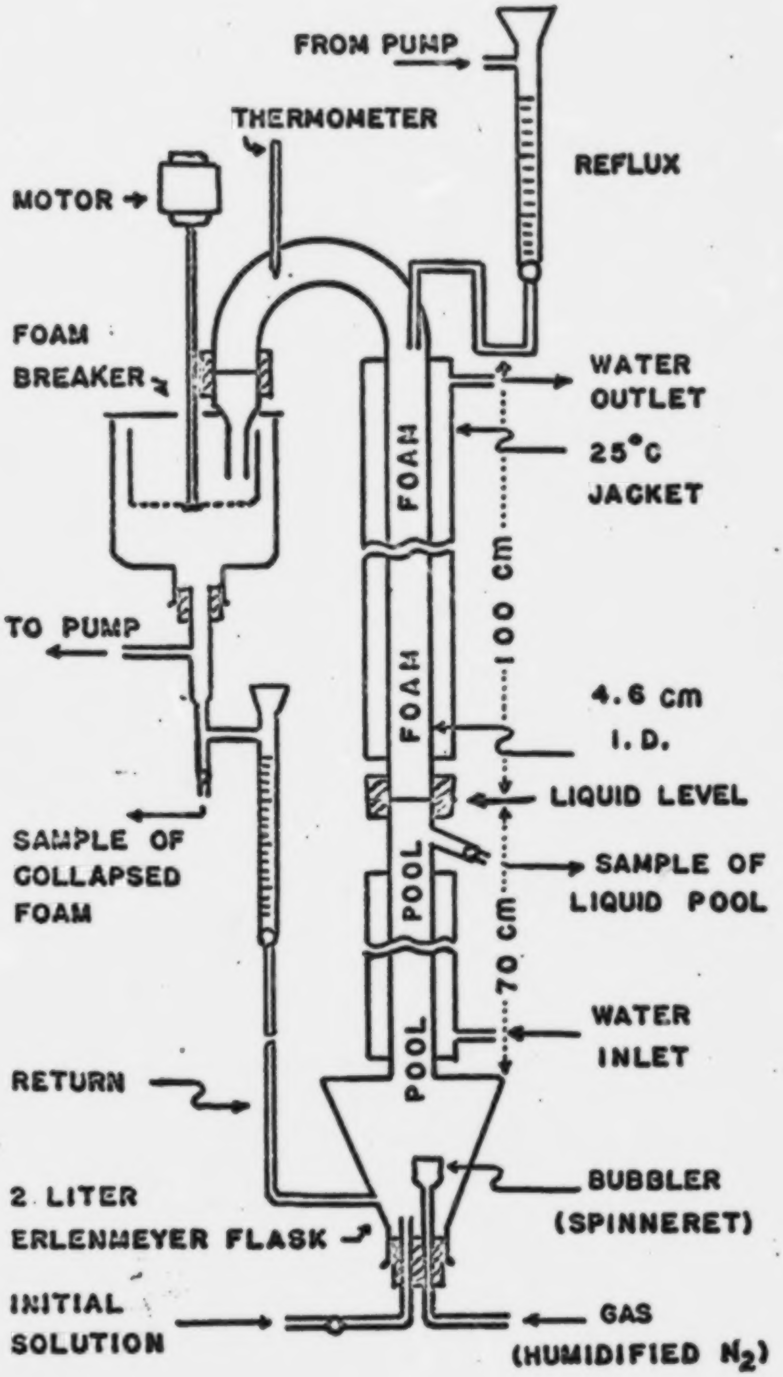
FROM PUMP
THERMOMETER
REFLUX
MOTOR
FOAM BREAKER
WATER OUTLET
25°C JACKET
FOAM
FOAM
100 cm
TO PUMP
4.6 cm I. D.
LIQUID LEVEL
SAMPLE OF COLLAPSED FOAM
POOL
SAMPLE OF LIQUID POOL
70 cm
POOL
WATER INLET
RETURN
BUBBLER (SPINNERET)
2 LITER ERLENMEYER FLASK
INITIAL SOLUTION
GAS (HUMIDIFIED N2)

Figure 19. Foam fractionation column equipped for reflux and return. Seven pairs of electrodes (not shown) are located within the column to measure the bulk foam density at various levels.

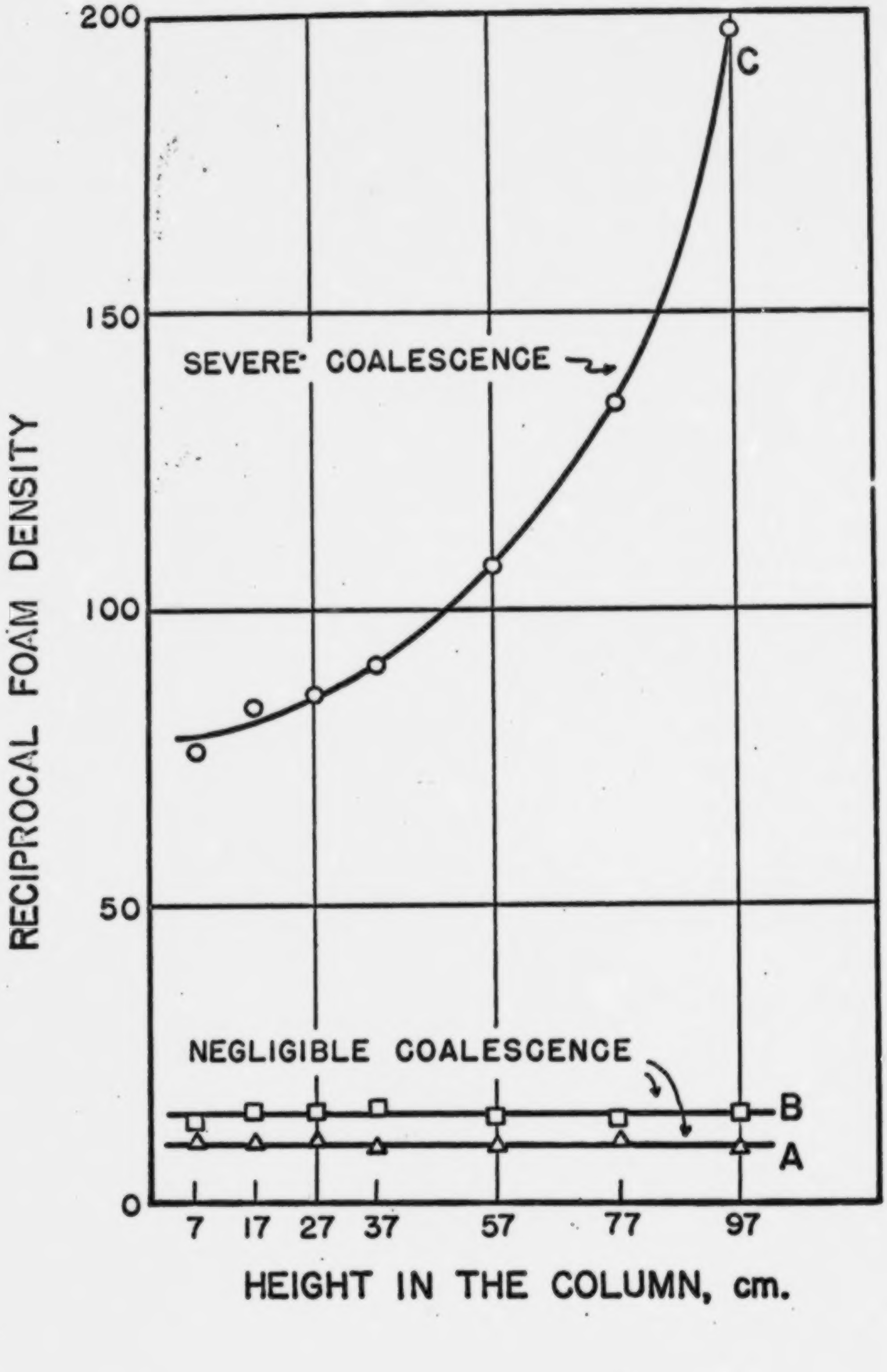

Figure 20. Typical measurements of bulk foam density at various levels within the vertical foam column.

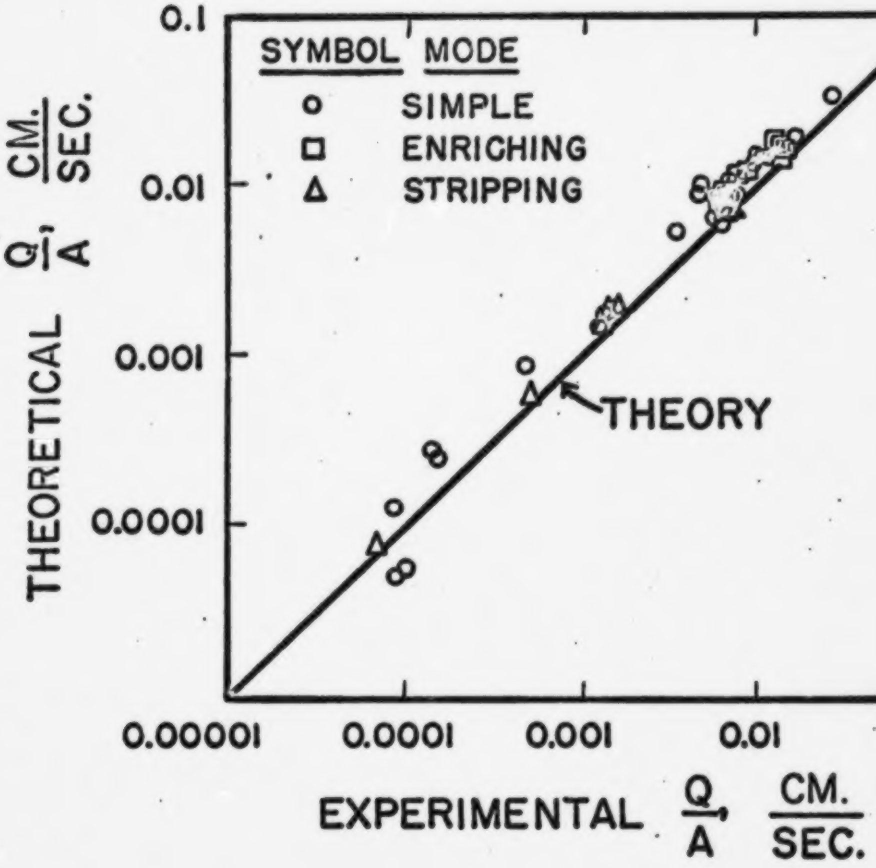

Figure 21. Test of theory for predicting the foam overflow rate.

Note: This paper has been accepted for publication in Industrial and Engineering Chemistry (1968).

ADSORPTIVE BUBBLE SEPARATION METHODS

Foam Fractionation and Allied Techniques

In recent years, interest has quickened in these unusual methods of separation. This review presents the pertinent fundamentals, and covers the reported results for many new systems.

by

Robert Lemlich
Chemical Engineering Department
University of Cincinnati
Cincinnati, Ohio 45221

INTRODUCTION

Over the years there has appeared a growing interest in the separation of materials by foam fractionation and related techniques. Procedures which were once just laboratory curiosities now appear to be feasible for purposes ranging from chemical analysis to plant scale operations.

A number of different systems have now been shown to be separable by these methods. A compilation which appeared in 1962 (120) lists 18 metals, 14 dyes, 4 organic anions, 21 fatty acids and detergents, 22 proteins and enzymes, and some miscellaneous inorganic ions and organic substances. Since then, many more studies have been reported in the literature. The present paper will endeavor to cite the most important of these more recent investigations.

Foam fractionation is based on the selective adsorption of one or more solutes on the surface of gas bubbles which rise through a solution. These bubbles then form a foam atop the main body of liquid. This foam is relatively rich in adsorbed material, and so when it is recovered overhead a partial separation of components results. This is illustrated in Figure 1a for ordinary batchwise operation and in Figure 1b for simple continuous flow operation. The overhead foam is usually collapsed in a foam breaker, and the resulting liquid is termed the foamate*.

The bubbles are usually produced by deliberate sparging. However, foam fractionation can also occur "incidentally" when a foamable solution is simply shaken, or when bubbles are formed by the release of dissolved gas. Indeed, any time a foam is produced, whether it be in the manufacture of rigid foam, the pouring of beer, or the frothing of sea water, some separation of components always takes place.

---

*Unfortunately, the same term foamate has occasionally been used to represent the pool or bottoms. This ambiguity has caused some confusion.

Foam fractionation should never be confused with gas desorption. The former is based on the surface adsorption of generally nonvolatile material. The latter is based on absorption of volatile material into the bubble interior. Furthermore, foam fractionation can enrich as well as strip. (This will be further discussed later.) Gas desorption can only strip.

Historically, foam fractionation in the laboratory goes back at least to the year 1900 (143). At that time foaming was used to remove sodium oleate from aqueous solution in an attempt to experimentally verify Gibbs' adsorption equation. More recently, prior to the wide-spread use of biodegradable detergents, foam fractionation was used on a large scale in several localities to remove detergents from municipal sewage (138).

Studies have shown that even surface inactive components (molecular or ionic) can be removed from solution if an appropriate surface active material is added to unite with the surface inactive material so that it can be adsorbed at the bubble surfaces (122,129). This can occur either through the formation of a chelate or other compound, or through electrostatic (counterionic) attraction by the surfactant layer adsorbed at the surface, or by both types of mechanism.

The surface inactive component so removed is termed the colligend (128) and the surfactant added to effect its removal is called the collector. Various substances, including trace radioactive metallic ions, have been removed this way on a laboratory and pilot plant scale.

CLASSIFICATION OF THE VARIOUS TECHNIQUES

While the body of literature has been growing, so unfortunately has the confusion regarding terminology. Overlap and even contradictions in nomenclature have appeared. In an effort to clarify the situation, five investigators recently proposed a joint set of recommendations for nomenclature (73). The proposal represents a compromise between current usage on the one hand and a more rational systemization on the other.

Figure 2 outlines the proposed scheme of classification. The generic name for all the techniques is Adsorptive Bubble Separation Methods. This name was first proposed by the present writer, along with Adsubble Methods as a convenient contraction (82). Of these methods, those which involve foam or froth are termed Foam Separation. This category is further divided into Foam Fractionation already described, and Froth Flotation or simply Flotation.

Froth flotation involves many subdivisions, as shown in the Figure. Ore Flotation is a special case for the separation of minerals. Typically, ore particles are separated from gangue particles by the selective attachment to rising bubbles (35). Ore flotation is a highly specialized subject for which a very substantial body of literature exists. Accordingly, it will not be dealt with in the present paper.

Other subdivisions of froth flotation include Macroflotation which is the removal of macroscopic particles; Microflotation which is the removal of microscopic particles, especially micro-organisms or colloids (28); Ion Flotation which is the removal of surface inactive ions through the use of a surfactant which yields an insoluble product, especially a removable scum (129); Molecular Flotation which is the removal of surface inactive molecules through the use of a surfactant which yields an insoluble product; Precipitate Flotation in which a precipitate is removed and the precipitating agent is other than the surfactant (5); and Adsorbing Colloid Flotation which is the removal of dissolved material "piggy back" by first being adsorbed on colloidal particles.

Clearly, these subdivisions have much in common with each other and with foam fractionation. For example, the microflotation of colloids (which can be termed simply Colloid Flotation) has often been included under foam fractionation (85). Indeed, much that will be said about the fundamentals of foam fractionation will apply to foam separations in general.

Even in the absence of foam, a separation may still be achieved by virtue of adsorption or attachment at the surfaces of the bubbles in the liquid. This is accomplished by elongating the liquid pool to form a vertical column. The rising bubbles then carry the material at their surfaces to the top of the column where it is deposited as the bubbles pass out. The resulting concentration gradient represents a partial separation.

This procedure is illustrated in Figure 3a for batch operation and in Figure 3b for continuous operation. The method has been named *Bubble Fractionation* (29). It can be used in tandem with foam separation to raise the concentration of an otherwise nonfoaming mixture up to the foaming threshold. This is shown in Figure 3c.

For certain purposes the separation achieved by bubble fractionation can be greatly increased by placing an immiscible liquid on top of the main liquid. This immiscible liquid "traps" the adsorbed material released by the exiting bubbles. This technique is termed *Solvent Sublation* (128).

While the preceding terms cover the recommended nomenclature, other terms have been used from time to time in the literature. Also, it is not unreasonable to expect that new terms for new adsubble methods will appear in time.

In connection with this last point, it is interesting to note that separations can also be achieved by adsorption or attachment at liquid-liquid interfaces. Such techniques of course are not adsorptive bubble separation methods but are rather their droplet analogs. Hence, for this analogous group, the present writer proposes the generic term *Adsorptive Droplet Separation Methods*, with *Adsoplet Methods* as the logical contraction.

In comparison to the adsubble methods, the adsoplet methods have attracted only little attention. Some separations have been reported for *Emulsion Fractionation* (30) which is the analog of foam fractionation. Some work (139) has also been carried out with the emulsionless analog of bubble fractionation which, by logical extension should be termed Droplet Fractionation. Further exploration of the adsoplet methods could prove very interesting.

ADSORPTION

The separation obtained in such methods as foam fractionation depends in part on the extent and selectivity of adsorption at the bubble surface. Under equilibrium conditions, the adsorption at a gas-liquid interface is given by Gibbs (37) as Equation 1.

$$d\gamma = -\underset{\sim}{R}T \sum \Gamma_i d \ln a_i \tag{1}$$

Γ_i is the so called "surface excess". In simple terms, it is essentially the concentration of adsorbed component i at the surface in units such as gm. moles per sq.cm. $\underset{\sim}{R}$ is the gas constant, T is the absolute temperature, a_i is the activity of the i-th component, and γ is the surface tension. For a more detailed discussion of Γ_i, the reader is referred to standard references (1,21,105).

Unfortunately, the practical utility of Equation 1 is limited by the paucity of information regarding activity coefficients and the difficulty in accurately measuring small changes in γ. However, one useful case is that of a nonionic surfactant in pure water at concentrations below the critical micelle concentration (often abbreviated c.m.c.). For such a simple two component system, a_i in Equation 1 can be replaced with the concentration C_i or simply C. This yields Equation 2 for the surfactant.

$$\Gamma = -\frac{1}{\underset{\sim}{R}T} \frac{d\gamma}{d \ln C} \tag{2}$$

With a uni-univalent ionic surfactant, the left-hand side of Equation 2 theoretically becomes 2Γ. However the presence of salts and certain other factors can suppress the coefficient (85).

Figure 4 shows typical variation of Γ, the surface concentration. At very low concentrations, the latter curve is inclined straight through the origin. At higher concentrations it bends and tends to level off. The adsorption isotherms for many substances follow the general profile of Figure 4. This holds true for many surfactants (collectors) as well as many adsorbed colligends. Equilibrium adsorption can often be approximated by a Langmuir type of isotherm (21).

The surface concentration of the major surfactant in a foam usually corresponds to the more or less level portion of the curve in Figure 4. This level portion is often taken as representing an adsorbed monolayer. The surface concentration for the major surfactant in the foam is thus roughly independent of its concentration in the liquid. However, such approximate independence need not apply to other (minor) surfactants or to colligends which may be present. Indeed, for the adsorption of trace colligends such as metallic ions the lower (inclined) linear portion of such a curve applies. This linear isotherm for trace colligends is represented by Equation 3 in terms of an equilibrium constant K.

$$\Gamma = K\ C \qquad (3)$$

Of course, for the nonfoaming adsubble methods such as bubble fractionation, Equation 3 will also apply at equilibrium to the major surfactant if its concentration is low enough. For other conditions, more complicated equilibrium relationships are available (21).

K for the adsorption of a colligend can be affected by the collector (surfactant) concentration. This can obviously come about through an insufficiency of collector. However, it can also be caused by an excess of collector which may compete against the colligend-collector complex for the available surface (122).

The excess collector may also form micelles which are themselves not adsorbed at the surface but which compete against the collector at the surface for the available colligend. In other words, the micelles of collector in the liquid may adsorb some of the colligend, say by electrostatic attraction, and so reduce the amount of colligend adsorbed by the collector at the surface. If this is the mechanism, then the change in the linear isotherm for the colligend, from K_1C at a collector concentration just below the c.m.c. to K_2C above the c.m.c. and therefore in the presence of micelles, is given theoretically (85) by Equation 4.

$$\frac{1}{K_2} = \frac{1}{K_1} + \frac{C_s - C_{sc}}{\Gamma_s E} \qquad (4)$$

C_s is the concentration of the collector in the liquid and C_{sc} is the c.m.c. of the collector. All the additional surfactant above the c.m.c. is assumed to form micelles. Γ_s is the surface concentration of the collector, which is assumed uniform over the range C_{sc} to C_s. E is the effectiveness of the collector molecules at the surface in adsorbing colligend, divided by the corresponding effectiveness of the collector molecules which constitute the micelles. If the two effectivenesses are equal, E is unity.

Various methods have also been proposed to determine Γ experimentally. One of the easiest involves measuring the performance of a foam fractionation column operating in the simple mode (14); i.e., operating as a single theoretical (equilibrium) stage. It can be used to find Γ for surfactants as well as colligends, with or without micelles (85). This method is considered next.

OPERATION IN THE SIMPLE MODE

Figure 1 shows a foam fractionation column operating in the simple mode. In the foam, the surfactant or colligend in question is to be found partly adsorbed at the bubble surfaces and partly in the interstitial liquid. However, the surface is essentially in equilibrium with the interstitial liquid. This liquid is virtually identical with pool liquid if there is no coalescence of bubbles in the rising foam. Thus Γ here is really Γ_W, where the subscript denotes equilibrium with C_W which is the concentration in the liquid pool. Simple material balance then yields Equation 5.

$$\Gamma_W = \frac{(C_Q - C_W) Q\, d}{6\, G} \qquad (5)$$

C_Q is the concentration in the foamate (collapsed foam), Q is the volumetric flow rate of foamate, G is the volumetric flow rate of gas, and d/6 is the volume to surface ratio for a spherical bubble where d is the bubble diameter. For nonuniform bubbles, a surface average is employed according to Equation 6, where n_i is the number of bubbles of diameter d_i in a representative portion of foam.

$$d = \frac{\sum n_i d_i^3}{\sum n_i d_i^2} \qquad (6)$$

In order to determine Γ_W accurately by Equation 5, the operation must be truly in the simple mode. In other words, the column must act as a single theoretical stage. Otherwise Equation 5 will not apply. This means that coalescence within the rising foam must be avoided or at least kept to a bare minimum. Such internal coalescence destroys surface and so releases adsorbed material which flows back down through the rising foam. This rich drainage acts as internal reflux, which enriches the foam. While such enrichment is very useful under certain circumstances, it is highly undesirable in the present context because it causes Equation 5 to yield an erroneously high Γ_W.

Coalescence can be minimized by employing a high gas rate. This keeps the liquid content of the foam high, which in turn keeps the films (lamellae) separating the foam bubbles relatively thick and more resistive to rupture. A high gas rate also holds down the residence time for the foam in the column. So does a very short height of foam. For this purpose, a height of less than 1 inch is desirable. In fact, it may be best to determine Γ_W at several small foam heights and then extrapolate the results to zero height, which of course corresponds to zero residence time. A short residence time minimizes the opportunity for film rupture and thus minimizes coalescence.

When determining Γ_W by operation in the simple mode, collapsed foam can be recycled to maintain the pool concentration, and hence the overall operation, at steady state. This is shown in Figure 5. However, when measuring Γ_W for a colligend, recycle may not be the preferred technique because collector micelles which form in the foamate may not dissociate fast enough upon dilution in the liquid pool. In this event, simple batch operation with a large liquid pool, or simple continuous operation may be employed. For this last case, Γ_W can be determined alternatively from Equation 7 which is derived by combining Equation 5 with an overall material balance for the column.

$$\Gamma_W = \frac{(C_F - C_W)Fd}{6G} \qquad (7)$$

F is the feed rate and C_F is the concentration in the feed. For reasons which will become evident later, Equation 7 is much less sensitive to internal coalescence than is Equation 5.

Bubble diameters in the foam can be measured photographically through the glass wall of the column. However, such measurements are subject to several sources of error including distortion of the individual bubbles at the wall, distortion of the distribution of bubble sizes at the wall, and the statistical bias inherent in sampling a size distribution at a plane rather than by count through its volume (26). At least the last two sources of error can be minimized by generating bubbles of fairly uniform size. This is often most easily accomplished by using a bubbler with identical orifices such as a spinneret, or simply a bubbler with a single orifice.

Bubble diameters can also be measured photographically in the liquid pool, utilizing an external surrounding pool bounded by flat walls to eliminate optical distortion. Alternatively, if a single orificed bubbler is employed, the bubble diameter can be determined by combining a stroboscopic count of the frequency with an external volumetric measurement of the gas flow rate (89).

Several other points are worth noting. A bubbler immersion of one foot or more should insure good contact. Prehumidifying the nitrogen (or other nonreactive gas) eliminates any spurious evaporative effects. A wide pool discourages vertical concentration gradients in the liquid. Such gradients are undesirable when measuring Γ_W

since they lend uncertainty to C_W.

Of course the simple mode is not merely a means for measuring surface concentration. For certain situations it is also an effective means of separation in its own right. When Γ_W is known, the separation achieved by steady continuous flow operation in the simple mode is expressed by rearranging Equations 5 and 7 to yield Equations 8 and 9 respectively.

$$C_Q = C_W + \frac{6\ G\ \Gamma_W}{Q\ d} \qquad (8)$$

$$C_W = C_F - \frac{6\ G\ \Gamma_W}{F\ d} \qquad (9)$$

OPERATION IN OTHER MODES

As with other methods of separation such as distillation or liquid extraction, operation in foam fractionation is not limited to one theoretical stage. Figure 6 shows three higher modes with the simple mode for comparison. Stripping operation further purifies the bottoms, enriching (refluxing) operation further concentrates the flow overhead, and combined operation does both.

In the stripping mode, the feed enters some distance above the pool and trickles down through the rising foam. With sufficient height, the interstitial liquid of pool concentration is replaced with liquid of feed concentration. Accordingly, the separation achieved by a tall stripping column in continuous flow operation is given by Equations 10 and 11.

$$C_Q = C_F + \frac{6.59\ G\ \Gamma_F}{Q\ d} \qquad (10)$$

$$C_W = C_F - \frac{6.59\ G\ \Gamma_F}{W\ d} \qquad (11)$$

While the stripping column should theoretically be infinitely tall in order for Equations10 and 11 to apply, a height of several feet is often more than sufficient to allow the concentration in the interstitial liquid to approach that of the feed.

While the bubbles are essentially spherical in the liquid pool, they press together in the foam to form blunted polyhedra. In foams of low liquid content, such as are generally desirable for foam fractionation, bubbles of uniform size may be approximated as regular dodecahedra (1,9,98). The factor of 6.59 in Equations 10 and 11 accounts for the resulting increase in surface. However, the factor 6 is retained in Equations 5, 7, 8 and 9 because in the simple mode the resulting increased adsorption is at the expense of material already trapped in an interstitial liquid which is not replaced by a richer feed.

In the enriching mode, some collapsed foam serves as reflux and drains back down through the rising foam. The resulting countercurrent contact enriches the rising interstitial liquid and, unless the surface is saturated with the component in question, enriches the surface as well. Either way, the result is to enrich the overflow. This has been well verified experimentally (86,125).

Reflux may be external as shown in Figure 6 , or it may be internal resulting from internal coalescence. The importance of internal reflux is too often overlooked.

Unlike the tall stripper, in a tall enricher the concentration pinch between the rising stream and the downcoming liquid (reflux) occurs just above the liquid pool (14,85). Material balances around the foam in the column and around the entire column yield Equations 12 and 13.

$$C_D = C_W + \left(6.59 - \frac{0.59}{R+1}\right)\frac{G\,\Gamma_W}{D\,d} \qquad (12)$$

$$C_W = C_F - \left(6.59 - \frac{0.59}{R+1}\right)\frac{G\,\Gamma_W}{F\,d} \qquad (13)$$

R is the reflux ratio. D is the net collapsed overhead product, Q/(R+1). Equations 12 and 13 are for continuous enriching in a tall column with external reflux. Equation 12 also applies to batch operation if the holdup in the foam is small relative to the pool.

In practice, an enriching height of several feet is often sufficient to qualify as "tall" (again theoretically infinite) provided the reflux ratio is not too high (14). For larger reflux ratios, greater height is needed in order for Equations 12 and 13 not to predict too high a separation. However, Equation 13 is much less sensitive than Equation 12 in this regard. Solving Equation 13 for Γ_W yields a result which is quite close to Equation 7. It is for this reason that Equation 7 was earlier characterized as relatively insensitive to internal coalescence (internal reflux).

The coefficient $\left(6.59 - \frac{0.59}{R+1}\right)$ comes about from the limited replacement available for the incremental adsorption by the dodecahedra in an enricher. Of course the entire coefficient only varies from 6 to 6.59, so that for convenience it could simply be approximated by 6.3.

A combined column consists of an enriching section atop a stripping section. If both sections are sufficiently tall, the concentration pinch between the counterflowing streams should occur at the level of the feed. This results in Equations 14 and 15 for a tall combined column (88).

$$C_D = C_F + \frac{6.59\ G\ \Gamma_F}{D\ d} \qquad (14)$$

$$C_W = C_F - \frac{6.59\ G\ \Gamma_F}{W\ d} \qquad (15)$$

Equation 15 is identical with Equation 11.

When separating a colligend, the presence of micelles in the reflux can shift the equilibrium adversely. But interestingly enough, for a sufficiently tall column the overall effect of the micelles should be nil. They should all be transferred from the downflowing interstitial liquid to the upflowing interstitial liquid by the time the downflowing liquid reaches the feed level (or the pool in the case of the enricher alone). As a result, the pertinent material balances should remain unaffected, and so Equations 12-15 should remain unchanged.

For stripping, enriching, and combined columns which are not sufficiently tall, Equations 10-15 may be viewed as upper limits of performance. Actual performance for shorter columns is given in terms of theoretical stages or transfer units. For this purpose, the use of a revised equilibrium diagram to allow for the upflowing liquid as well as the upflowing surface is recommended (85). An effective upflowing stream concentration $\overline{C}$ is defined according to Equation 16.

$$\overline{C} = C + \frac{GS\Gamma}{U} \qquad (16)$$

Γ is taken in equilibrium with the upflowing interstitial liquid concentration C in accordance with Figure 4 or its equivalent. S is the surface to volume ratio for the foam bubbles, say 6.59/d. U is the upflow rate. For the sake of simplicity (85), U can be equated to Q. Equation 16, with $\overline{C}^{*}$ replacing $\overline{C}$, is now the revised equilibrium relationship. Foam fractionation is thus analogous in a sense to distillation with entrainment. The bubble surfaces correspond to the vapor and the rising interstitial liquid corresponds to the entrainment.

Next, operating lines are derived in the usual manner from material balances. Such lines have as their slope $\frac{\Delta\overline{C}}{\Delta C} = \frac{L}{U}$, where L is the downflow rate and C is now the downflow concentration. Finally, theoretical stages are calculated or "stepped off" graphically. This is shown in Figure 7 for the case of a combined column separating out a surfactant with a constant Γ.

Alternatively, transfer units can be employed. Based on the upflowing stream, the number of transfer units in the foam is given by Equation 17.

$$\text{N.T.U.} = \int_{\overrightarrow{C_W}}^{C_Q} \frac{d\overline{C}}{\overline{C}^{*}-\overline{C}} \qquad (17)$$

For the case of a stripper separating a colligend for which the linear equilibrium isotherm $\Gamma = KC$ applies, Equation 17 becomes Equation 18.

$$\text{N.T.U.} = \frac{F}{GSK-W} \ln \frac{F(GSK-W)\frac{C_F}{C_W} + FW}{GSK(GSK+F-W)} \qquad (18)$$

The liquid pool is generally considered to be one theoretical stage, unless it is deliberately elongated and narrowed to furnish additional separation by bubble fractionation.

The height equivalent to a theoretical stage or to a transfer unit depends on the conditions of operation. Fortunately, foam is a good packing when its liquid content is less than say 10%. The curvature of the capillary walls within the foam acts to suck liquid from wetter portions to drier portions, thus opposing the channeling of liquid and improving its distribution. Under reasonably favorable operating conditions, an H.T.U. on the order of several inches or better can be expected, at least with simple surfactants. In a column exceeding several inches in diameter, feed and reflux distributors are advisable, especially for wetter foam (58).

Increasing the gas velocity increases the rate of surface generation. However, it also increases the liquid content of the foam. When the volume fraction of liquid in the foam rises much above 0.30, the bubbles become highly mobile relative to one another. Channeling becomes excessive and countercurrent contact becomes poor (58,104). The dispersion is no longer a true foam but a so called "gas emulsion" (10). Such conditions are poorly suited to refluxing or other countercurrent operations. However, for operation in the simple mode when maximum throughput is desired and the high liquid content in the foam can be readily handled, a gas emulsion may be employed (145).

Columns with bubble caps passing foam through their slots show efficiencies of up to 30% (145). Sieve plates, with foam passing up the former downcomers and liquid dripping down through the holes, yielded separations no better than those obtained with the bare column (89). Of course, if desired, individual columns can be connected in countercurrent array (6).

In practice, the gas employed can be air if its chemically reactive properties pose no problem, or are beneficial. Similarly, prehumidification can be omitted if the evaporative effects are unimportant.

FOAM DRAINAGE AND OVERFLOW

With the regular dodecahedron as the model for a typical foam bubble in a reasonably dry foam, the bubble films (faces) meet three at a time to form capillaries with a cross section that may be idealized by Figure 8. Drainage in such a foam occurs primarily through these capillaries rather than through the films (98,103).

The linear velocity of flow at any point in such a capillary has been calculated from the pertinent independent variables by means of the partial differential equation for steady incompressible rectilinear flow of a Newtonian liquid, plus appropriate boundary conditions (88). These latter include momentum transfer to and within the capillary wall. In general, the wall is not rigid. Rather, it experiences flow subject to a surface viscosity, μ_s.

Surface viscosity is a measure of the resistance to flow in a surface. It has the units of dyne sec/cm. This compares with the conventional viscosity, μ, which has the units of dyne sec/cm^2 and measures resistance to flow within a volume. The importance of μ_s

as a factor for foam drainage is well established (21,105).

The calculations were carried out for Newtonian μ_s by means of finite difference approximations (90) with a digital computer. The resulting velocity profile for a typical capillary was combined vectorially with the upward velocity of the bulk foam moving in plug flow. The net velocities so obtained were then integrated over the horizontal cross sections of all capillaries cut by an arbitrary horizontal plane, with due regard for the essentially random positions of the capillaries (85,88).

For a fairly dry foam, the results for a vertical column are given by Equation 19.

$$Q = \frac{G^2\mu}{Ag\rho\, d_o^2}\,\phi\left(\frac{\mu^3 G}{\mu_s^2 g\rho A}\right) \qquad (19)$$

where A is the cross section of the empty column, g is the acceleration of gravity, and ρ is the liquid density. For nonuniform bubble sizes, the average bubble diameter d_o is evaluated according to Equation 20.

$$d_o^2 = \frac{\sum n_i d_i^3}{\sum n_i d_i} \qquad (20)$$

Since appreciable internal coalescence is almost always present, d_o should be evaluated near the top of the vertical column. However, d for Equations 5-15 is theoretically better evaluated at the bottom.

Function ϕ depends on the detailed relationship between interstitial downflow and bulk foam upflow. Figure 9 shows a solid curve and a dashed curve as the results of two alternative theoretical evaluations (32,88). Use of the solid curve is recommended, although the difference between the two curves is small, especially in the usual region of interest.

If the foam is wetter, the results are more complicated than Equation 19. They are expressed by certain interrelated dimensionless relationships (88). However, these can be conveniently approximated by simply multiplying Q from Equation 19 by the quantity $\left(1 + \frac{3Q}{G}\right)$. For extremely wet or highly coalescing foam the theoretical model breaks down.

Equations 19 and 20 together with Figure 9, plus the wetness factor of 1 + 3Q/G if needed, predict the rate of foam overflow by means of theory alone. No empirical factors are involved.

So far as the present writer is aware, the above theory is by far the most highly developed to date. Other approaches (11,37,59, 69,101,113) are more empirical. They do not quantitatively include the proper shape of the capillary cross section, the randomness of capillary orientation, or the fluidity of the capillary walls. As a result, these other approaches involve various empirical constants.

A recent paper (121) compares the trend of some independently gathered experimental data for foam overflow against the trends predicted by the present theory (88) and another (59). Closer agreement was reported with the trend of the other theory. However, the range of the data was small compared to that of theory. Subsequent calculation of absolute values (83), rather than merely trends, reveals that agreement is actually closer with the present theory.

While the present theory does not involve empirical factors, certain physical properties must nevertheless be known. The liquid viscosity, μ , and liquid density, ρ , can be easily measured by conventional means. However, μ_s is another matter. Probably the best method of measuring surface viscosity for subsequent use in foam overflow calculations is to actually run a foam column with the system in question, measure or otherwise determine Q, G, μ , A, g, ρ , and d_o, substitute in Equation 19 (utilizing the wetness correction factor if needed), and solve for μ_s. This method of finding μ_s reduces the ultimate effect of both the experimental error and the limitations of theory.

Surface viscosity values determined in this manner (89) for aqueous solutions of the nonionic surfactant Triton X-100 agree reasonably well with the independent value obtained (89) by the rough but simple method (103) of timing the rise of "black" spots in the silver-white films of well-drained standing foam. This latter method yielded a μ_s of 1 x 10^{-4} dyne sec/cm at 25°C.

Surface viscosities on the order of 10^{-4} dyne sec/cm are common for simple detergents. For certain protein and other solutions they are considerably higher. These higher surface viscosities are likely to be less Newtonian. They may also decrease sharply at certain temperatures (8). Based on incomplete studies (131), the surface viscosities for some of these solutions as determined by foaming may not agree with the high values obtained by other methods.

It is worth mentioning in passing that surface viscosities which are high enough to reduce the two-dimensional surface mobility in the films may significantly decrease the mass transfer between counterflowing streams by increasing the H.T.U. This would come about as a result of decreased transport between the capillaries and the more rigid films.

Figure 10 shows the result of a test (132) of the aforementioned theory for predicting the rate of foam overflow. The theoretical prediction is obtained from Equation 19 together with the solid curve of Figure 9 and the wetness correction factor $(1 + \frac{3Q}{G})$. Several aqueous systems are considered. The experimental data (6, 13,14,31,32,87,89) cover a wide range of variables. Simple, stripping, and refluxing operations are included. For the sake of impartiality, the independent μ_s value of 1×10^{-4} dyne sec/cm determined by the black spot method is employed for Triton X-100. Inspection of the figure reveals reasonably good agreement between theory and experiment.

The general theory for foam drainage (88) also offers a method for predicting the rate of steady interstitial flow through a stable stationary foam fed continuously at its top with liquid (132). The prediction is in terms of d_o, A, ρ, g, μ, μ_s, and bulk foam density. Results so obtained have generally been good, and in accord with other aspects of the theory.

The general drainage theory also predicts uniformity in the bulk foam density along any one section of the vertical column provided there is no coalescence in the rising foam. This means a single value for bulk foam density throughout the stripping section, another throughout the enriching section, and another throughout the vertical top disengaging section. Due to interstitial downflow, this last density is considerably greater than $\frac{Q}{Q+G}$. For simple operation, there would of course be just one value of bulk foam density throughout the vertical column. Again, it would be greater than $\frac{Q}{Q+G}$. All this presupposes no coalescence in the column section or sections in question.

The uniformity prediction also neglects the very small effect of hydrostatic head on bubble volume which, for an aqueous foam with a bulk density of say 0.1, is only about 0.3% per foot of foam height. The small effect on the bubble volume of the friction head in moving the bulk foam is also neglected. It is worth mentioning in passing that by measuring gas rate and timing foam rise, it is easy to verify that foam generally rises through a column of uniform cross section in essentially plug flow.

These predictions of theory relating to bulk foam density may at first glance appear to run counter to casual intuition. For this reason it is well to remember that a continuously generated uncoalescing foam in a foam fractionation column is in a sense at steady state, while a standing unfed foam is not.

The theoretically predicted uniformity in bulk foam density has been amply borne out by experiments using columns equipped with a series of calibrated electrical conductivity cells to measure the local foam density in situ during operation (32,131). Once again, this uniformity presumes no coalescence. When coalescence is present to an appreciable extent, and it often is, the bulk foam density then decreases up the column.

COALESCENCE

Coalescence in foam is of two types. The first arises from the small difference in pressure between adjacent bubbles of differing size. As a result of the surface tension, the smaller bubble has a higher pressure than the larger (1,10). This causes gas to diffuse from the smaller bubble, across the film, to the larger bubble. The larger bubble accordingly grows larger while the smaller continues to shrink. Given sufficient time, the smaller bubble will disappear entirely. The overall effect, of course, is a decrease in film surface area.

The manner in which the bubble size distribution changes due to interbubble gas diffusion can be estimated (26). The phenomenon can be quite significant in a standing foam. It can also be significant in say the slowly generated scum-bearing froth of batchwise ion flotation. However, it is usually not important with the continuously overflowing foams employed in foam fractionation due to their short times of existence.

The second cause of coalescence is the rupture of film between bubbles. This can be significant in a standing foam as well as in the moving foam of a foam separation device.

The stability of film is commonly ascribed in large measure to the so called Marangoni effect. This is the inability of surfactant molecules to diffuse instantaneously to any locally stretched area in the film surface. The resulting lag permits the stretched surface to be momentarily depleted of surfactant. This produces a local rise in surface tension which opposes the stretching force, thus tending to "heal the wound".

A second but somewhat similar mechanism of foam stability is called the Gibbs effect. It involves the possible insufficiency of molecules within the film liquid to completely recoat the stretched surface regardless of diffusion rate.

A third mechanism, which may be important with some ionic surfactants, is the electrostatic repulsion between the charged parallel surfaces of the film. This repulsion opposes film thinning and hence also opposes rupture.

The second and third mechanisms are more likely to be operative in thin films. Actually, the relative importance of the three effects is still a matter of controversy.

In view of such uncertainty, it is not surprising that film rupture is very difficult to predict. Some approaches which have been employed (78) yield activation energies of rupture which are proportional to the square of the film thickness. However, there is poor agreement as to the cause of the rupture. The various suggestions which have been put forth from time to time include external vibration, pressure fluctuation, thermal fluctuation, spontaneous vapor nucleation, cosmic radiation, and local stresses related to readjustment of the bubble matrix as a result of interbubble gas diffusion.

Whatever the cause, coalescence within the rising foam furnishes internal reflux. For external reflux, either "dephlegmation" or external coalescence is required.

By analogy with distillation, dephlegmation is the deliberate partial collapse of the foam at the top of the column. This is accomplished by some suitable mechanical or thermal means, and/or widening the top of the column so as to decrease the upward linear foam velocity and increase the residence time. By whatever means accomplished, the reflux so created drains back down through the rising foam thus enriching it. The uncollapsed portion of the foam simply flows off overhead. It can then be separately broken later.

With external coalescence, all the overhead foam is broken in some suitable manner. A portion of this collapsed foam is then returned as reflux.

Mechanical methods for collapsing foam include slowly rotating perforated centrifuges (85) which can be improved by discharging aqueous foamate on to Teflon instead of glass (58); running foamate on to the foam in order to break it (15) (which works if the foam stability is not too high); discharging the foam on to a rotating disk (38); applying sonic or ultrasonic vibration; and other means (38). Where thermal degredation is not a problem, it may be convenient to break the foam by passing it through a short conduit surrounded by a steam or hot water jacket (74,77). Chemical methods of foam breaking (112) may be employed, but obviously they are generally not desirable for producing reflux.

RECENTLY REPORTED ADSUBBLE SEPARATIONS

During the past few years a number of publications have appeared describing the separation of various substances by foaming. These have usually involved aqueous systems.

The separation from water of the anionic surfactant Aresket 300 (14), the nonionic surfactant Triton X-100 (61) [as corrected (85)], the cationic surfactant ethylhexadecyldimethylammonium bromide (57,147) at various temperatures (45) in the presence of inorganic acids and bases (44), and other surfactants (49,51) have been studied. The last named surfactant has been used to remove orthophosphate with optimum results at a pH of 8 to 9 (48), to remove phenol with optimum results at a pH of 11.6 (41), and to remove dichromate (52,56). This last separation has also been accomplished through the release of dissolved air with the aid of a nonionic polymer as a flocculant (50). Sodium phenolate has been removed by diazo coupling (75), and by the action of the surfactant cetyltrimethylammonium bromide (65). The removal of other phenolic compounds has also been reported (67). The components of various surfactant mixtures have been selectively separated (77,133,134).

Methyl orange and protonated 1-naphthylamine have been removed by foam fractionation utilizing the oppositely charged surfactant sodium lauryl sulfate (72,107). With total reflux, the recovery of methyl orange was essentially complete (74).

The foam fractionation of sodium dodecylbenzene sulphonate from water (104) and its use in foaming off the metallic cations Cs^+, Sr^{++} and Ce^{++} has been studied (6). In a combined column with external reflux, a strontium decontamination factor (defined as C_F/C_W) in excess of 1000 was obtained with a volume reduction (F/D) of 3700 for a feed rate of 40 gal/hr per ft^2 of column cross section in a

3.8 cm. i.d. column (125). The performance was considerably better than that obtained without the external reflux.

Some 107 surfactants have been tested for use in the removal of Cs^+, Sr^{++}, and Ce^{++} (146). A two-step process combining foam separation and scavenging precipitation has been studied (25). Strontium ions have also been well-removed by ion flotation with α-sulphopalmitic acid as collector (22,23). Obviously, much of the interest in separating these various cations stems from their objectionable presence as radioactive isotopes at trace levels of concentration in certain effluents.

The removal of ferric, ferrous, silver, and malachite green cations by means of the anionic surfactant sodium dodecylsulfate, has been reported, as well as the removal of the ferric cation with a cationic surfactant utilizing an anionic chelating agent as a "bridge" (4). With appropriate collectors, concentration by ion flotation of the fluorozirconate ion (111) and the ions of europium, cesium, and strontium have been reported, and compared favorably with flocculation (17). The batch removal rates of lead, iron, and copper have been studied (115).

Selective separations of one ion from another have been reported. Aluminum has been separated from beryllium at a pH of 4 by the ion flotation of an oxalato-aluminate complex with long chain fatty amines, especially tretradecylamine (94). Uranium has been separated from thorium in hydrochloride medium by means of ion association between the cationic surfactant benzethonium chloride and the uranyl choroanionic complex (68). With the same surfactant, uranium has been separated from vanadium in carbonate medium (64) and otherwise (7). Cu^{++} has been separated from Zn^{++} by raising the pH (66). A proposed study of the effect of micelles in ion flotation has been reported (142).

The determination of surfactant ions by ion flotation has been studied for analytical purposes (93,140). Ion flotation has also been examined for use in toxicology (63). The ingenious "ring test" (19) for roughly determining trace surfactants in water has been shown to operate by virtue of foam fractionation (84).

Separations of enzyme mixtures have been carried out, including the foaming of catalase out of amylase (18). Foaming does not necessarily destroy enzyme activity -- some enzymes are quite stable. In related connection, it is worth restating the findings of earlier investigators to the effect that the foam fractionation of protein may be most effective at the isoelectric pH (120). Lowering solubility, say by adding salt, may also increase surface adsorption.

Several investigators have studied the foam separation of microorganisms (36,91,92,114). In some cases the key to accomplishing the separation was the addition of a collector of opposite charge; viz., a cationic surfactant to coat the negatively charged particles and carry them to the surface (12,27,54,55,116). A similar mechanism may be involved in the separation of inorganic colloids such as ferric oxide, stannic oxide, kaolin clay, and ferrocyanide complexes (42,43,47,136).

Laboratory studies have demonstrated the successful removal of alkyl benzene sulphonate detergents from municipal sewage by foaming (20,79,97,119,137). However, more important are the large scale studies. A pilot sized foaming unit, operating on a feed of 0.5 million gallons of sewage per day with a gas-to-feed volume ratio of 5, reduced the ABS concentration of the bottoms stream to nearly 1 part per million while producing a foamate volume equal to no more than 3% of the feed volume (15,138). A full scale unit treating more than 12 million gallons per day performed almost as well. Besides ABS, some other organic pollutants were also removed. The output of secondary treatment was recommended as the preferred location for the foaming unit (70). Foamate could then be recycled back to the activated sludge reactor for further exposure to microbial action (71). However, large scale foam separation of municipal sewage has now fallen into disuse due to the industry-wide changeover from nondegradable to degradable detergents (2). Whether this abandonment will be permanent or temporary remains to be seen.

Of related interest are the removal of radium from uranium mill wastewater (124), the removal of iron salts from contaminated natural streams (99), the foaming of acid mine water deliberately combined with municipal sewage (100), the foam fractionation of black liquor from sulphate pulping which yields tall oil as a by product (62), the flotation of algae in water reclamation (141), and the upgrading of low quality raw water by lowering its turbidity (102) through the use of a cationic surfactant (40,53) or bentonite as a flotation aid (48). The problem of treating such raw waters is often important for small communities and remote military installations.

The precipitate flotation of copper was studied and compared favorably against ion flotation (117,118). The selective precipitate flotation of some 14 metals was discussed and also compared favorably against ion flotation (96). Also, aluminum was separated from beryllium by precipitate flotation (95), and uranium removed from chemical waste waters (135). The flotation of certain organic precipitates without the aid of a surfactant collector was reported (106). An impressive array of radioactive isotopes has been separated by means of suitable precipitate carriers (such as iron hydroxide) which were then foamed off with appropriate collectors (24,108,109,110,144).

The foaming off of surfactants from mineral oils has been studied (76). A review article describes the separation of vanadium from crude oil (30).

Other review articles have also recently appeared (3,39,123). So have pertinent patents (33,34,126,130) and a discussion of design calculations (80).

In the area of nonfoaming adsubble methods, the separation ratio achieved in a batch bubble fractionation column at steady state has been shown by theory (81) and by experiment with aqueous dye solution (60) to increase with column height but to be substantially independent of gas rate or charge concentration. Solvent sublation studies of methyl orange and rhodamine B in aqueous media have been carried out utilizing hexadecyltrimethylammonium bromide as the surfactant and 2-octanol as the immiscible liquid on top (16,72).

CLOSURE

It is evident from the foregoing, that the adsubble methods offer particular promise as means for removing material present in relatively small amounts from large volumes of liquid. Under these conditions, the appropriate adsubble methods are potentially competitive with conventional techniques. For example, even though only low concentrations of suspended matter may be involved, filtration still requires that all the liquid be forced through the filter media. In effect, filtration removes the liquid, leaving the solids behind. On the other hand, the flotation methods deal passively with the liquid. The liquid remains behind. Only the small amount of solid is removed. Similarly, when low concentrations of dissolved material are involved, methods such as foam fractionation or ion flotation may be competitive with fixed bed adsorption or ion exchange.

The adsubble methods can also be used to separate the components of certain systems which might be difficult to handle by conventional techniques. Substances which differ, or which can be made to differ, in their surface affinities can be so separated. By judicious selection of the physical parameters, and/or proper control of the chemical environment, the removal or separation can often be made highly selective. An increasing portion of the published work in recent years has been directed toward examining and improving this selectivity.

ACKNOWLEDGMENT

The present work is supported by F.W.P.C.A. Research Grant WP-00161 from the U. S. Department of Interior.

NOMENCLATURE

A = horizontal cross sectional area of the column, cm.^{2}

a_i = activity of component i.

C = concentration in the liquid, gm. mol/cm^3.

C_i = concentration of component i in the liquid, gm. mol/cm^3.

$\overline{C}$ = effective upflow concentration, gm. mol/cm^3. on a gas-free basis.

$\overline{C}^*$ = effective upflow concentration in equilibrium with C, gm. mol/cm^3. on a gas-free basis.

D = volumetric rate of collapsed net overflow product, cm^3./sec.

d = bubble diameter or surface average bubble diameter, cm.

d_i = individual bubble diameter, cm.

d_o = edge average bubble diameter, cm.

E = relative adsorptive effectiveness of surfactant in the surface versus surfactant in the micelles.

F = volumetric feed rate, cm^3./sec.

G = volumetric gas rate, cm^3./sec.

g = acceleration of gravity, cm./sec^2.

K = equilibrium constant for adsorption, cm.

L = volumetric rate of interstitial liquid downflow, cm^3./sec.

N.T.U. = number of transfer units in the foam, based on the upflowing stream.

n_i = number of bubbles with diameter d_i.

Q = volumetric rate of foam overflow on a gas-free basis, cm^3./sec.

$\underset{\sim}{R}$ = gas constant, erg/gm.mol°K.

R = reflux ratio.

S = ratio of surface to volume, cm.$^{-1}$

T = absolute temperature, °K.

U = volumetric rate of interstitial liquid upflow, cm.^{3}/sec.

Greek:

Γ = concentration at the surface, gm.mol/cm.^{2}

Γ_i = concentration of component i at the surface, gm.mol/cm.^{2}

γ = surface tension, dyne/cm.

Δ = difference.

μ = viscosity, dyne sec./cm.^{2}

μ_s = surface viscosity, dyne sec./cm.

ρ = liquid density, gm./cm.^{3}

ϕ = dimensionless function of A, g, G, ρ, μ and μ_s.

Other Subscripts:

D = collapsed net overhead product.

F = feed.

Q = foam overflow on a gas-free basis.

s = surfactant.

sc = critical micelle.

W = pool or bottoms.

1 = in the absence of micelles.

2 = in the presence of micelles.

LITERATURE CITED

1. Adamson, A. W., The Physical Chemistry of Surfaces, 2nd ed., Interscience, New York, 1967.

2. Anon., Chem. Eng. News 45(50), 44 (1967).

3. Anon., Environmental Science and Technology 1, 116 (1967).

4. Aoki, N., Sasaki, T., Bul. Chem. Soc. Japan 39, 939 (1966).

5. Baarson, R. E., Ray, C. L., "Precipitate Flotation, a New Metal Extraction and Concentration Technique", presented at the Am. Inst. Mining, Metallurgical, and Petroleum Engineers Symp., Dallas, Texas, 1963.

6. Banfield, D. L., Newson, I. H., Alder, P. J., A.I.Ch.E.-I.Chem.E. (London) Symposium Series, No. 1, 3 (1965).

7. Barocas, A., Iacobelli-Turi, C., Salvetti, F., J. Chromatog. 14, 291 (1964).

8. Becher, P., Del Vecchio, A. J., J. Phys. Chem. 68, 3511 (1964).

9. Bikerman, J. J., Foam: Theory and Industrial Applications, Reinhold, New York, 1953.

10. Bikerman, J. J., Ind. Eng. Chem. 57 (1), 56 (1965).

11. Brady, A. P., Ross, S., J. Am. Chem. Soc. 66, 1348 (1944).

12. Bretz, H. W., Wang, S. L., Grieves, R. B., Appl. Microbiol. 14, 778 (1966).

13. Brunner, C. A., Ph.D. Dissertation, Univ. Cincinnati (1963).

14. Brunner, C. A., Lemlich, R., Ind. Eng. Chem. Fundamentals 2, 297 (1963).

15. Brunner, C. A., Stephan, D. G., Ind. Eng. Chem. 57 (5), 40 (1965).

16. Caragay, A. B., Karger, B. L., Anal. Chem. 38, 652 (1966).

17. Cardozo, R. L., Dejonghe, P., Nature 199, 687 (1963).

18. Charm, S. E., Morningstar, J., Matteo, C. C., Paltiel, B., Anal. Biochem. 15, 498 (1966).

19. Crits, G. J., "The 'Crits organic ring test': A simple test for trace organic substances in water", presented before the American Chemical Society, Division of Water and Waste Chemistry, Chicago, Sept. 1961.

20. Daboo, R. F., M.S. Thesis, Univ. Missouri, School of Mines and Metallurgy (1963).

20. Daboo, R. F., M.S. Thesis, Univ. Missouri, School of Mines and Metallurgy (1963).

21. Davies, J. T., Rideal, E. K., *Interfacial Phenomena*, 2nd ed., Academic Press, New York, 1963.

22. Davis, B. M., Sebba, F., J. Appl. Chem. 16, 293 (1966).

23. Davis, B. M., Sebba, F., J. Appl. Chem. 16, 297 (1966).

24. Davis, B. M., Sebba, F., J. Appl. Chem. 17, 40 (1967).

25. Davis, W., Jr., Kibbey, A. H., Schonfeld, E., U. S. At. Energy Comm. ORNL - 3811 (1965). C. A. 64, 4784 h (1966).

26. deVries, A. J., *Foam Stability*, Rubber-Stichting, Delft, 1957.

27. Dobias, B., Vinter, V., Folia Microbiologia 11, 314 (1966).

28. Dognon, A., Dumontet, H., Comp. Rend. 135, 884 (1941).

29. Dorman, D. C., Lemlich, R., Nature, 207, 145 (1965).

30. Eldib, I. A., "Foam and Emulsion Fractionation" in *Advances in Petroleum Chemistry and Refining* vol. 7, p. 66, Kobe, K. A., and McKetta, J. J., Jr., Eds., Interscience, New York, 1963.

31. Fanlo, S., Ph.D. Dissertation, Univ. Cincinnati (1964).

32. Fanlo, S., Lemlich, R., A.I.Ch.E.-I.Chem.E. (London) Symposium Series No. 9, 75, 85 (1965).

33. Gaden, E. L., Jr., Schnepf, R. W., U. S. Patent 3,054,746 (Sept. 18, 1962).

34. Gaden, E. L., Jr., Schnepf, R. W., U. S. Patent 3,054,747 (Sept. 18, 1962).

35. Gaudin, A. M. *Flotation*, McGraw-Hill, New York, 1957.

36. Gaudin, A. M., Davis, N. S., Bangs, S. E., Biotechnol. Bioeng. 4, 211, 223 (1962).

37. Gibbs, J. W., *Collected Works*, Longmans Green, New York, 1928.

38. Goldberg, M., Rubin, E., Ind. Eng. Chem. Process Design Devel. 6, 195, (1967).

39. Grieves, R. B., British Chem. Eng. *13*, 77 (1968).

40. Grieves, R. B., Proc. Am. Soc. Civil Engrs., J. Sanitary Eng. Div., 92, SA1, 41 (1966).

41. Grieves, R. B., Aronica, R. C., Int. J. Air Water Poll. 10, 31 (1966).

42. Grieves, R. B., Bhattacharyya, D., A.I.Ch.E. J. 11, 274 (1965).

43. Grieves, R. B., Bhattacharyya, D., Can. J. Chem. Eng. 43, 286 (1965).

44. Grieves, R. B., Bhattacharyya, D., Nature 204, 441 (1964).

45. Grieves, R. B., Bhattacharyya, D., J. Am. Oil Chem. Soc. 42 (3), 174 (1965).

46. Grieves, R. B., Bhattacharyya, D., Separation Science 1, 81 (1966).

47. Grieves, R. B., Bhattacharyya, D., Crandall, C. J., J. Appl. Chem. 17, 163 (1967).

48. Grieves, R. B., Crandall, C. J., Water Sewage Works, 113, 432 (1966).

49. Grieves, R. B., Crandall, C. J., Wood, R. K., Int. J. Air Wat. Poll. 8, 501 (1964).

50. Grieves, R. B., Ettelt, G. A., A.I.Ch.E. J. 13, 1167 (1967).

51. Grieves, R. B., Kelman, S., Obermann, W. R., Wood, R. K., Can. J. Chem. Engr. 41, 252 (1963).

52. Grieves, R. B., Schwartz, S. M., A.I.Ch.E. J. 12, 746 (1966).

53. Grieves, R. B., Schwartz, S. M., J. Am. Wat. Works Assoc. 58, 1129 (1966).

54. Grieves, R. B., Wang, S. L., Appl. Microbiol. 15, 76 (1967).

55. Grieves, R. B., Wang, S. L., Biotech. Bioeng. 8, 323 (1966).

56. Grieves, R. B., Wilson, E., Shih, K. Y., A.I.Ch.E. J. 11, 820 (1965).

57. Grieves, R. B., Wood, R. K., A.I.Ch.E. J. 10, 456 (1964).

58. Haas, P. A., Johnson, H. F., A.I.Ch.E. J. 11, 319 (1965).

59. Haas, P. A., Johnson, H. F., Ind. Eng. Chem. Fundamentals 6, 225 (1967).

60. Harper, D. O., Lemlich, R., A.I.Ch.E. J. 12, 1220 (1966).

61. Harper, D. O., Lemlich, R., Ind. Eng. Chem. Process Design and Development 4, 13 (1965).

62. Hendrickson, E. R., Harding, C. J., J. Air Pollution Control Assoc. 14 (12), 491 (1964).

63. Hofman, M., Angew Chem. Intern., Ed. Engl. 6:373 (1967).

64. Jacobelli-Turi, C., Barocas, A., Torenzi, S., Ind. Eng. Chem. Process Design Devel. 6, 161 (1967).

65. Jacobelli-Turi, C., Palmera, M., Gaz. Chim. Ital. 96, 1432 (1966).

66. Jacobelli-Turi, C., Palmera, M., Margani, A., Ric. Sci. 36, 1198 (1966).

67. Jacobelli-Turi, C., Palmera, M., Perinelli, S., Ric. Sci. 36, 1219 (1966).

68. Jacobelli-Turi, C., Torenzi, S., Palmera, M., Ind. Eng. Chem. Process Design Devel. 6, 162 (1967).

69. Jacobi, W. M., Woodcock, K. E., Grove, C. S., Jr., Ind. Eng. Chem. 48, 2046 (1956).

70. Jenkins, D., J. Water Pollution Control Fed. 38, 1737 (1966).

71. Karassik, I. J., Sebald, J. F., "Foaming detergents offer new opportunities for advanced sewage treatment; the 'scat' process for suds control and transfer". Worthing Corp., Harrison, New Jersey (1963).

72. Karger, B. L., U. S. Army Natick Labs., Tech. Report 66-25-FD (1966).

73. Karger, B. L., Grieves, R. B., Lemlich, R., Rubin, A. J., Sebba, F., Separation Science, 2, 401 (1967).

74. Karger, B. L., Poncha, R. P., Miller, M. M., Anal. Chem. 38, 764 (1966).

75. Karn, J. L., Undergraduate Senior Project Report, Univ. Cincinnati (1961).

76. Keil, G., Richter, R., Erdol Kohle Erogas Petrochemie 19, 187 (1966).

77. Kishimoto, H., Kolloid Z. 192, 66 (1963).

78. Kitchener, J. A., "Foam and Free Liquid Films", Chapt. 2 in Recent Progress in Surface Science, vol. 1, Danielli, J. F., Pankhurst, K. G. A., Riddiford, A. C., Editors, Academic Press, New York, 1964.

79. Klein, S. A., McGauhey, P. H., J. Water Pollution Control Fed. 35, 100 (1963).

80. Lambert, C. W., M.S.Ch.E. Thesis, Carnegie Inst. Technology (1967).

81. Lemlich, R., A.I.Ch.E. J., 12, 802 (1966). Also correction, 13, 1017 (1967).

82. Lemlich, R., Chem. Eng. 73 (21), 7 (1966).

83. Lemlich, R., Chem. Eng. Sci., in press. Presently, Tech. Note 9-67, Univ. Cincinnati (1967).

84. Lemlich, R., Env. Sci. Tech., submitted for publication. Presently, Tech. Note 1-68, Univ. Cincinnati (1968).

85. Lemlich, R., "Principles of Foam Fractionation", Chapt. 1 in Progress in Separation and Purification, vol. 1, Perry, E. S., Editor, Interscience, New York, 1968.

86. Lemlich, R., Lavi, E., Science 134 (3473), 191 (1961).

87. Leonard, R. A., Ph.D. Dissertation, Univ. Cincinnati (1964).

88. Leonard, R. A., Lemlich, R., A.I.Ch.E. J. 11, 18 (1965).

89. Leonard, R. A., Lemlich, R., A.I.Ch.E. J. 11, 25 (1965).

90. Leonard, R. A., Lemlich, R., Chem. Eng. Sci., 20, 790 (1965).

91. Levin, G. B., Barnes, J. M., Proc. Purdue Industrial Waste Conference 19, 421 (1964).

92. Levin, G. V., Clendenning, J. R., Gibor, A., Bogar, F. D., Appl. Microbiol. 10, 169 (1962).

93. Lovell, V. M., Sebba, F., Anal. Chem. 38, 1926 (1966).

94. Lusher, J. A., Sebba, F., J. Appl. Chem. 15, 577 (1965).

95. Lusher, J. A., Sebba, F., J. Appl. Chem. 16, 129 (1966).

96. Mahne, E. J., Pinfold, T. A., Chem. Ind. 30, 1299 (1966).

97. Malik, A. S., M.S. Thesis, Univ. Missouri, Rolla, (1964).

98. Manegold, E., Schaum, Strassenbau, Chemie und Technik Verlagsgesellschaft, Heidelberg, 1953.

99. McLean, D. C., Item no. 5.0965 in Water Resources Research Catalog, vol. 2, U. S. Dept. Interior, Nov. 1966.

100. McLean, D. C., Item no. 5.0966 in Water Resources Research Catalog, vol. 2, U. S. Dept. Interior, Nov. 1966.

101. Miles, G. D., Shedlovsky, L., Ross, J., J. Phys. Chem. 49, 93 (1945).

102. Murphy, R. S., Item no. 5.0052 in Water Resources Research Catalog, vol. 2, U. S. Dept. Interior, Nov. 1966.

103. Mysels, K. J., Shinoda, K., Frankel, S., Soap Films, Studies of their Thinning, Pergamon, New York, 1959.

104. Newson, I. H., J. Appl. Chem. 16, 43 (1966).

105. Osipow, L. I., Surface Chemistry, Theory and Industrial Applications, ACS Monograph Series 153, Reinhold, New York, 1962.

106. Pinfold, T. A., Mahne, E. J., Chem. Ind. 1917 (1967).

107. Poncha, R. P., Karger, B. L., Anal. Chem. 37, 422 (1965).

108. Pushkarev, V. V., Radiokhimicheskie Metody Opredeleniya Mikroelementov, pp. 124-9, Izdatel'stvo Nauka, Moscow - Leningrad, 1965. Nucl. Sci. Abs. 20, 20628 (1966).

109. Pushkarev, V. V., Bagretsov, V. F., Puzako, V. D., Radiokhimiya 6, 120 (1964). Nucl. Sci. Abs. 18, 23735 (1964).

110. Pushkarev, V. V., Egorov, Y. V., Tkachenko, E. V., Zoltavin, V. L., Atomic Energy USSR 16, 48 (1964). Nucl. Sci. Abs. 18, 19452 (1964).

111. Rice, H. W., Sebba, F., J. Appl. Chem. 15, 105 (1965).

112. Ross, S., Chem. Eng. Prog. 63 (9), 41 (1967).

113. Ross, S., J. Phys. Chem. 47, 266 (1943).

114. Rubin, A. J., Biotechnol. Bioeng. 10, 89 (1968).

115. Rubin, A. J., J. Am. Wat. Works Assoc., in press.

116. Rubin, A. J., Cassel, E. A., Henderson, O., Johnson, J. D., Lamb, J. C., III, Biotech. 8, 135 (1966).

117. Rubin, A. J., Johnson, J. D., Anal. Chem. 39:298 (1967).

118. Rubin, A. J., Johnson, J. D., Lamb, J. C., III, Ind. Eng. Chem. Process Design Devel. 5, 368 (1966).

119. Rubin, E., Everett, R., Jr., Ind. Eng. Chem. 55 (10), 44 (1963).

120. Rubin, E., Gaden, E. L., Jr., "Foam Separation", Chapter 5 in New Chemical Engineering Separation Techniques, Schoen, H. M., Editor, Interscience, New York, 1962.

121. Rubin, E., LaMantia, C. R., Gaden, E. L., Jr., Chem. Engr. Sci. 22, 1117 (1967).

122. Schnepf, R. W., Gaden, E. L., Jr., Mirocznik, E. Y., Schonfeld, E., Chem. Eng. Prog. 55 (5), 42 (1959).

123. Schoen, H. M., Ann. New York Acad. Sci., 137, Art. 1, 148 (1966).

124. Schoen, H. M., Rubin, E., Ghosh, D., J. Water Pollution Control Fed. 34, 1026 (1962).

125. Schonfeld, E., Kibbey, A. H., Nuclear Applications 3,353 (1967).

126. Sebba, F., Belg. Patent 623,140 (Jan. 31, 1963). C. A. 59, 3575 h (1963).

127. Sebba, F., Ger. Patent 1,163,265 (Feb. 20, 1964). C. A. 64, 6139 a (1966).

128. Sebba, F., *Ion Flotation*, Elsevier, New York, 1962.

129. Sebba, F., Nature 184, 1062 (1959).

130. Sebba, F., Jonaitis, C. W., Ray, C. I., Baarson, R. E., Ger. Patent 1,175,622 (Aug. 13, 1964). C. A. 61, 14244 d (1964).

131. Shih, F. S., Ph.D. Dissertation in preparation, Univ. Cincinnati.

132. Shih, F. S., Lemlich, R., A.I.Ch.E. J. 13, 751 (1967).

133. Shinoda, K., Kinoshita, K., J. Colloid Sci. 18, 174 (1963).

134. Shinoda, K., Nakanishi, J., J. Phys. Chem. 67, 2547 (1963).

135. Skrylev, L. O., Mokrushin, S. G., Zhur. Priklad. Khim. 34, 2403 (1961). Nucl. Sci. Abs. 16, 12799 (1962).

136. Skrylev, L. D., Mokrushin, S. G., Zh. Prikladnoi Khimii *37* (1), 211 (1964).

137. Stander, G. J., Chairman, Steering Committee of the Windhoek Sewage Reclamation Project, National Institute for Water Research, Council for Scientific and Industrial Research, City Engineers' Department, Windhoek Municipality. *Final Report on Reclamation of Purified Sewage Effluent for Augmentation of Domestic Water Supply of Windhoek.* WNNR,CSIR Contract Report no. C WAT 4 (1965)., Pretoria, South Africa.

138. Stephan, D. G., Civil Eng. 35 (9), 46 (1965).

139. Strain, H. H., J. Phys. Chem. 57, 638 (1953).

140. Tomlinson, H. S., Sebba, F., Anal. Chim. Acta, 27, 596 (1962).

141. van Vuuren, L. R. J., Meiring, P. G. J., Henzen, M. R., Kolbe, F. F., Int. J. Air Wat. Poll. 9, 823 (1965).

142. Venable, R. L., Item no. 5.0626 in *Water Resources Research Catalog*, vol. 2, U. S. Dept. Interior, Nov. 1966.

143. von Zawidzki, J., Z. Phys. Chem. 35, 77 (1900).

144. Voznesenskii, S. A., Sereda, G. A., Baskov, L. I., Tkachenko, E. V., Bagretsov, V. F., Kernenergie (USSR) 4, 316 (1961). C. A. 62, 2610 e (1965).

145. Wace, P. F., Banfield, D. L., Chem. Proc. Eng. 47 (10), 70 (1966).

146. Weinstock, J. J., Mook, S., Schonfeld, E., Rubin, E., Sanford, R., U. S. At. Energy Comm. NYO - 10038 (1963). C. A. 61, 12900 d (1964).

147. Wood, R. K., Tran, T., Canadian J. Chem. Eng. 44, 322 (1966).

LIST OF FIGURES

Figure 1. Foam fractionation in the simple mode: (a) Batchwise operation; (b) Continuous operation.

Figure 2. Classification scheme for the various adsorptive bubble separation methods (73).

Figure 3. Bubble fractionation (29): (a) Batchwise operation; (b) Continuous operation; (c) Continuous operation in tandem with foam fractionation.

Figure 4. Typical variation of concentration at the surface, Γ, with concentration in the liquid, C.

Figure 5. Foam fractionation in the simple mode with recycle.

Figure 6. Four modes for continuous foam fractionation.

Figure 7. Graphical stagewise calculation for a continuous foam fractionation column operating in the combined mode. Liquid feed enters at the match point. The straight 45° portion of the equilibrium curve represents a constant Γ.

Figure 8. Cross section of capillary and films in foam.

Figure 9. Theoretical evaluations of $\phi\left(\frac{\mu^3 G}{\mu_s^2 g \rho A}\right)$. The solid curve (32) approaches a horizontal asymptote of 2.41. The broken curve (88) approaches a horizontal asymptote of 2.27. Use of the solid curve is recommended (132).

Figure 10. Test of the present theory for predicting the rate of foam overflow (132). The surfactants involved include Triton X-100 (31,32,87,89), Aresket 300 (13,14), and sodium dodecylbenzene sulphonate (6).

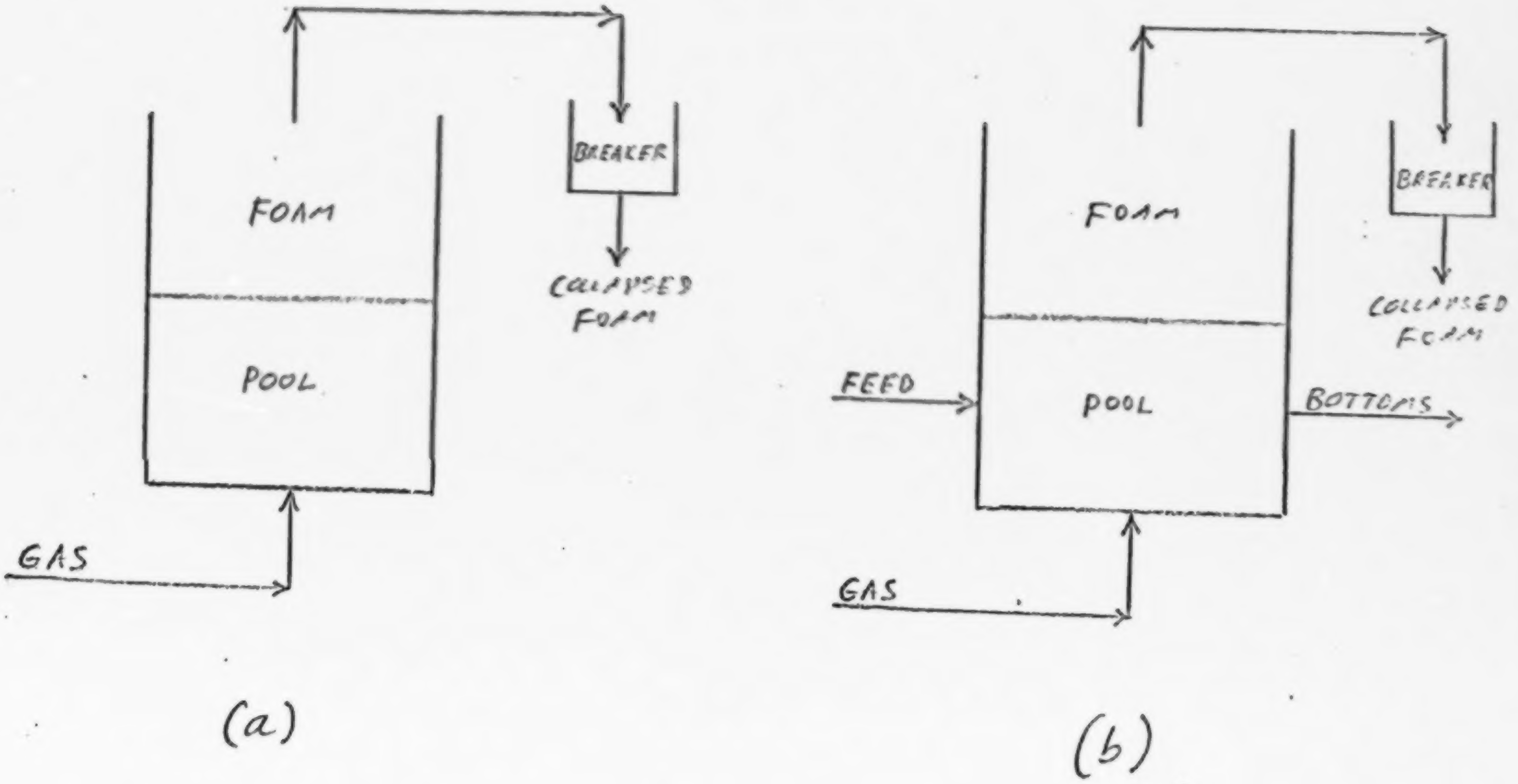
FOAM
POOL
BREAKER
COLLAPSED FOAM
GAS
(a)
FOAM
POOL
BREAKER
COLLAPSED FOAM
FEED
BOTTOMS
GAS
(b)

Figure 1. Foam fractionation in the simple mode: (a) Batchwise operation; (b) Continuous operation.

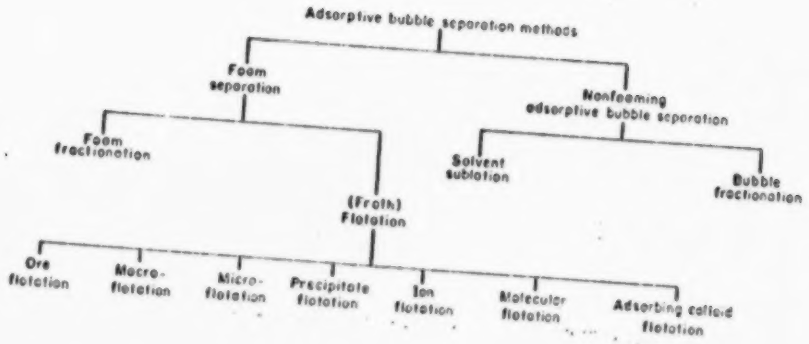
Adsorptive bubble separation methods
Foam separation
Nonfoaming adsorptive bubble separation
Foam fractionation
(Froth) Flotation
Solvent sublation
Bubble fractionation
Ore flotation
Macro-flotation
Micro-flotation
Precipitate flotation
Ion flotation
Molecular flotation
Adsorbing colloid flotation

Figure 2. Classification scheme for the various adsorptive bubble separation methods (73).

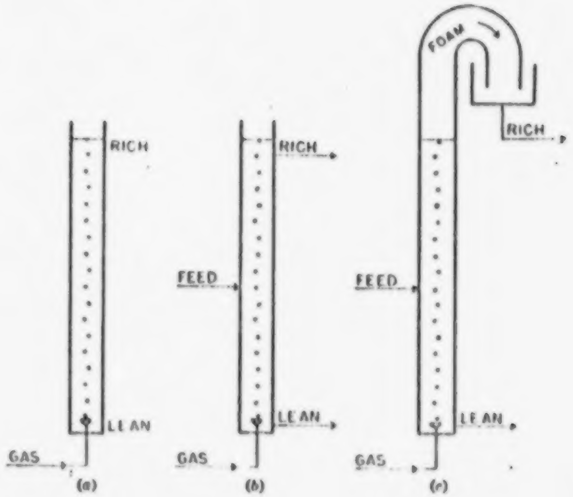
RICH
LEAN
GAS
(a)
FEED
RICH
LEAN
GAS
(b)
FOAM
RICH
FEED
LEAN
GAS
(c)

Figure 3. Bubble fractionation (29): (a) Batchwise operation; (b) Continuous operation; (c) Continuous operation in tandem with foam fractionation.

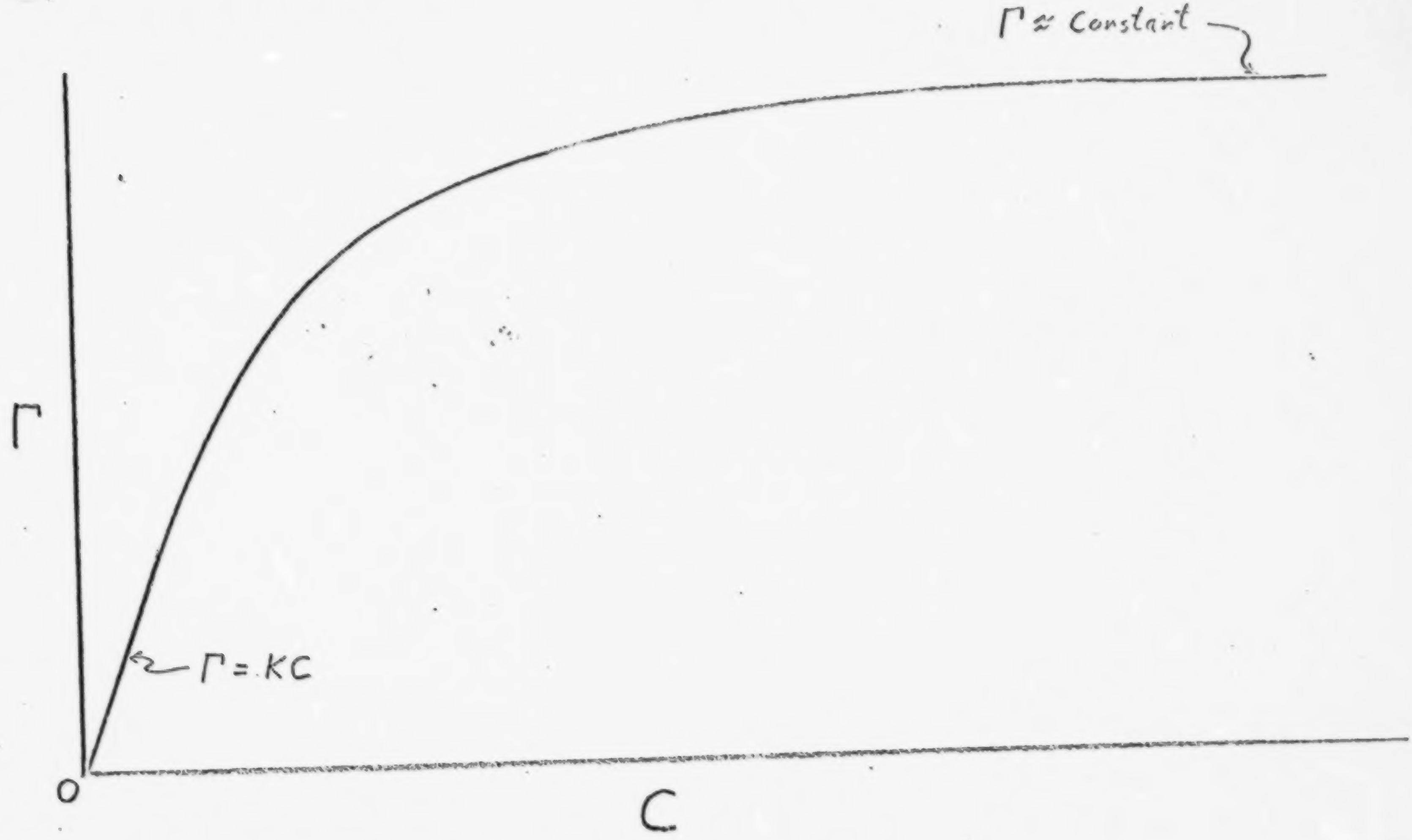

Figure 4. Typical variation of concentration at the surface, Γ, with concentration in the liquid, C.

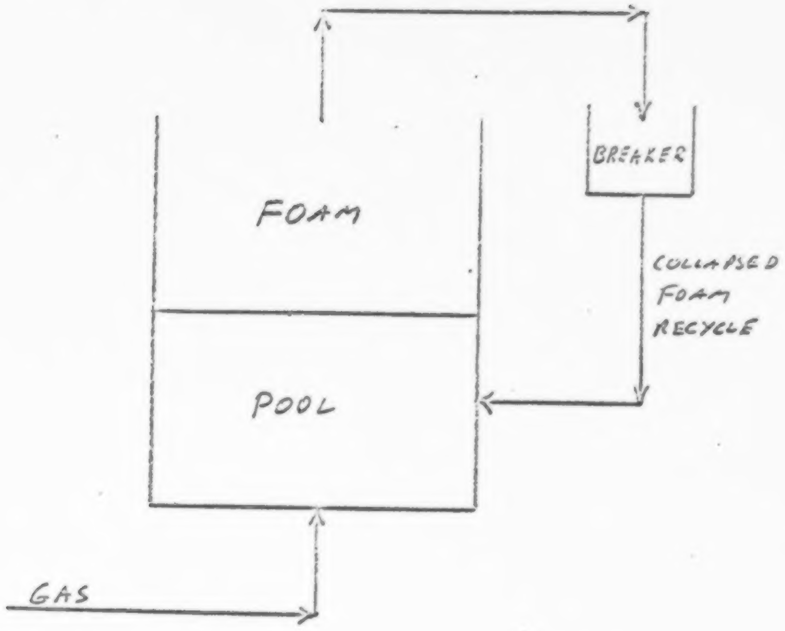
BREAKER
FOAM
COLLAPSED
FOAM
RECYCLE
POOL
GAS

Figure 5. Foam fractionation in the simple mode with recycle.

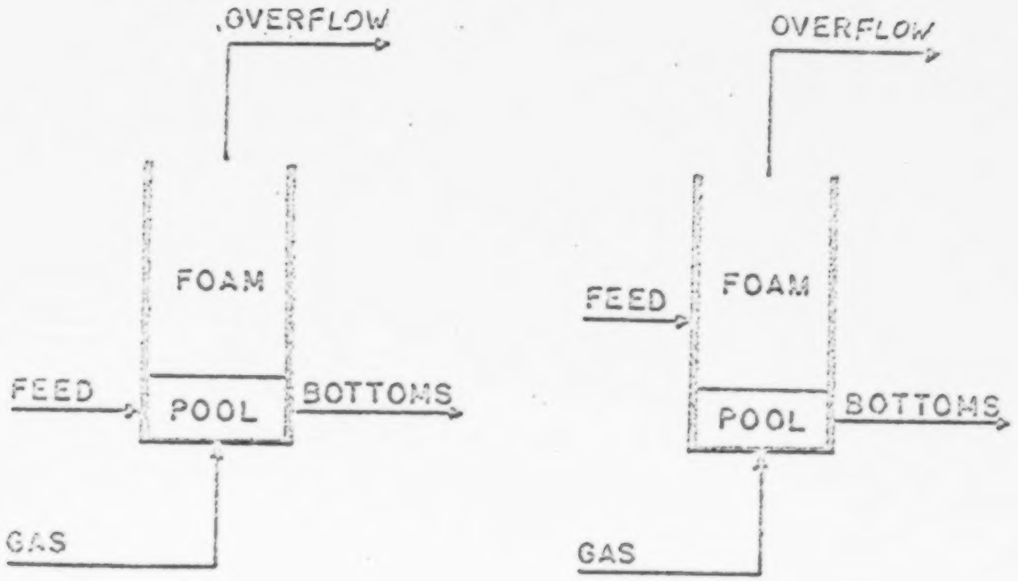
OVERFLOW
FOAM
FEED
POOL
BOTTOMS
GAS
OVERFLOW
FEED
FOAM
POOL
BOTTOMS
GAS

SIMPLE STRIPPER

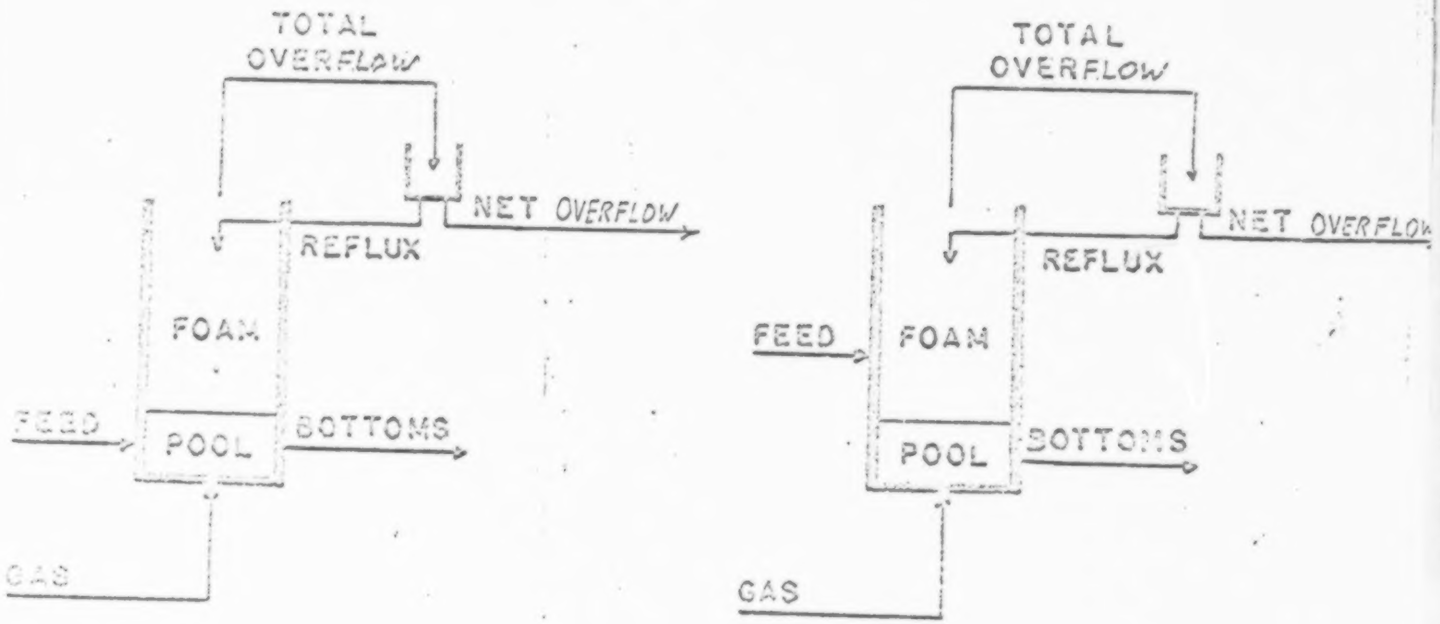
TOTAL OVERFLOW
NET OVERFLOW
REFLUX
FOAM
FEED
POOL
BOTTOMS
GAS
TOTAL OVERFLOW
NET OVERFLOW
REFLUX
FEED
FOAM
POOL
BOTTOMS
GAS

ENRICHER COMBINED

Figure 6. Four modes for continuous foam fractionation.

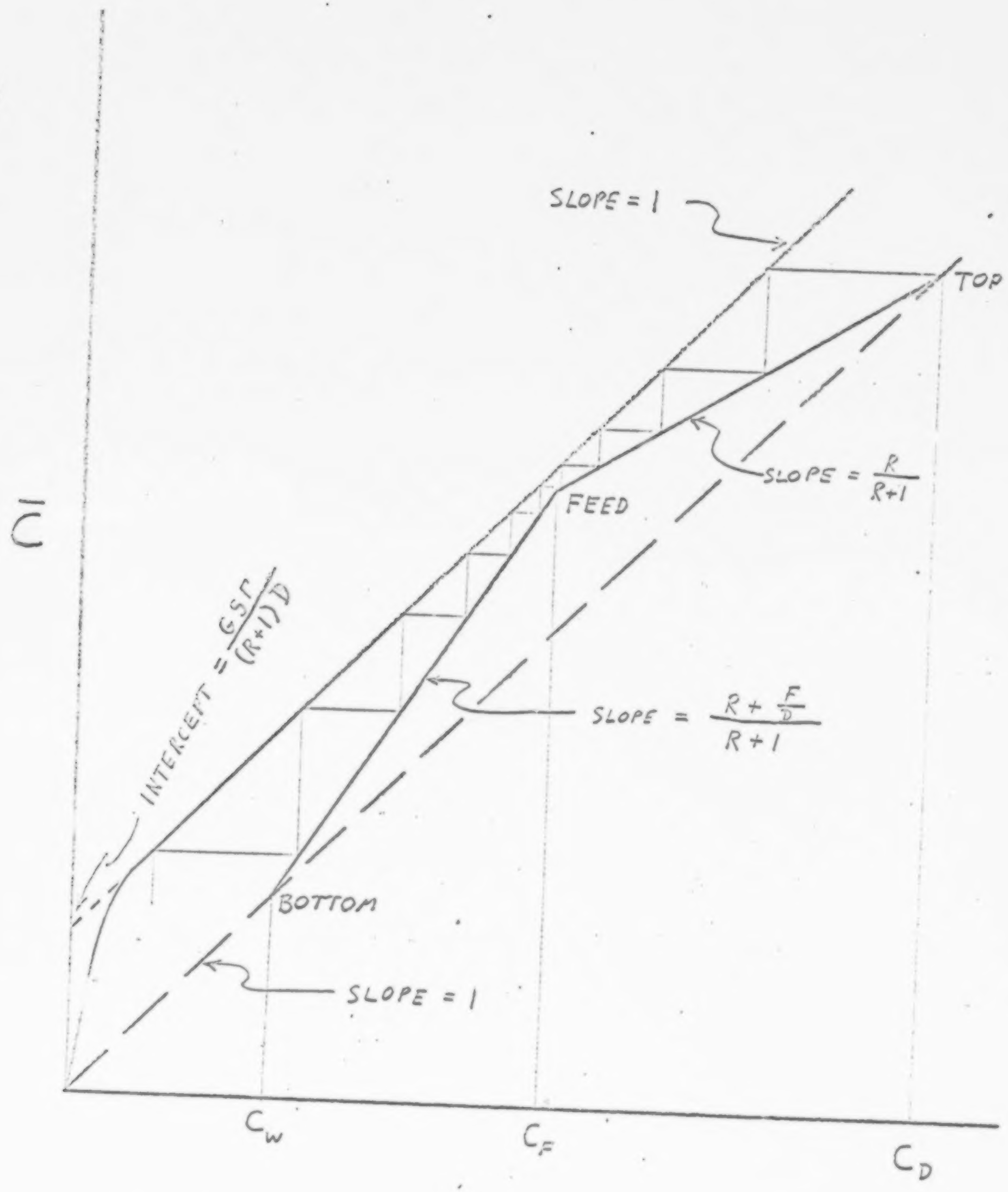
SLOPE = 1
TOP
$SLOPE = \frac{R}{R+1}$
FEED
$INTERCEPT = \frac{G S \Gamma}{(R+1) D}$
$SLOPE = \frac{R + \frac{F}{D}}{R+1}$
BOTTOM
SLOPE = 1
$\bar{C}$
C_W
C_F
C_D

Figure 7. Graphical stagewise calculation for a continuous foam fractionation column operating in the combined mode. Liquid feed enters at the match point. The straight 45° portion of the equilibrium curve represents a constant Γ.

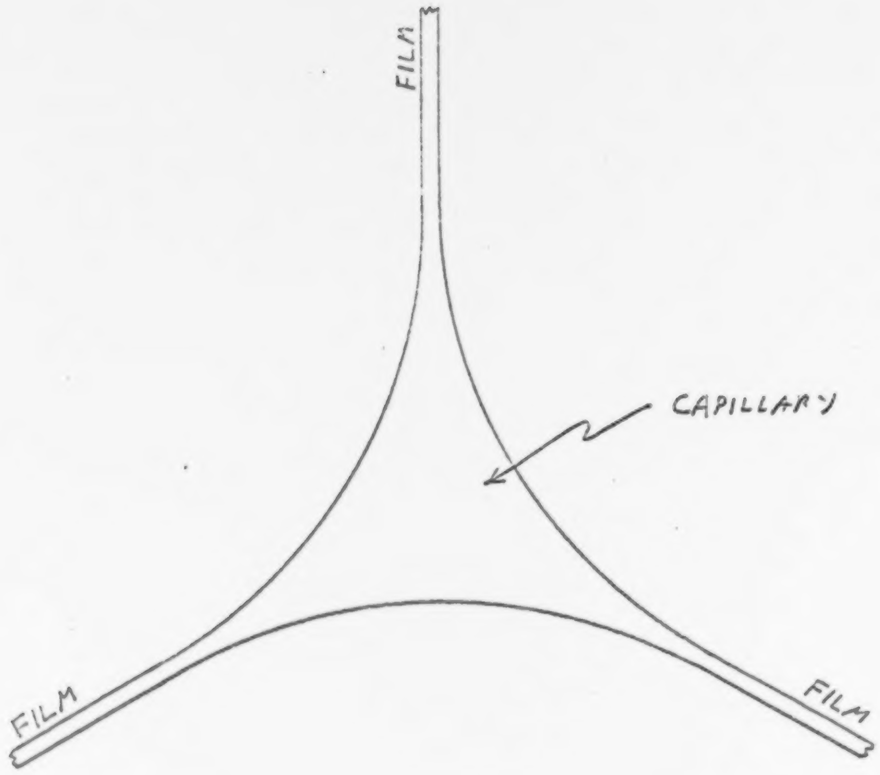

FILM
CAPILLARY
FILM
FILM

Figure 8. Cross section of capillary and films in foam.

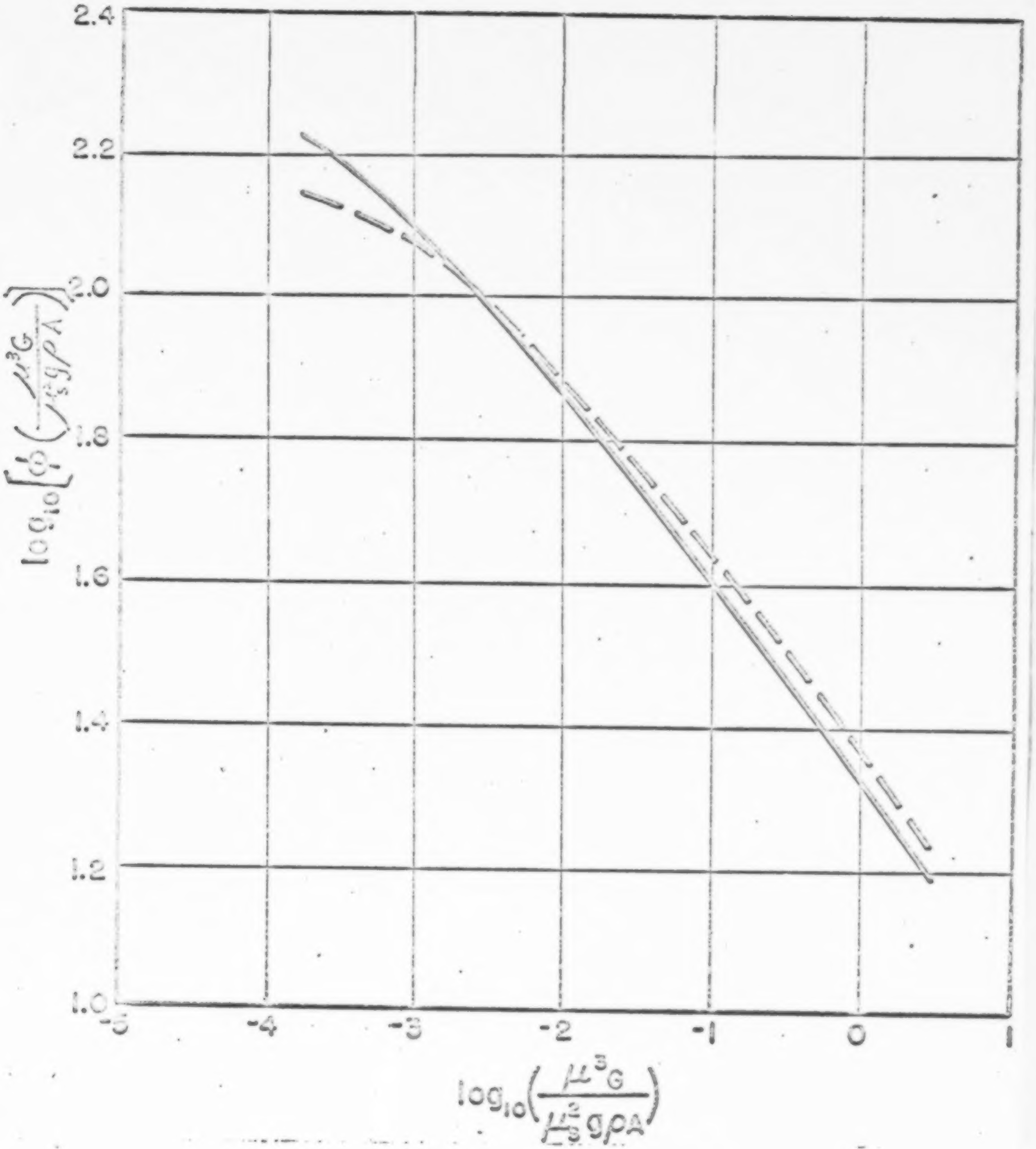

Figure 9. Theoretical evaluations of $\phi\left(\frac{\mu^3_G}{\mu_S^2 g \rho_A}\right)$. The solid curve (32) approaches a horizontal asymptote of 2.41. The broken curve (88) approaches a horizontal asymptote of 2.27. Use of the solid curve is recommended (132).

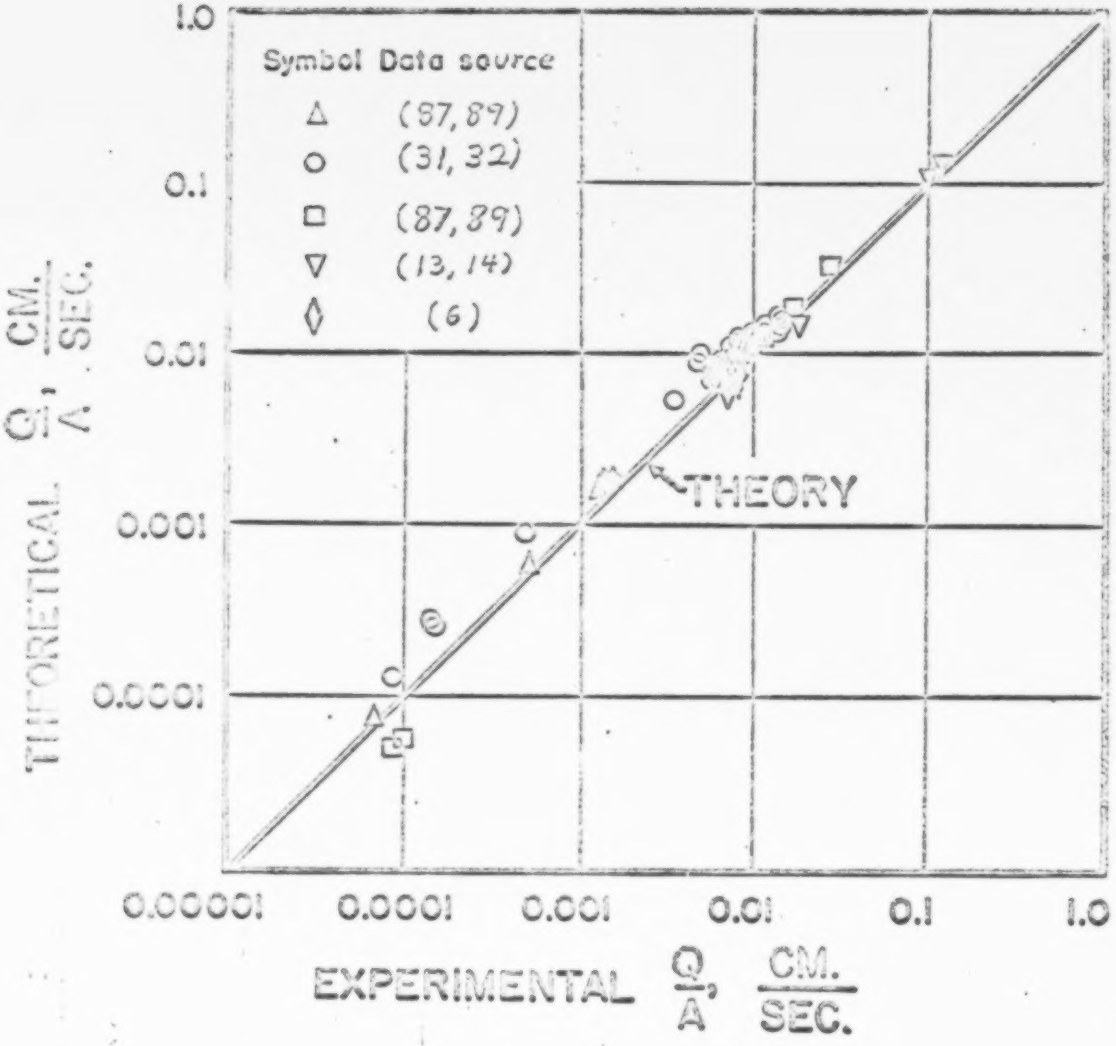

Figure 10. Test of the present theory for predicting the rate of foam overflow (132). The surfactants involved include Triton X-100 (31,32,87,89), Aresket 300 (13,14), and sodium dodecylbenzene sulphonate (6).

Note: This paper has been accepted for publication
in Chemical Engineering Science (1968).

FOAM OVERFLOW RATE: COMPARISON OF THEORY WITH EXPERIMENT

by

Robert Lemlich

Department of Chemical Engineering

University of Cincinnati

Cincinnati, Ohio 45221

U.S.A.

Recently, Rubin, LaMantia, and Gaden (5) presented some experimental results for the rate of foam overflow from vertical foam fractionation columns. They then compared the trend of their data against the trends predicted by the model of Leonard and Lemlich (4) and the model of Haas and Johnson (2,3).

While a comparison of trends can sometimes be useful, it is by its nature limited. This is especially so when the range of experimental data is modest in comparison with the scope of the theory being tested. More information can be obtained by testing the theoretical prediction itself, rather than merely its trend.

The writer has prepared such a test in Fig. 1. The dashed curve represents the theoretical prediction of Lemlich and Leonard for foam of low liquid content. The theory includes the random orientation of the capillaries, their curved triangular cross section, and the surface viscosity at their walls. The solid curve is a later refinement (1,6).

The dotted horizontal line represents the more empirical prediction of Haas and Johnson. It is flat because it makes no allowance for surface viscosity. It also does not incorporate the capillary orientation or cross section in any fundamental way.

The shaded portion represents experimental results of Rubin et.al. (5). It was plotted in the following way. First a band was drawn covering the data points of their Fig. 4. This band proved to be thick in the middle and thin at the ends. Next a band was drawn covering the data of their Figure 5. This band was thin at the bottom, thick elsewhere, and slightly curved. Then both bands were mapped on to the present Fig. 1 by direct calculation using $g = 981$ cm/sec^2, $\rho = 1.0$ g/cm^3, and the approximate viscosities suggested by Rubin et.al., namely $\mu = 0.01$ dyne sec/cm^2 and $\mu_s = 10^{-4}$ dyne sec/cm.

Actually, the present writer has found a μ_s of 1.8×10^{-4} dynes sec/cm for aqueous Aresket 300, but based on very limited experimental data (6). Use of this value for μ_s would shift the shaded regions in Fig. 1 somewhat to the left. On the other hand, since d was reportedly measured in the lowest part of the column (5), correcting for any coalescence in the foam before it reached the top would elevate the shaded regions somewhat. Incorporating additional data for the small effect of column diameter which was reported (5) would extend the overall shaded region upward and downward, but not by very much.

All in all, Fig. 1 shows reasonable agreement between the shaded experimental regions and the theoretical prediction of Leonard and Lemlich. Agreement with Haas and Johnson is not as good.

NOTATION

d	average bubble diameter, cm.
f	foam ratio (volume fraction of liquid in collected uncollapsed foam), dimensionless
g	gravitational acceleration, cm/sec^2
v_f	rising foam velocity, cm/sec
ρ	liquid density, g/cm^3
μ	liquid viscosity, dyne sec/cm^2
μ_s	surface viscosity, dyne sec/cm

REFERENCES

1. Fanlo S. and Lemlich R., A.I.Ch.E.-I.Chem.E. Symposium Series (Instn. Chem. Engrs., London) 1965 9 75.
2. Haas P. A., Ph.D. Dissertation, University of Tennessee 1965.
3. Haas P. A. and Johnson H. F., Ind. Engrg. Chem. Fundls. 1967. 6 225.
4. Leonard R. A. and Lemlich R., A.I.Ch.E. Jl 1965 11 18.
5. Rubin E., LaMantia C. R., and Gaden E. L. Jr., Chemical Engineering Science 1967 22 1117.
6. Shih F. S. and Lemlich R., A.I.Ch.E. Jl 1967 13 751.

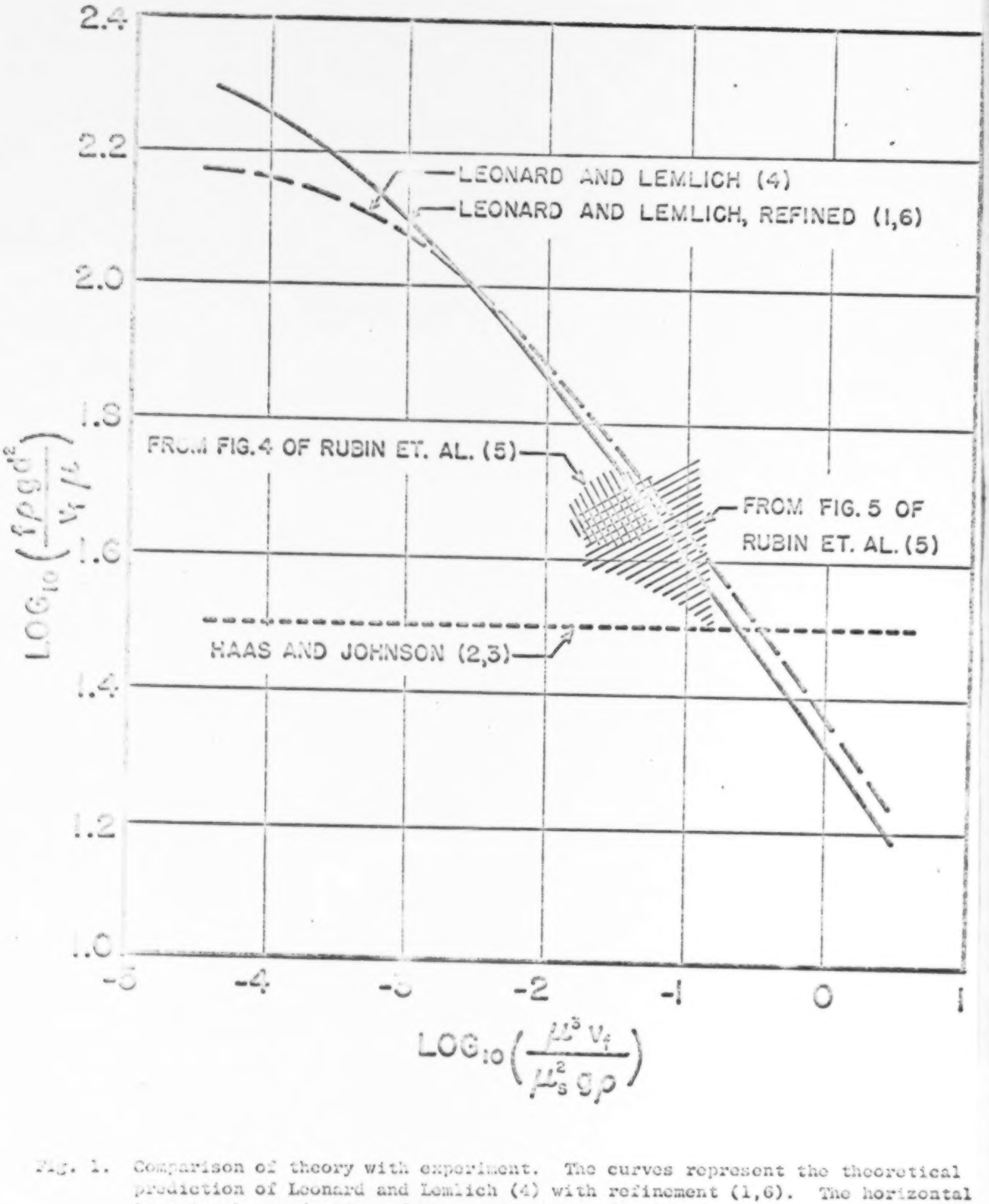

Fig. 1. Comparison of theory with experiment. The curves represent the theoretical prediction of Leonard and Lemlich (4) with refinement (1,6). The horizontal line is the prediction of Haas and Johnson (2,3). The shaded areas represent experimental results of Rubin et.al. (5).

Reprinted from A.I.Ch.E. JOURNAL, July 1967

A Study of Interstitial Liquid Flow in Foam

Part III. Test of Theory

FANG-SHUNG SHIH and ROBERT LEMLICH

University of Cincinnati, Cincinnati, Ohio

The theory for foam drainage and overflow recently proposed by the authors' group is tested with extensive experimental data gathered from foam fractionation columns and also from stationary foams at steady state. The experimental results support the theory.

Recently the authors' group presented a theory for foam drainage and overflow (*7*). It is based on interstitial Newtonian flow through randomly oriented capillaries (Plateau borders) of noncircular cross section with surface viscosity at the capillary boundaries. It involves no empirical constants.

This theory permits the estimation of the rate at which foam flows off overhead from a foam fractionation column. Such columns are used to partially separate the constituents of solutions via differences in surface activity. Gas is bubbled up through a liquid pool at the bottom of the column, thus forming a foam which rises up the column and overflows the top. This overflow carries off solute which has been adsorbed at the bubble surfaces.

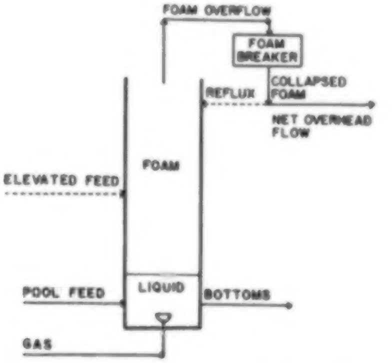

Fig. 1. Four alternative modes of flow operation with a foam fractionation column. 1. Solid lines show the simple mode. 2. The dotted reflux line is for operation as an enricher. 3. For stripping operation, pool feed is replaced with elevated feed to the foam. 4. For combined operation, reflux and elevated feed are both employed.

The degree of overhead enrichment, which may be considerable, can be increased even further through the use of internal or external reflux (*3*). The degree of stripping can be increased by injecting the feed into the foam some distance above the liquid pool (*7*). Figure 1 shows a foam fractionation column in these alternative modes of operation. The theory predicts the rate of foam overflow for all modes.

The theory incidentally also provides a relationship at steady state between the bulk density of a stationary foam in a column and the rate of deliberate liquid feed draining through the foam keeping it moist. In this situation there is no pool feed and no gas flow, and therefore no foam overflow or reflux. There is only elevated feed, stationary foam up to the feed inlet (with empty column above it), and bottoms withdrawal. This is illustrated in Figure 2.

The theory has already been compared against limited experimental data (*8*). The purpose of the current paper is to present the results of a more extensive test; details have been placed on file (*10*).

In accordance with the theory (*5, 7*) the rate of overhead flow for a fairly dry foam (meaning a foam of low liquid content) is given by Equation (1):

$$D = \frac{G^2\mu}{Ag\rho d^2}\,\phi\left(\frac{\mu^3 G}{\mu_s^2 g\rho A}\right) \qquad (1)$$

The function ϕ was evaluated theoretically in accordance with two alternatives regarding the detailed relationship between the interstitial downflow and the bulk foam upflow. The two evaluations are shown in Figure 3. The difference between them is minor, especially in the region of current interest.

Density ρ and viscosity μ are for the liquid in the capillaries. For dilute solutions these properties can be conveniently taken as those of the solvent which is usually water. Surface viscosity μ_s is a separate property which involves resistance to flow in a surface, as compared with

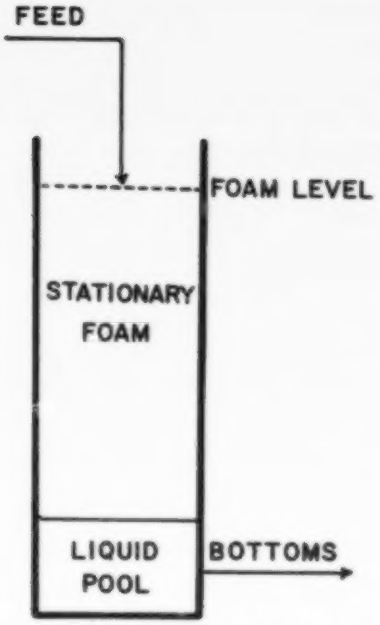

Fig. 2. Steady state drainage through a stationary foam.

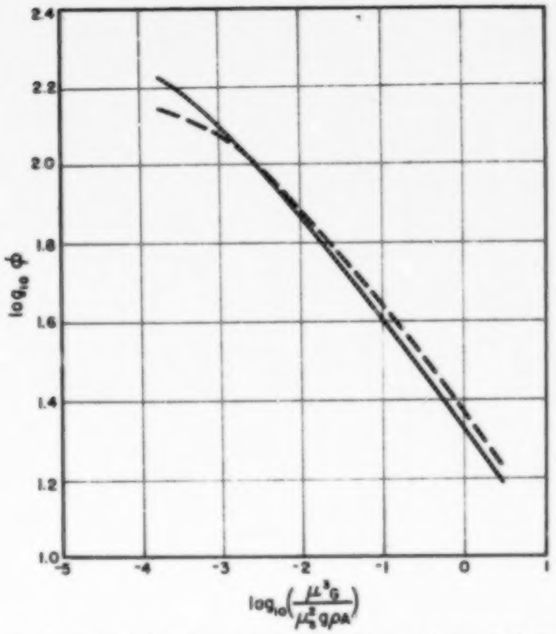

Fig. 3. Theoretical evaluation of ϕ. The solid curve is based (4, 5) on $\overline{v}_{z,\max,MO} = v_{f,SO}$. It has an asymptote of $\log_{10} \phi = 2.41$. The dashed curve is based (7) on $v_{z,\max,MO} = (3/2)\, v_{f,SO}$. It has an asymptote of $\log_{10} \phi = 2.27$.

μ which involves resistance to flow within a volume. Thus the dimensions of μ_s are force times time per length, while those for μ are of course force times time per area. The determination of μ_s is discussed later.

When there is appreciable variation in bubble diameter within the foam, an average d is employed in accordance with Equation (2):

$$d^2 = \frac{\Sigma n_i d_i^3}{\Sigma n_i d_i} \qquad (2)$$

For foam of high liquid content, the theoretical procedure for estimating D is more complicated (7). However, if the foam has only a moderate liquid content, then the complicated procedure can be greatly simplified into just multiplying D from Equation (1) by the quantity $(1 + 3D/G)$ to give a corrected D. The interested reader is referred to the aforementioned earlier publications for further details.

If bubble coalescence is present within the foam column, d must be taken at the top of the column. This is important. Experiments conducted by the authors' group have shown that a small but very significant degree of coalescence can easily go unnoticed to the eye (5). It is also worth mentioning here that such coalescence furnishes internal reflux. Thus column operation which is nominally in the simple mode can in fact constitute operation in the enriching mode.

When d is not directly measured at the top of the column, it can be estimated from the average bubble diameter lower down the column by means of the ratio of corresponding bulk foam densities (7), should this ratio be known from measurement (4, 5, 8) or some other source.

For severe internal coalescence, highly nonuniform bubble sizes, or extremely high liquid content in the foam, the theoretical evaluation of ϕ breaks down since the model is based on flow through capillaries bounding regular polyhedral bubbles. For such cases, one can resort to an empirical evaluation of ϕ.

COMPARISON BETWEEN THEORY AND EXPERIMENT FOR FOAM OVERFLOW

Table 1 summarizes the data sources and results for the present test involving foam overflow. For the first three sets of data, the system employed was aqueous Triton X-100 with pool concentrations ranging from 2×10^{-7} to 20×10^{-7} g.-mole/cc. Of course with reflux the range of interstitial concentrations was even greater.

TABLE 1. APPROXIMATE RANGE OF DATA, AND RESULTS FOR THE TEST OF THEORY PRESENTED IN FIGURE 4

Set	Reference	Aqueous System	Feed inlet	External reflux ratio	d, cm.	G, cc./sec.	D, cc./sec.	A, sq. cm.	μ_s, (dyne) (sec.)/cm.	No. of runs	Average deviation, %
1	*6, 8*	Triton X-100	Pool	0	0.11 to 0.24	1.3 to 3.2	0.001 to 0.028	16.6	1.0×10^{-4}	5	16
2	*4, 5*	Triton X-100	Pool	0 to 13	0.10 to 0.22	1.7 to 9.6	0.002 to 0.305	16.6	1.0×10^{-4}	31	29
3	*6, 8*	Triton X-100	Foam	0	0.05 to 0.40	1.3 to 10.4	0.001 to 0.405	13.1 to 13.8	1.0×10^{-4}	10	25
4	*2, 3*	Aresket 300	Pool	0	0.042 to 0.046	1.5 to 1.7	0.20 to 0.38	2.8 to 9.1	1.8×10^{-4}	3	12
5	*1*	Essentially NaDBS	Pool	0	0.055 to 0.071	2.7 to 2.9	0.09 to 0.12	11.4	0.8×10^{-4}	10	13
										Total = 59	

Triton X-100 is a commercial nonionic surfactant with the nominal formula C_8H_{17}-C_6H_4-$(OCH_2CH_2)_{9.7}$-OH.

For the first set of data, the column was operated in the simple mode. For the second set, nineteen runs were conducted with the column operating in the simple mode, and the remaining twelve runs were conducted with external reflux to operate the column deliberately in the enriching mode. For the third set, feed entered the foam rather than the pool so that operation was in the stripping mode.

Some of the early experiments (6) which yielded this third set of data involved very large slugs of gas in the foam and a very uncertain d at the tops of the columns. Such runs are not included here.

The fourth set of data is for aqueous Aresket 300 (commercial monobutyl biphenyl sodium monosulfonate) with pool concentrations ranging from 8×10^{-7} to 16×10^{-7} g.-mole/cc. This set of early results is very small owing to the fact that most of the data from which the set is drawn are unusable here. This is because for these data the bubble diameter was not measured at the top of the column and there was an undetermined degree of internal coalescence. The small set selected here constitutes those runs for which coalescence seemed the least, and furthermore represents D data extrapolated to zero column height (zero residence time) to further minimize the effect of coalescence.

The fifth set is from the work of another group of investigators who used aqueous sodium dodecylbenzene sulfonate in the range of 1.5×10^{-7} to 2.6×10^{-7} g.-mole/cc. in the presence of trace radioactive ions. Their photographs seem to show a wider range of bubble sizes within each bubble population than was usually the case for the authors' group of investigators who used special spargers to achieve more uniform bubble sizes within each run. Accordingly, with small bubbles fitting between larger bubbles, for a given bulk foam density their bubbles can be expected to have been more nearly spherical (and hence less polyhedral) than those of the authors' group. Their photographs seem to confirm this. There is also the question of internal coalescence in their foam. So, all in all, there is some doubt as to whether the theory is applicable to their case. Nevertheless, for the sake of completeness, their data are included in the present test.

The detailed bubble data required for applying Equation (2) to this fifth set were not published. Accordingly, d was obtained by dividing the spherical geometric factor 6 by their published values of average specific bubble surface. This does not give quite the same results as Equation (2) but is the best that can be done with the information available.

The surface viscosity for the first three sets of data, that is, for aqueous Triton X-100, has been measured independently (8) by the black spot method of Mysels (9). Its value was found to be 1.0×10^{-4} (dyne)(sec.)/cm. at 25°C.

Unfortunately, no μ_s measurements are known to the present authors for the systems employed in the last two data sets. Accordingly, for these two sets, μ_s was determined by applying the theory to the foam data. This was accomplished by combining Equation (1) with the wetness factor $(1 + 3D/G)$ and the solid curve of Figure 3, and then substituting for the quantities involved so as to solve for μ_s for each run. Results were then averaged. This yielded a μ_s of 1.8×10^{-4} (dyne)(sec.)/cm. for the aqueous Aresket 300, and 0.8×10^{-4} (dyne)(sec.)/cm. for the aqueous sodium dodecylbenzene sulfonate. Naturally, values of μ_s so determined incorporate not only any error in the data but also any limitations in the foam theory. On the other hand, they obviously improve the theoretical estimation of D over what might be expected from independently measured values of μ_s.

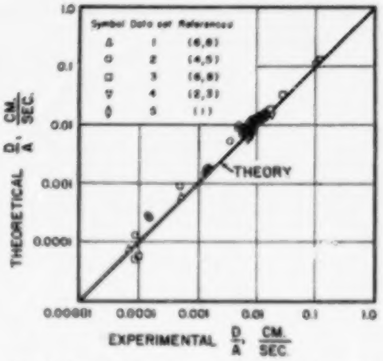

Fig. 4. Test of theory (5, 7) for predicting the foam overflow rate. Data set numbers refer to Table 1.

For the first four sets of data, the temperature was 25°C. Conditions for the fifth set were apparently near ambient too. Accordingly, for all five sets, μ is taken as 8.94×10^{-3} (dyne)(sec.)/sq. cm., ρ as 1.00 g./cc., and g as 980 cm./sec.^{2}. There is evidence which indicates that μ_s, at least for Triton X-100, can vary markedly with temperature (4, 5). Impurities can also affect μ_s.

Figure 4 shows the test. The ordinate represents D/A calculated from theory, that is, from Equation (1), the wetness factor $(1 + 3D/G)$, and the solid curve of Figure 3. (Use of the dashed curve of Figure 3 would have yielded nearly the same results.) The abscissa of Figure 4 represents experimental values of D/A. The diagonal is the line of theoretical perfection.

Examination of Figure 4 reveals reasonably good agreement between the plotted points and the theoretical line. The average deviation of theory from experiment is listed in Table 1 for each set of data. The average deviation is 26% for the points involving the independently measured μ_s, and 23% for all the points. In view of the wide range of variables covered (more than 1,000-fold for D/A) and the experimental difficulties involved, this is deemed to be good agreement between theory and experiment.

Of course the agreement can be improved further by using foam determined μ_s for the first three sets of data as well. In this connection, the apparent effect of concentration in the interstitial liquid on μ_s, as exhibited in Figure 5 of reference 5, can be incorporated. However, this would reduce the independence of the test and so, for the sake of maximum objectivity, has not been done here.

COMPARISON FOR STEADY STATE DRAINAGE

As mentioned earlier, the theory also furnishes a theoretical steady state relationship between the bulk density of a stable stationary foam trapped in a column and the rate of a liquid stream fed on to the top of the foam so as to drain through to the bottom.

In this connection, two sets of experimental data are available to test the drainage theory. For the first set (6, 8) d was 0.37 cm. and A was 13.1 sq.cm., while for the second set (4, 5) d ranged from 0.10 to 0.19 cm. and A was 16.6 sq.cm. Aqueous Triton X-100 was employed for both sets. Accordingly, the independent μ_s value of 1.0×10^{-4} (dyne)(sec.)/cm. is used here for the test. The temperature was 25°C. Since the foam was stationary, G of course was zero.

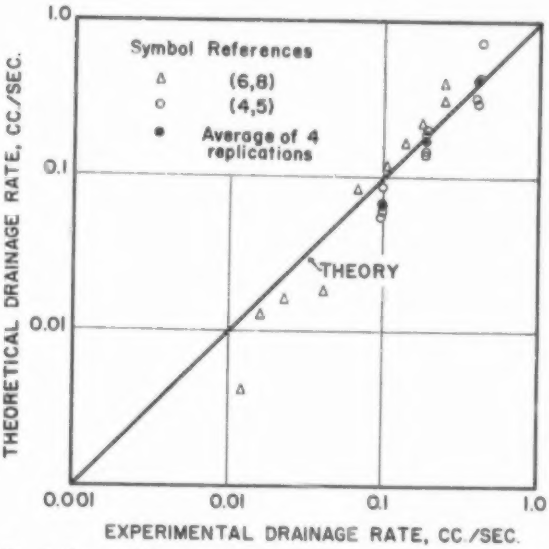

Fig. 5. Test of theory (7) for predicting the rate of steady state drainage through a stationary foam.

Figure 5 shows this drainage test. The ordinate represents the drainage rate predicted by theory from the measured bulk foam density and other pertinent information. This theoretical drainage rate was calculated in accordance with the information flow diagram of Figure 6 in which all notation, equation numbers, and figure numbers refer to reference 7. The aforementioned function ϕ does not enter the calculation in any way. Input information is encircled. Input t is of very small effect here. It was determined from Figure 5 of reference 8 but could just as well have been neglected.

The abscissa of the present Figure 5 represents the experimentally measured drainage rate. As before, the diagonal is the line of theoretical perfection. Inspection of this figure reveals fair agreement except at the lower drainage rates where experimental error is likely to be greatest. The average deviation of theory from experiment is 29%.

If one considers the experimental scatter apparent in the three sets of quadruplicated runs (shown as open circles in Figure 5), and then compares the three corresponding averages against the diagonal (so as to minimize the effect of individual error), better agreement between theory and experiment becomes immediately evident. The average deviation for these three averages is only 18%.

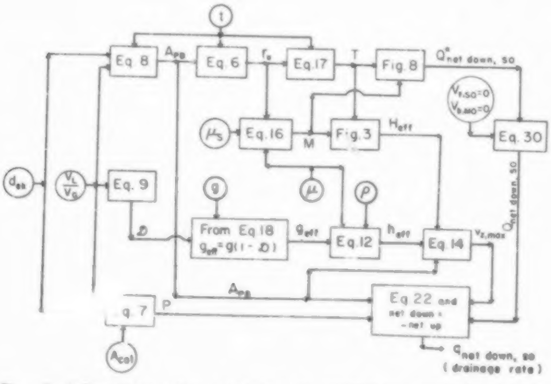

Fig. 6. Information flow diagram for predicting from theory (7) the rate of steady state drainage through a stationary foam. Input information is encircled. Since $v_{f,SO} = 0$ and $v_{b,MO} = 0$, $BO = MO = SO$. Notation, equations, and figures refer to reference 7.

In view of the range of variables, the experimental difficulties, and the use of the independently determined value for μ_s, the test represented in Figure 5 appears to yield fair agreement between theory and experiment.

CONCLUSIONS

The experimental results appear to support the theory. This is especially evident in light of the wide range of variables involved. Over more than a 400-fold range of foam overflow rate, the average deviation of theory from experiment is only 26%, even with μ_s independently determined.

ACKNOWLEDGMENT

This work was supported by U. S. Public Health Service Research Grant WP-00161.

NOTATION

A = horizontal cross-sectional area of a foam column, sq.cm.
D = volumetric flow rate of the entire foam overflow on a gas-free basis, cc./sec.
d = average bubble diameter, cm.
d_i = individual bubble diameter, cm.
G = volumetric flow rate of gas, cc./sec.
g = gravitational acceleration, cm./sec.^{2}
n_i = number of bubbles with diameter d_i
t = interstitial film (face) thickness, cm.
$v_{f,SO}$ = upward velocity of the aggregate of foam bubbles relative to a stationary observer, cm./sec.
$v_{z,max,MO}$ = maximum velocity downward within a vertical capillary relative to the aggregate of foam bubbles, cm./sec.
$\bar{v}_{z,max,MO}$ = average velocity downward within a vertical capillary relative to the aggregate of foam bubbles, cm./sec.

Greek Letters

μ = liquid viscosity, (dyne)(sec.)/sq.cm.
μ_s = surface viscosity, (dyne)(sec.)/cm.
ϕ = function
ρ = liquid density, g./cc.

LITERATURE CITED

1. Banfield, D. L., I. H. Newson, and P. J. Alder, *AIChE-I. Chem. E. Symp. Ser. (London)*, preprint 1.1; also private communication.
2. Brunner, C. A., Ph.D. dissertation, Univ. Cincinnati, Ohio (1963).
3. ———, and Robert Lemlich, *Ind. Eng. Chem. Fundamentals*, **2**, 297 (1963).
4. Fanlo, S., Ph.D. dissertation, Univ. Cincinnati, Ohio (1964).
5. ———, and Robert Lemlich, *AIChE-I. Chem. E. Symp. Ser. (London)*, **9**, 75 (1965).
6. Leonard R. A., Ph.D. dissertation, Univ. Cincinnati, Ohio (1964).
7. ———, and Robert Lemlich, *AIChE J.*, **11**, 18 (1965).
8. *Ibid.*, 25.
9. Mysels, R. J., K. Shinoda, and S. Frankel, "Soap Films, Studies of their Thinning," Pergamon Press, New York (1959).
10. Shih, F. S., Ph.D. dissertation, Univ. Cincinnati, Ohio, in preparation.

Manuscript received August 17, 1966; revision received November 21, 1966; paper accepted November 21, 1966.

SEPARATION SCIENCE, 2(3), 401–404 (1967)

NOTE

Nomenclature Recommendations for Adsorptive Bubble Separation Methods

---

Recently several separation techniques employing adsorption on bubbles have been introduced. As these methods must be added to the already well-established techniques using this general mechanism for separation, certain confusions have arisen in the literature in regard to the naming of these operations. In this note we should like to recommend nomenclature for these techniques. These recommendations have also been submitted to the I.U.P.A.C. subcommittee on nomenclature in the field of surface activity.

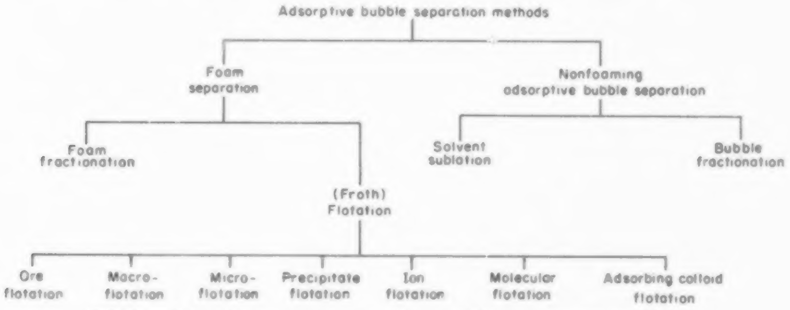
Adsorptive bubble separation methods
Foam separation
Nonfoaming adsorptive bubble separation
Foam fractionation
(Froth) Flotation
Solvent sublation
Bubble fractionation
Ore flotation
Macro-flotation
Micro-flotation
Precipitate flotation
Ion flotation
Molecular flotation
Adsorbing colloid flotation

FIG. 1. Schematic representation of nomenclature recommendations.

Figure 1 represents the total nomenclature scheme. As a generic name for the entire subject we propose *adsorptive bubble separation methods* (*1*). This general heading can then be divided into two catagories: *foam separation* and *nonfoaming adsorptive bubble separation*, the distinction being whether the formation of a foam (froth) is required for the separation.

Examination of Fig. 1 reveals the foam separation methods can be further subdivided into two parts:

Foam fractionation (2):	The removal of dissolved material by foaming.
Flotation (3):	The removal of particulate material by foaming (frothing). (Synonymous with *froth flotation.*)

Flotation presently includes seven subdivisions, not all of which are mutually exclusive:

Ore flotation (3):	A special case of froth flotation for the separation of minerals.
Macroflotation:	The removal of macroscopic particles by foaming (frothing).
Microflotation (4):	The removal of microscopic particles by foaming (frothing), especially microorganisms or colloids. (For the latter, *colloid flotation* may be used.)
Precipitate flotation (5):	A special case of froth flotation where a precipitate is removed, the precipitating agent being other than the surfactant.
Ion flotation (6):	The removal of a non-surface-active ion by foaming (frothing) through the use of a surfactant which yields an insoluble product, especially if removed as a scum.
Molecular flotation:	The removal of a non-surface-active molecule by foaming (frothing) through the use of a surfactant which yields an insoluble product.
Adsorbing colloid flotation (7):	The removal of dissolved material by adsorption on colloidal particles followed by removal of such particles by flotation.

Nonfoaming adsorptive bubble separations presently include two subdivisions:

Bubble fractionation (8):	The removal of material (whether molecular in size or particulate) by virture of adsorption at the surface of rising

bubbles followed by redeposition at or just under the main surface of the liquid pool.

Solvent sublation (9): The removal of material (whether molecular in size or particulate) by virtue of adsorption at the surface of rising bubbles followed by deposition within, or at either horizontal interface of, an immiscible liquid atop the main liquid.

REFERENCES

1. R. Lemlich, *Chem. Eng.*, **73**(21), 7 (1966).
2. H. G. Cassidy, *Technique of Organic Chemistry*, Vol. X, Wiley-Interscience, New York, 1957, Chap. 11.
3. A. M. Gaudin, *Flotation*, McGraw-Hill, New York, 1957, Chap. 1 (historical survey).
4. A. Dognon and H. Dumontet, *Comp. Rend.*, **135**, 884 (1941).
5. R. E. Baarson and C. L. Ray, Precipitate Flotation, a New Metal Extraction and Concentration Technique, *Am. Inst. Mining, Metallurgical, and Petroleum Engineers Symposium, Dallas, Texas, 1963.*
6. F. Sebba, *Nature*, **184**, 1062 (1959).
7. S. G. Mokrushin, *Ref. Zh. Khim.*, **1954**, No. 30406; CA, **49**, 2149i(1955).
8. D. C. Dorman and R. Lemlich, *Nature*, **207**, 145 (1965).
9. F. Sebba, *Ion Flotation*, Elsevier, New York, 1962, Chap. 10.

BARRY L. KARGER

Department of Chemistry,
Northeastern University,
Boston, Massachusetts

ROBERT B. GRIEVES

Department of Civil Engineering,
Illinois Institute of Technology,
Chicago, Illinois

ROBERT LEMLICH

Department of Chemical Engineering,
University of Cincinnati,
Cincinnati, Ohio

ALAN J. RUBIN

Environmental Health Engineering,
University of Cincinnati,
Cincinnati, Ohio

FELIX SEBBA

Department of Chemistry including Biochemistry,
University of Witwatersrand,
Johannesburg, South Africa

Received by editor March 4, 1967
Submitted for publication March 14, 1967